A subnational analysis of burden of disease in South Africa: mortality levels, causes of death and their forecasts.

William Tinashe Msemburi

A dissertation
submitted in partial fulfillment of the
requirements for the degree of

Doctor of Philosophy

University of Washington

2020

Reading Committee:

Eric Vos, Chair

Laura Dwyer-Lindgren

Aleksandr Aravkin

Debbie Bradshaw

Program Authorized to Offer Degree:
Global Health

University of Washington

Abstract

A subnational analysis of burden of disease in South Africa:
mortality levels, causes of death and their forecasts.

William Tinashe Msemburi

Chair of the Supervisory Committee:
Professor Eric Vos
Global Health

Empirical and model based approaches have provided estimates of South Africa's national and provincial mortality. However, little is known about district-level mortality patterns and differentials. The purpose of this research is to provide reliable estimates of these over three aims. Firstly, district-specific all-cause deaths for each age, sex and year are estimated by adjusting observed vital registration (VR) death numbers using a Bayesian regression model that concurrently addresses under-reporting of deaths and the random noise which typifies small-area samples. For the second aim, district-specific cause-of-death proportions for selected causes are determined using a Dirichlet-Multinomial regression model that leverages the South Africa province cause-of-death estimates from the 2017 Global Burden of Disease study to correct the district cause-of-death numbers from VR. In the final aim, the results from the previous aims are forecasted within a compositional data framework (CoDa) by first applying Singular Value Decompositions (SVDs) to the estimated all-cause and multiple decrement life table death matrices for all district-years. Next, estimated time-varying parameters from the resultant low-rank matrix approximations are forecasted using additive models that assume first order autoregressive residuals. Finally, full life table death matrices are reconstructed by combining these forecasts with the non-varying principal components estimated using the SVD-CoDa.

TABLE OF CONTENTS

LIST OF FIGURES

LIST OF TABLES

ACRONYMS

CODA: Compositional Data analysis

DDM: Death Distribution Method

DHA: Department of home affairs

DM: Dirichlet-Multinomial

ICD-10: Tenth revision of the International Statistical Classification of Diseases

GAM: Generalized Additive Model

GBD: Global Burden of Disease

GGB: Generalized Growth Balance

NBD: National Burden of Disease

SEG: Synthetic Extinct Generations

SVD: Singular Value Decomposition

VR: Vital Registration

ACKNOWLEDGMENTS

The African proverb, “it takes a village to raise a child”, is an apt description of how this research has come about; I have most certainly only been able to accomplish it through the support of a village whose members span the globe.

Foremost, I would like to thank my advisor, Theo Vos. You have been patient and encouraging throughout my graduate career, generously providing support and wisdom, and you created a space in which I was propelled to succeed. I have learnt a great deal from what you have said and the passion for a healthier world that you have consistently displayed. Our many discussions on Zimbabwe, global health, methods and soccer were truly an oasis for me, thank you Theo.

I would also like to thank the members of my reading committee who each uniquely contributed to my being able to complete this work. In particular, Laura Dwyer-Lindgren, thank you for reading through my research with such attention to detail and sharing of your knowledge. Many improvements in the rigour of the methods came about after having talked to you and received insightful comments and advice. Sasha Aravkin, thank you for the contribution you made to improve the mathematical components of this research. Your enthusiasm was infectious and your input was timely. To Debbie Bradshaw, thank you for introducing me to this field. Working with and learning from you at the SAMRC was foundational to what is pursued here. I am immensely grateful for your contribution over the years which has routinely been in line with the advice you gave me many moons ago, “to think globally, and to act locally”. And finally Suzanne Withers, in taking your class I was struck by your passion for health, justice and equity and how these relate to demography. Thank you for representing me on the committee.

I am tremendously grateful for the leadership at the Institute for Health Metrics and Evaluation. I am particularly thankful for Emmanuela Gakidou who from our first meeting to joining the PhD program and now beyond that, has been supportive, approachable and a champion working behind the scenes, thank you for creating opportunities for me. I am thankful to Chris Murray. Not only for your overall leadership, but as a research assistant for the GBD HIV estimation team, I had the adventure of learning from you and to this day it remains a highlight. Your depth of understanding of so many aspects of health measurement including the higher level demographic and statistical aspects, is something I aspire towards. And lastly, thank you to Haidong Wang. You are someone I consider to be a mentor and a friend and your quiet leadership and strong work ethic are in every way admirable.

I would like to extend my gratitude to a number of people who have supported me on this journey in various ways and at different points. Firstly Rob Dorrington and Tom Moultrie (CARe), your instruction was foundational and you remain wells of wisdom in this field. Thank you David Watkins and the BCEPS/DCP3 team (UW) and many mentors in Francesca Little, Allan Clark (UCT), Victoria Pillay-Van-Wyk (MRC), Willem Hanekom, Damian Walker (Gates Foundation), Hope Johnson, Dan Hogan (GAVI), Samira Asma and Somnath Chatterjee (WHO).

To my comrades in arms, the PhD colleagues who paved the way and gave invaluable advice and support throughout - David Phillips, Roy Burstein, Sarah Wulf-Hanson, Gloria Ikilezi and Gregoire Lurton - intellectual hour was the best hour of the week, thank you for enriching the journey.

Finally, thank you to all my friends and family. Special thank you to my mother Hellen who made innumerable sacrifices for me and on whose shoulders I stand. Lastly to my wife Hilda and our daughter Sarah, thank you for getting me here, this degree is as much yours as it is mine because we carried each other through it.

Chapter 1

INTRODUCTION

The endeavour to improve global health is contingent on accurate and detailed mortality data. The most appropriate actions to improve the health of populations result from granular specifications of place, age, sex, timing and cause of death. Obtaining the relevant data hinges on vital registration systems that can cover the affected and record these identifiers. In the absence of good quality data, indirect analytical tools are required to derive the desired information at sufficient levels of detail to insure that data needs are met. Ideally, appropriate data driven responses will in turn lead to improved health outcomes. In addition to responding based on retrospective data, correctly predicting future health trends and proactively preparing for them has the potential to increase health gains even further. Mortality forecasts play an important role in providing such predictions, informing on expected mortality levels if trends follow certain trajectories into the future. Benchmarking mortality projections against predefined optimal targets e.g. the sustainable development goals [1], highlights where health improvements are needed or where targets are unlikely to be reached.

Low- and middle-income countries have lagged behind in the development of strong vital registration systems that could be used to monitor health trends and provide good quality mortality data [2]. The Global Burden of Disease (GBD) [3] study has taken great strides to respond to this measurement need, producing detailed estimates of condition-specific mortality and morbidity for all countries of the world at national and for some, even at state, province or county level [4]. However, the level of specification of derived estimates

is conditional on how specific the data that are available for the location are. Countries range widely on the development spectrum and correspondingly, in the quality of the empirical data that are available for them. A large number of low- and middle-income countries are on a development journey which will see them having improved data over time; data that can be used to produce health estimates at higher spatial resolutions. One country which is well on its way in this journey, and can be seen as something of a burden of disease template for other low- and middle-income countries, is South Africa.

South Africa is made up of 52 metropolitan and district municipalities requiring information on the numbers and causal compositions of those deceased and estimates of the populations exposed - crucial information for monitoring health status, assessing how effective health-related programmes are, and identifying emerging health issues [5]. South Africa also has a turbulent history to overcome. The health sector of South Africa has the monumental task of undoing the health related legacy of apartheid. Laws such as the controversial Group Areas Act of 1950 forced people to only own or occupy homes in designated towns based on legally-defined racial groups with the objective of establishing completely segregated areas [6]. Apartheid's systematic discrimination is foundational to current extreme income inequalities, large variations in educational attainment, excessive violence, migrant labour and the proliferation of HIV/AIDS infection and mortality [7]. Post-apartheid South Africa inherited a health care system in which 60% of the resources were used by the private sector, serving only about 20% of the population [8]. This has led to sustained differential health access and wide variations in quality of care, both contributing to the vast differences in health outcomes across South Africa's socio-demographic spectrum. To address this, the National Health Act of 2004 decentralised health care through the establishment of a district health system to optimise quality and access across all districts. Subsequently, the day to day responsibilities for redressing the health inequities of the past and meeting the current health needs of all South Africans have been shifted to district health management teams [9].

The problem is obtaining complete and accurate health data for all districts. Although some information can be gleaned from population censuses, vital registration and the community surveys, the information that these data sources provide is currently not suitable for health monitoring at the district level [10, 11, 12]. Each of these data sources has potential weaknesses and there currently isn't a process that synthesizes the information they contain to produce estimates in a format that can help district level decision making.

Considering the 1996, 2001 and 2011 censuses, self-reported data are available at the district level to inform on the numbers in the population. Answers to questions on the survival of relatives can be used to estimate both adult and child mortality using indirect demographic techniques [13, 14]. Summary birth histories are recorded for all women aged 15–49 counting the number of live-births for each woman and the number still alive. This allows for a measure of fertility and the reported age-specific proportions of children who have died can help to estimate under-5 mortality by demographic methods [15]. However, census results can suffer from recall bias as the data are retrospective in nature [16, 17]. Other issues affecting response validity are under-coverage and selection bias. Bias can be introduced due to household collapse or mother's death, inaccurate age reporting, inaccurate responses from respondents, misunderstanding of the questions or incorrect capture by interviewers, and incorrect coding structures by coders. Finally, for South Africa the censuses do not provide a continuous time-trend but have a 5-yearly collection (although better than many other countries that conduct censuses every 10 years) [18, 19].

The vital registration system (VR) captures mortality information for the years 1997 to 2015 through death notification forms which are administrated by the national department of home affairs (DHA). These forms are processed by the national statistics agency, Statistics South Africa (Stats-SA), to capture cause-of-death information and selected socio-demographic and health data [20]. The captured information is coded according to the tenth revision of the International Statistical Classification of Diseases and Related Health

Problems (ICD-10) [21]. These data are available for the years 1997-2015 by age, sex, race, province and district. South African VR data are not immune to the quality issues that plague other low- and middle-income countries [22]. These include inaccurate coding of causes of death and under-reporting of deaths [2].

The community Surveys of 2007 and 2016 were large-scale nationally representative inter-census household surveys. Sampling was at the municipality level aggregated to provide district level information [23, 24]. The community surveys effectively provide much of the same information as in the census albeit using a smaller sample size and thus with greater uncertainty for smaller areas like districts. The community surveys also have similar limitations as described for the census.

The unadjusted mortality estimates derived using these data sources do not give a comprehensive picture of district-specific health burden. For most districts, little is known of the relative ranking of the mortality causes to note those accounting for the highest burden [25]. For many years and areas, VR data are known to be incomplete [5]. The magnitude of the impact of incompleteness on the estimates of mortality is generally larger for smaller areas as the missing deaths may not be missing completely at random and could be a significant proportion of specific districts. Also, little is known about the risk factors that would drive burden of disease levels and trends at the small area level [26].

Due to these data deficits, the delivery of particular services such as those necessary to intervene in a geographically clustered cause, age or sex-specific mortality scenario, may not match the true needs [27]. South Africa is experiencing a quadruple burden of disease comprising of HIV/AIDS, high rates of injury, other infectious diseases excluding HIV/AIDS and a burgeoning tide of non-communicable diseases [28, 29]. It becomes increasingly necessary to fill any knowledge gaps that impede on the district health system's ability to respond adequately and appropriately.

The GBD has produced detailed national mortality estimates for South Africa and the recent 2017 publication provides province level results as well, but not the district [4]. This is an opportunity to build on the GBD to produce estimates of particular relevance to the health district of South Africa. In this dissertation, I have completed three research aims. Aims 1 and 2 respectively outline methodology that can be used to disaggregate all-cause and cause-of-death GBD estimates to subnational and derive such estimates for South Africa's 52 health districts for the period 1997–2015. Aim 3 describes how the estimates can be forecasted to 2030 in a coherent way. Specifically:

Aim 1: Estimate South Africa all-cause mortality by district (1997–2015)

- True all-cause death numbers are estimated for each district by age, sex and year for the period 1997–2015. District-specific VR data by sex and year are adjusted through a Bayesian regression model that smooths the observed age-specific mortality rates using the corresponding parent province's log-mortality age-pattern and age-specific offsets determined using a spline function. Together with the smoothing, the model simultaneously quantifies the level and uncertainty of completeness of death registration for each district based on the observed district VR, the district-specific completeness of child deaths and the completeness of reporting at older ages that is estimated in GBD2017 for the province the district lies within.

Aim 2: Estimate South Africa cause-specific mortality by district (1997–2015)

- Estimates of all-cause death numbers by year, age, sex and district are disaggregated to expected true causes through a Dirichlet-Multinomial compound model that predicts the GBD2017 provincial cause-specific results by year, age and sex using the observed province-specific VR cause-of-death numbers. The model determines the most likely posterior distributions for the district true causes given the observed district-specific VR as well as the age, sex, year and province of death.

Aim 3: Derive South Africa mortality forecasts by district (2016–2030)

- The third aim of this study is to forecast district, province and national mortality profiles from 2016 to 2030. The forecasting approach is according to a Compositional Data Analysis (CoDa) framework applied to district specific life table deaths. The dimensions of the deaths matrix are reduced using a Singular Value Decomposition (SVD) to determine principle components and time-varying parameters which are then forecasted using generalized additive models (GAMS) that assume first order autoregressive residuals. These parameters are used to reconstruct the life table death matrix for both the observed and forecasted period. The single-decrement life table formulation and a multiple-decrement variant are used to forecast the Aims 1 and 2 estimates, respectively. Finally, the forecasted cause-specific mortality rates are scaled to sum to the forecasted all-cause rates for the corresponding location, age, year and sex, maintaining coherence.

The next three chapters expand on these three aims. They outline the methods and studies that have produced estimates of all-cause and cause-specific mortality for the provinces of South Africa, as well as nationally, before detailing the methods used to generate district level estimates in this research. Summary results of key measures such as death-numbers and rates, probabilities of death and life-expectancy at birth for Aims 1 and 3, and leading causes-of-death and cause-patterns for Aims 2 and 3, are provided in the relevant chapters. More detailed results are then provided in the attached supplementary appendices.

REFERENCES

[1] Jeffrey D Sachs. From millennium development goals to sustainable development goals. *The Lancet*, 379(9832):2206–2211, 2012.

[2] Colin D Mathers, Doris Ma Fat, Mie Inoue, Chalapati Rao, and Alan D Lopez. Counting the dead and what they died from: an assessment of the global status of cause of death data. *Bulletin of the world health organization*, 83(3):171–177c, 2005.

[3] Daniel Dicker, Grant Nguyen, Degu Abate, Kalkidan Hassen Abate, Solomon M Abay, Cristiana Abbafati, Nooshin Abbasi, Hedayat Abbastabar, Foad Abd-Allah, Jemal Abdela, et al. Global, regional, and national age-sex-specific mortality and life expectancy, 1950–2017: a systematic analysis for the global burden of disease study 2017. *The lancet*, 392(10159): 1684–1735, 2018.

[4] Haidong Wang, Amanuel Alemu Abajobir, Kalkidan Hassen Abate, Cristiana Abbafati, Kaja M Abbas, Foad Abd-Allah, Semaw Ferede Abera, Haftom Niguse Abraha, Laith J Abu-Raddad, Niveen ME Abu-Rmeileh, et al. Global, regional, and national under-5 mortality, adult mortality, age-specific mortality, and life expectancy, 1970–2016: a systematic analysis for the global burden of disease study 2016. *The Lancet*, 390(10100):1084–1150, 2017.

[5] N Massyn, N Peer, A Padarath, P Barron, and C Day. District Health Barometer 2014/15. *Durban: Health Systems Trust*, 2015.

[6] Anthony J Christopher. Changing patterns of group-area proclamations in South Africa, 1950–1989. *Political Geography Quarterly*, 10(3):240–253, 1991.

[7] Hoosen Coovadia, Rachel Jewkes, Peter Barron, David Sanders, and Diane McIntyre. The health and health system of South Africa: historical roots of current public health challenges. *The Lancet*, 374(9692):817–834, 2009.

[8] Jørn Braa and Calle Hedberg. The struggle for district-based health information systems in South Africa. *The information society*, 18(2):113–127, 2002.

[9] Mickey Chopra, Joy E Lawn, David Sanders, Peter Barron, Salim S Abdool Karim, Debbie Bradshaw, Rachel Jewkes, Quarraisha Abdool Karim, Alan J Flisher, Bongani M Mayosi, et al. Achieving the health Millennium Development Goals for South Africa: challenges and priorities. *The Lancet*, 374(9694):1023–1031, 2009.

[10] Henry S Shryock, Jacob S Siegel, and Elizabeth A Larmon. *The methods and materials of demography*. US Bureau of the Census, 1973.

[11] Donald T Rowland et al. Demographic methods and concepts. *OUP Catalogue*, 2003.

[12] Kenneth Hill, Alan D Lopez, Kenji Shibuya, Prabhat Jha, Monitoring of Vital Events (MoVE) writing group, et al. Interim measures for meeting needs for health sector data: births, deaths, and causes of death. *The Lancet*, 370(9600):1726–1735, 2007.

[13] Kenneth Hill. Approaches to the measurement of childhood mortality: a comparative review. *Population Index*, pages 368–382, 1991.

[14] Georges Reniers, Bruno Masquelier, and Patrick Gerland. Adult mortality in Africa. In *International handbook of adult mortality*, pages 151–170. Springer, 2011.

[15] United Nations. Department of International Economic and Social Affairs. Population Division and others. *Manual X: indirect techniques for demographic estimation*. UN, 1983.

[16] Martin Bangha, Alioune Diagne, Ayaga Bawah, and Osman Sankoh. Monitoring the millennium development goals: the potential role of the INDEPTH Network. *Global health action*, 3, 2010.

[17] Ian M Timæus. Adult mortality. 1993.

[18] The United Nations. Africa addendum to the United Nations principles and recommendations for population and housing censuses. *Addis Ababa, Ethiopia: Economic Commission for Africa*, ACS/WPS2/2008, 2008.

[19] John Blacker. The impact of AIDS on adult mortality: evidence from national and regional statistics. *Aids*, 18:S19–S26, 2004.

[20] Statistics South Africa. *Mortality and Causes of Death in South Africa, 2007: Findings from Death Notification. Statistical release P0309.3. Pretoria:*. Statistics South Africa, 2009.

[21] World Health Organization. *International statistical classification of diseases and related health problems*, volume 1. World Health Organization, 2004.

[22] Elisabeth França, Daisy Xavier de Abreu, Chalapati Rao, and Alan D Lopez. Evaluation of cause-of-death statistics for Brazil, 2002–2004. *International journal of epidemiology*, 37(4): 891–901, 2008.

[23] Statistics South Africa. *Community survey 2007*. Statistics South Africa, Pretoria, 2007.

[24] Statistics South Africa. *Community survey 2016*. Statistics South Africa, Pretoria, 2016.

[25] Bongani M Mayosi, Alan J Flisher, Umesh G Lalloo, Freddy Sitas, Stephen M Tollman, and Debbie Bradshaw. The burden of non-communicable diseases in south africa. *The Lancet*, 374 (9693):934–947, 2009.

[26] Mickey Chopra, Joy E Lawn, David Sanders, Peter Barron, Salim S Abdool Karim, Debbie Bradshaw, Rachel Jewkes, Quarraisha Abdool Karim, Alan J Flisher, Bongani M Mayosi, et al. Achieving the health millennium development goals for south africa: challenges and priorities. *The Lancet*, 374(9694):1023–1031, 2009.

[27] Salim S Abdool Karim, Gavin J Churchyard, Quarraisha Abdool Karim, and Stephen D Lawn. Hiv infection and tuberculosis in south africa: an urgent need to escalate the public health response. *the Lancet*, 374(9693):921–933, 2009.

[28] D. Bradshaw, K. Steyn, N. Levitt, and B. Nojilana. Non-communicable diseases A race against time. Burden of Disease Research Unit and Chronic Disease Initiative for Africa, Dept of Medicine, University of Cape Town Policy Brief, September 2011.

[29] Victoria Pillay-van Wyk, William Msemburi, Ria Laubscher, Rob E Dorrington, Pam Groenewald, Tracy Glass, Beatrice Nojilana, Jané D Joubert, Richard Matzopoulos, Megan Prinsloo, et al. Mortality trends and differentials in South Africa from 1997 to 2012: second National Burden of Disease Study. *The Lancet Global Health*, 4(9):e642–e653, 2016.

Chapter 2

SOUTH AFRICA ALL-CAUSE MORTALITY BY DISTRICT (1997–2015)

2.1 Introduction

Estimates of South Africa's true national and provincial all-cause mortality have been provided through approaches that utilize statistical models as well as others based on more empirical methods, most notably in the Global Burden of Disease (GBD) [1] and the 2nd National Burden of Disease (NBD) [2] studies. However, no study has generated the same for South Africa's 52 health districts and this research aims to fill this gap. The next few sections explore the current state of knowledge, reviewing the methods that have been used to estimate provincial and national mortality and describing these studies that have used them. Following which, the estimation approach used in this research is discussed in more detail.

2.2 Review of national and provincial all-cause mortality estimation

Estimates of all-cause mortality are crucial for assessing district health status and evaluating the performance of the district health sector. They define the mortality envelope which can be used in the derivation and/or validation of cause-specific estimates. Ideally, these estimates should come from complete VR; a data source that is potentially all-inclusive regardless of socio-economic status, death location, age and sex. Even incomplete VR data can still be used in research depending on the extent of under-reporting, whether or not the incompleteness biases the data randomly or systematically, and most importantly, if the bias can be quantified and corrected.

In the absence of usable VR data or to correct it using population trends, census or survey data can be used to estimate key mortality metrics, in particular ${}_5q_0$ and ${}_{45}q_{15}$, which are measures of child and adult mortality, respectively. The ${}_nq_x$ give the probability that a person aged x will die within n years if mortality rates remain constant and they can be related to model life tables to generate age-specific estimates. As estimation requires a number of assumptions to be made which can lead to biased results, the final age-specific numbers generated are less accurate than those based on a complete VR time series.

A third option is the use of statistical models applying mathematical relationships to derive estimates of all-cause mortality. The demographic balancing equation takes the numbers in a population at the beginning and end of a period of t years, P_1 and P_2, respectively, and connects them according to the following equation:

$$P_2 = P_1 + B - D + M$$

where births are represented by B, deaths by D and net-migration by M. By making assumptions about P_1, P_2, B and M, it is possible to solve for D. What we currently know about South Africa mortality comes from studies that typically utilise combinations of the three options above. Broadly speaking, these studies can either be classified as being empirical or model based.

2.2.1 Empirical methods

There have not been many empirical studies that provide subnational or even national mortality estimates because of the historically poor quality of reported data and the time-lag between year of death and Stats-SA dissemination of collated reported deaths. The most comprehensive of the empirical studies has been the NBD study [2].The NBD aimed to analyse cause of death data for the 1997–2012 period and to develop national, population group, and provincial estimates of the levels and causes of mortality. The

study used underlying cause of death data from death notification forms covering this period and obtained from Stats-SA. The national reported adult deaths were adjusted for under-reporting using death distribution methods i.e. the generalized growth balance (GGB) and synthetic extinct generations (SEG) methods [3, 4]. For the completeness of the province, deaths reported by households from the 2001 and 2011 censuses and 2007 community survey were used to generate mortality rate values for those aged 15 and older for specific years, and the ASSA2008 model [5] was used to set the mortality rate value for 1996. ASSA2008 is an MS Excel AIDS and demographic model developed by the Actuarial Society of South Africa. It is calibrated to child mortality and adult mortality based on surveys, census and vital statistics as well as antenatal HIV seroprevalence survey data. The ASSA2008 model was then used to derive a trend through these four point estimates with the ratio of the derived to observed rates providing base estimates of completeness which were then scaled so that the sum of the adjusted would match that calculated using the DDMs for the national [6]. There are multiple sources of uncertainty in this approach from the reference result from the DDM to the province estimates derived using the census/surveys as well as the initial estimate and the trend derived using ASSA2008.

The child mortality estimates generated from VR were adjusted for incomplete reporting using estimates generated by applying an indirect demographic method originally developed by Brass [7, 8] to census and community survey summary birth history responses. The method uses the ratio of children ever born to children dying to estimate ${}_5q_0$. For the NBD, the Ward and Zaba [9] correction was further applied to the child mortality estimate to correct for the non-response due to high HIV/AIDS mortality [10].

Death distribution methods to estimate completeness of reporting of adult deaths and this standard indirect approach to estimating child mortality play a significant role in providing mortality estimates for countries like South Africa that have imperfect albeit functional VR and that utilize population census and surveys to estimate child mortality. As such, these indirect demographic methods are discussed in greater detail below.

2.2.1.1 Death distribution methods for adult mortality

There are three main classes of mortality estimation methods that have been used by demographers for countries with incomplete vital registration and those lacking regular and accurate censuses [11, 12]. These are death distribution methods (DDMs), intercensal survival methods and indirect methods based on sibling survival. Hill [11] found that specific DDMs, namely the Generalized Growth Balance (GGB) and the Synthetic Extinct Generations (SEG) method, gave superior results by virtue of their generating period- and age-specific mortality rate estimates.

The Generalized Growth Balance (GGB) Method:

Based on the Growth Balance method which was developed by Brass et al. [13], Hill [14] proposed the Generalized Growth Balance (GGB) method to estimate the completeness of reporting of deaths. The method uses the census to derive a mortality rate for those aged x and older and compares it to that derived using the reported deaths. According to the demographic balancing equation for a closed population, the population numbers at the end of the period are the result of deaths being subtracted from and births being added to the population at the beginning of the period. Mathematically, this can be expressed as

$$ {}_{\infty}P_0(t_2) = {}_{\infty}P_0(t_1) + N_0 - {}_{\infty}D_0 \implies N_0 + {}_{\infty}P_0(t_1) - {}_{\infty}P_0(t_2) = {}_{\infty}D_0 \tag{2.1} $$

where ${}_{\infty}P_0(t_1)$ and ${}_{\infty}P_0(t_2)$ are the numbers of people aged 0 and older at time points t_1 and t_2, respectively, ${}_{\infty}D_0$ are the deaths aged 0 and older occurring in the period t_1 to t_2, and N_0 are the number reaching age 0 over the period. For any age x and older, this relationship can be generalized to:

$$ N_x - \left({}_{\infty}P_x(t_2) - {}_{\infty}P_x(t_1) \right) = {}_{\infty}D_x \tag{2.2} $$

The GGB method is based on equation 2.2. We let ${}_{\infty}YL_x(t_1, t_2)$ represent the number of person-years aged x and over lived between t_1 and t_2, which can be estimated using the geometric mean [15]:

$$ {}_{\infty}YL_x(t_1, t_2) = (t_2 - t_1) \times \sqrt{{}_{\infty}P_x(t_1){}_{\infty}P_x(t_2)} $$

Dividing equation 2.2 through by ${}_{\infty}YL_x(t_1, t_2)$ gives

$$ n(x) - r(x+) = d(x+) \tag{2.3} $$

where the death, birth and growth rates are respectively

$$ \begin{aligned} d(x+) &= \frac{{}_{\infty}D_x}{{}_{\infty}YL_x(t_1, t_2)} \\ n(x) &= \frac{N_x}{{}_{\infty}YL_x(t_1, t_2)} \\ r(x+) &= \frac{{}_{\infty}P_x(t_2) - {}_{\infty}P_x(t_1)}{{}_{\infty}YL_x(t_1, t_2)} \end{aligned} \tag{2.4} $$

Equation 2.3 gives terms that are functions of true, not reported, quantities. Letting k_1 and k_2 represent the census coverage at time points t_1 and t_2 and c the completeness of reporting of deaths, then the reported quantities defined as:

$$ \begin{aligned} {}_{\infty}P^r_x(t_1) &= k_1 \times {}_{\infty}P_x(t_1) \\ {}_{\infty}P^r_x(t_2) &= k_2 \times {}_{\infty}P_x(t_2) \\ {}_{\infty}D^r_x &= c \times {}_{\infty}D_x \end{aligned} \tag{2.5} $$

where r represents the reported quantity calculated in place of the true ones given in preceding equations. Additional approximations and assumptions are made to estimate death, birth and growth rates:

- Equation 2.6 is used to approximate the true numbers reaching age x between times t_1 and t_2. Numbers are aggregated by 5 yearly age-groups to work quinquennially following standard convention to approximate:

$$N_x \approx (t_2 - t_1)\frac{\sqrt{{}_5P_{x-5}(t_1)\,{}_5P_x(t_2)}}{5} \tag{2.6}$$

  $N_x^r \approx 0.2(t_2 - t_1)\sqrt{{}_5P_{x-5}^r(t_1)\,{}_5P_x^r(t_2)}$ is used to generate

$$n(x) = \frac{N_x}{{}_\infty YL_x(t_1, t_2)} = \frac{N_x^r}{{}_\infty YL_x^r(t_1, t_2)} = n^r(x) \tag{2.7}$$

  where ${}_\infty YL_x^r(t_1, t_2) = (t_2 - t_1) \times \sqrt{{}_\infty P_x^r(t_1)\,{}_\infty P_x^r(t_2)}$.

- The population numbers are used to approximate the observed growth rates $r^r(x+)$ and true growth rates $r(x+)$ according to equation 2.8:

$$\begin{aligned} r(x+) &\approx \frac{ln\left(\frac{{}_\infty P_x(t_2)}{{}_\infty P_x(t_1)}\right)}{t_2 - t_1} \\ r^r(x+) &\approx \frac{ln\left(\frac{{}_\infty P_x^r(t_2)}{{}_\infty P_x^r(t_1)}\right)}{t_2 - t_1} = \frac{ln\left(\frac{k_2 \times {}_\infty P_x(t_2)}{k_1 \times {}_\infty P_x(t_1)}\right)}{t_2 - t_1} = \frac{ln\left(\frac{{}_\infty P_x(t_2)}{{}_\infty P_x(t_1)}\right) - ln\left(\frac{k_1}{k_2}\right)}{t_2 - t_1} \\ \implies r(x+) &= r^r(x+) + \frac{ln\left(\frac{k_1}{k_2}\right)}{t_2 - t_1} \end{aligned} \tag{2.8}$$

- The observed death rates $d^r(x+)$ and true death rates $d(x+)$ are estimated according to equation 2.9:

$$\begin{aligned} d(x+) &= \frac{{}_\infty D_x}{(t_2 - t_1) \times \sqrt{{}_\infty P_x(t_1)\,{}_\infty P_x(t_2)}} \\ d^r(x+) &= \frac{{}_\infty D_x^r}{(t_2 - t_1) \times \sqrt{{}_\infty P_x^r(t_1)\,{}_\infty P_x^r(t_2)}} = \frac{c \times {}_\infty D_x}{(t_2 - t_1) \times \sqrt{k_1 \times {}_\infty P_x(t_1) k_2 \times {}_\infty P_x(t_2)}} \\ \implies d(x+) &= \frac{\sqrt{k_1 k_2}}{c} d^r(x+) \end{aligned} \tag{2.9}$$

Equation 2.3 is rewritten using these three approximations of true values which are based on reported to give:

$$n^r(x) - r^r(x+) - \frac{ln\left(\frac{k_1}{k_2}\right)}{t_2 - t_1} = \frac{\sqrt{k_1 k_2}}{c} d^r(x+) \tag{2.10}$$

The elements of equation 2.10 can also be expressed in terms of an equation of a straight line:

$$\underbrace{n^r(x) - r^r(x+)}_{\text{Dependent variable}} = \underbrace{\frac{1}{t_2 - t_1} ln\left(\frac{k_1}{k_2}\right)}_{\text{Intercept term}} + \underbrace{\frac{1}{c}\sqrt{k_1 k_2}}_{\text{Slope term}} \times \underbrace{d^r(x+)}_{\text{Independent variable}} \tag{2.11}$$

The method assumes the coverage of the more recent census to be 1, assuming it is better enumerated, such that the relative coverage of censuses, k_1 and k_2, as well as coverage of reported deaths, c, are estimated using the line of best fit. The GGB method is found to be most vulnerable to errors in the reported age [14].

The Synthetic Extinct Generations (SEG) method:

As with the GGB, the SEG method estimates the completeness of death reporting using the death numbers implied by censuses. The method is based on Vincent's 1951 extinct generations method [16] which used the death numbers from members of a cohort aged a at time t, from time t till the final death of the entire cohort, to estimate the original number of people in the cohort at the initial time point t i.e.

$${}_1P_a(t) = {}_1D_a(t) + {}_1D_{a+1}(t+1) + {}_1D_{a+2}(t+2) + \ldots + {}_1D_{a+\omega-a}(t+\omega-a) \tag{2.12}$$

where ${}_1P_a(t)$ and ${}_1D_a(t)$ are the population and death numbers of age $\in [a, a+1)$ at time t and ω is the age at which the last cohort member dies. This method was generalized to a stable population relationship by Preston *et al* [16] under assumptions of discrete time

and age. Under the stable population assumption,

$$ {}_1D_a(t+y) =_1 D_a(t)\mathrm{e}^{ry} $$

where r is the population growth rate independent of age. ${}_1P_a(t)$ can be rewritten

$$ {}_1P_a(t) = \sum_{y=0}^{\omega-a} {}_1D_{a+y}(t)\mathrm{e}^{ry} \tag{2.13} $$

which can be generalized for continuous age and time for ages a at time t to

$$ {}_1P_a(t) = \int_0^{\omega-a} {}_1D_{a+y}(t)\mathrm{e}^{ry}\mathrm{d}y = \int_a^{\omega} {}_1D_x(t)\mathrm{e}^{r(x-a)}\mathrm{d}x \tag{2.14} $$

for the transformation $y = x - a$. Bennett and Horiuchi [16] derived the SEG method based on equation 2.14 to correct the reported deaths between two censuses for incompleteness by determining the levels of coverage. The underlying assumption for the SEG method is that if relative to census enumeration, death reporting was complete, the population numbers derived using the deaths would be the same as the population numbers derived using the censuses. Conversely, if death reporting is incomplete with completeness assumed constant by age, then the levels of incompleteness can be estimated using the ratio of the population number according to the census relative to the population number derived using the reported deaths.

The SEG method works quinquennially and requires:

- ${}_5P_x(t_1)$ and ${}_5P_x(t_2)$: census counts by age at time points t_1 and t_2.
- ${}_5D_x$: reported deaths by age for the same population over the intercensal period.

Assuming age x with bounds $[0, A)$ where A is the open interval lower bound, the method also requires the population and death numbers at the open interval age A, represented by

${}_{\infty}P_A(t_1)$, ${}_{\infty}P_A(t_2)$ and ${}_{\infty}D_A$, respectively.

The observed growth rates by age ${}_5r_x$ can be estimated from the census using:

$$ {}_5r_x \approx \frac{ln\left(\frac{{}_5P_x(t_2)}{{}_5P_x(t_1)}\right)}{t_2 - t_1} \tag{2.15}$$

The estimate of the population aged x based on the reported deaths, ${}_5\bar{P}_x$, is first estimated for the open interval ${}_{\infty}\bar{P}_A$ according to:

$$ {}_{\infty}\bar{P}_A = {}_{\infty} D_A\left[\exp\left({}_{\infty}r_A e_A\right) - \left({}_{\infty}r_A e_A\right)^{2/6}\right] \tag{2.16}$$

where e_A is the life expectancy at the open interval lower bound and ${}_{\infty}r_A$ is growth rate for the open interval. The population is then estimated for all other ages below the open interval iteratively downwards:

$$ {}_5\bar{P}_{x-5} = {}_5\bar{P}_x \exp\left[5{}_5r_{x-5}\right] + {}_5D_{x-5}\exp\left[2.5{}_5r_{x-5}\right] \tag{2.17}$$

The number attaining age x between time points t_1 and t_2 according to the census data is estimated:

$$ {}_5P_x = \frac{(t_2 - t_1) \times \sqrt{{}_5P_x(t_1){}_5P_{x+5}(t_2)}}{5} \tag{2.18}$$

and then overall completeness, c, is derived from the $c(x)$ age-specific estimates where each compares the census based population number to that derived using the reported VR for each age-group $[x, x+5)$:

$$ c(x) = \frac{{}_5\bar{P}_x}{{}_5P_x} \tag{2.19}$$

Assuming differential completeness by age with lower coverage for the youngest and

oldest age-groups an age-independent estimate of completeness c is required. The median or mean of the $c(x)$ is generally chosen for this purpose, also taking a subset of the available age-range to minimize the effect of extreme fluctuations while retaining as much information about the level of completeness as possible. After c is calculated, the reported deaths are corrected for under-reporting using:

$$ {}_5D_x^* = \frac{{}_5D_x}{c} \tag{2.20} $$

with $D^*(x)$ being the true death number after correcting for any under-count. Adjusted death-rates ${}_5m_x$ can be calculated using the adjusted death numbers according to:

$$ {}_5m_x \approx_5 M_x = \frac{{}_5D_x^*}{(t_2 - t_1)\sqrt{{}_5P_x(t_1)\,{}_5P_x(t_2)}} \tag{2.21} $$

and key probabilities of death can be generated using standard approximations e.g.

$$ {}_5q_x = \frac{5\,{}_5m_x}{1 + 2.5\,{}_5m_x} \tag{2.22} $$

An estimate of adult mortality, ${}_{45}q_{15}$, can be calculated using the ${}_5m_x$ by assuming that the mortality rates estimate hazard rates represented by $\mu_{x+2.5}$. Assuming $T(x)$ represents the still to be experienced lifetime of an individual aged x, then its survival function of $T(x)$ can be defined

$$ S_{T(x)}(t) = Pr(T(x) > t) \triangleq_t p_x $$

and the force of mortality is

$$ \mu_x = -\frac{\mathrm{d}}{\mathrm{d}t} ln S_{T(x)}(t) $$

Assuming a constant force of mortality between x and $x+t$, the hazards are estimated:

$$ {}_tp_x = \frac{S(x+t)}{S(x)} = \exp\left[-\int_x^{x+t} \mu_y \mathrm{d}y \right] \implies {}_5p_x \approx \exp\left[-5\mu_{x+2.5} \right] $$

and so

$$ {}_{45}q_{15} = 1 - \exp\left[-5 \sum_{x=15[5]}^{55} {}_5m_x \right] \tag{2.23} $$

Bennett and Horiuchi [16] propose allowing for differential census coverage using an adaptation the describe in end note number 10 i.e. determining a level $c(x)$ series by finding an optimal value of a constant δ to add to the growth rates,

$$ {}_5\hat{r}_x = {}_5 r_x + \delta, \tag{2.24} $$

where ${}_5\bar{P}_{x+5}$, ${}_5D_x$ and ${}_5r_x$ are used to determine ${}_5\bar{P}_x$ as described above. The value of δ, which van be determined through optimization, quantifies the difference in coverage between the two censuses, that is

$$ k_1/k_2 = \exp(\delta[t_2 - t_1]) \tag{2.25} $$

where k_1 and k_2 represent the completeness of censuses 1 and 2, respectively, with the larger assumed to be 100% complete.

DDMs assume closed populations in terms of migration, levels of death registration are uniform by age, coverage of census enumeration by age is uniform across censuses, accurate reporting of ages in the deaths and census, and for the SEG, that the coverage of the two censuses is the same. Various researchers have looked at the impact of violations of these assumptions on the performance of these methods. Hill et al. [17] used the West model life table for females to simulate a population with predefined mortality. Hill et al. [17] assumed the population was non-stable and specified age-specific growth rates to impose a

fertility decline to it. In addition, two censuses occurring five years and 25 error scenarios were applied to the simulated population to replicate collection and data quality issues for real life data. The error scenarios fell into four broad categories:

1. Age misreporting for reported deaths and in censuses,
2. Differences in census coverage (aggregate and age-specific),
3. Age-specific differences in the completeness of reporting of deaths (decreasing/increasing by age),
4. Non-zero net-migration.

Hill et al. [17] compared the GGB, SEG, a combined GGB+SEG variant and the extended SEG+δ by assessing the error in the estimated ${}_{45}q_{15}$ after applying these methods to the simulated data. The results showed that DDMs accurately correct the errors for which they are designed but are each vulnerable to specific assumption violations. For the GGB it is age misreporting whereas for the SEG it is differential census coverage and migration. The SEG+δ was most accurate in 80% of scenarios and the GGB+SEG was best for the remainder.

Dorrington et al. [18] performed a similar exercise with the same scenarios to validate the results by Hill et al. [17] but also included male and female African datasets of populations with a high prevalence of HIV. Dorrington et al. [18] confirmed that the SEG+δ performed the best for many of the scenarios applied by Hill et al. [17] albeit for a smaller number with the African datasets that were not included previously.

Murray et al. [19] also assessed these various DDMs using simulations and the same approach of applying errors to data with known mortality. Error patterns were first derived empirically and were then used to simulate errors in vital registration completeness, coverage of censuses and reporting of age in both. Murray et al. [19] used four population types:

- Static - constant mortality, constant fertility and no migration
- Closed - declining mortality, declining fertility and no migration
- Immigrant - declining mortality, declining fertility and a positive net migration rate per population citizen
- Emigrant - declining mortality, declining fertility and a negative net migration rate per population citizen

As was done by Hill et al. [17], the DDMs were assessed using the estimated ${}_{45}q_{15}$ error for each scenario and population. The study reiterated the findings by Hill et al. [17] and Dorrington et al. [18], highlighting the vulnerability of DDMs to migration, although the GGB was found to be less so. The GGB was found to have higher error variance for scenarios with age misreporting whereas the SEG had higher variance under differential coverage of censuses. The SEG also had a higher variance when all the errors were applied simultaneously. Uniquely, Murray et al. [19] observed a significant correlation between the bias and the choice of ages used to summarise completeness. DDMs produce estimates of completeness by age which in turn need to be summarized to provide a single measure of adult completeness using the mean or the median for a selected age-range. Generally, the selection of the age-range or the age-trim has been according to qualitative criteria viewed as part of the art that is demography with selection not formalized by set rules but at the discretion of the demographer.

In other research, Murray et al. [20] propose more formal criteria for deciding on the optimal DDM versions to apply. In their research, optimization is carried out by varying the age-trim option to select the calibration that leads to the most accurate results in the simulated datasets previously described [19]. Despite observing that on average these age-trims lead to the most accurate estimates of completeness, Murray et al. [20] emphasize that these results should not be interpreted without caution as the uncertainty around them is likely to be at least 20% of the estimated level. These optimal DDM versions have

been used in adjusting specific country VR for the Global Burden of Disease (GBD) studies [21] and more details are provided about them in subsection 2.2.2 that describes mortality estimation in the GBD.

2.2.1.2 Birth history methods for child mortality

The South African census includes a summary birth history (SBH) module which provides the data the NBD has used to estimate completeness of child mortality in the VR. In SBH, mothers are asked a key question - the number of children they have given birth to versus the number of them that have died by the time of survey. As there is no additional information on age or timing of death, an indirect demographic method must be used to estimate child mortality. Over the next section, the standard indirect method originally developed by Brass [8] is described. The NBD applied this method with some adjustments to account for the violation of assumptions due to the impact of HIV on the mortality pattern of the country. This adjustment is described as well.

Standard approach using SBH data

The method requires information on the numbers of women $W(i)$ in five-year age groups i aged 15-49 obtained from census/survey, the numbers of children ever born to them by age of mother, and the numbers of child survivors to the time of the census/survey. If we denote the number of children ever born to the women in age group i by $CEB(i)$ and those children who died by $CD(i)$, this gives the proportion of children dead $D(i) = \frac{CD(i)}{CEB(i)}$. The proportions dead are converted into ${}_zq_0$ which denote the probability of dying between birth and age z according to the equation,

$$ {}_zq_0 = k(i)D(i) $$

where $k(i)$ are correction factors corresponding to age i and are related to the patterns of fertility. Trussell [22] derived a robust set of these correction factors, making use of

parities P_1, P_2 and P_3 for women aged 15-19, 20-24 and 25-29, respectively, such that:

$$k(i) = a(i) + b(i)\frac{P_1}{P_2} + c(i)\frac{P_2}{P_3} \tag{2.26}$$

where the $a(i)$, $b(i)$ and $c(i)$ were calculated by Trussell [22] using regression and simulation for each Princeton model life table . The underlying assumptions behind this model are that (1) the fertility patterns for the population have not changed in the recent 15 years (2) the chosen model life table and population are the same (3) child mortality risk is independent of the age of the mother, and (4) the coverage of reporting of the children ever born is independent of the age of mother. The estimates generated using this method are mapped to specific time-points in the recent past derived using a similar approach to equation 2.26 but with different multipliers.

The method links the age distribution of the mothers to the timing of deaths to generate a time trend of mortality estimates. One weakness resulting from this is that the method should not be used to estimate child mortality within 3-6 years of the census/survey as that timing would be biased towards the mortality experience of the youngest mothers. For this age-group of women, the estimate is based on smaller numbers of them who have given birth and as such is prone to sampling bias [23], and will typically be higher than average as many of them are first time mothers with pregnancies at high risk [24].

Ward and Zaba adjustment for HIV mortality

Certain base assumptions for the CEB/CD method are violated under a high HIV mortality pattern such as that resultant from South Africa's generalized epidemic. In this setting, HIV prevalence, transmission rates and consequently child mortality risk, are dependent on the age of the mother. The age pattern of mortality is selective for the duration of infection which results in higher mortality risk associated with increasing age. When sampling from such a population there is potential of surveys missing the births and/or

deaths of children born to women who have died due to HIV with this bias being related to age. There is potential underestimation of mortality rates due to the increased mortality of HIV infected women and their children [25].

Ward and Zaba [9] simulated a stable population model in an HIV population and used it to assess the extent of biases in the estimates produced by the CEB/CD technique - deriving correction factors in the process. For a simulated population with a known HIV/AIDS prevalence and a known true level of child mortality ${}_zq_0$, data for an SBH module based on a simulated survey was also generated. The CEB/CD was then used to estimate the child mortality estimates according to the simulated survey, represented by ${}_zq_0^*$. Using the true child mortality ${}_zq_0$, the estimated child mortality ${}_zq_0^*$ and the known levels for prevalence, Ward and Zaba derived some correction factors using the OLS regression model:

$$ {}_zq_0 - {}_z\,q_0^* = \alpha(PREV) + \beta(PREV^2) + \gamma(PREV15) + \epsilon $$

where $\epsilon \sim N(0, \sigma^2)$, $PREV$ is the prevalence at the time of the survey for women of childbearing age, expressed as a proportion, $PREV15$ is the prevalence in women aged 15-19 years (set to 0 if unknown) and α, β and γ are regression coefficients. For any given estimates of child mortality based on the CEB/CD method and corresponding prevalence, these coefficients can be used to be estimate the adjusted for HIV/AIDS "true" estimate. This correction assumes a stable population with stable HIV prevalence [26].

2.2.2 Statistical and demographic models

Model based approaches have played an important role in providing South Africa mortality levels and trends, particularly to help guide policy priorities related to child survival and HIV treatment. For instance, the Spectrum model, designed to examine the impact of HIV interventions on health outcomes [27, 28], together with the Estimation and Projection Package (EPP) module for estimating HIV incidence based on antenatal prevalence [29],

has been used to estimate mortality for South Africa [30, 31]. The Spectrum/EPP suite can be calibrated to run at the provincial level but requires as an input the HIV-free mortality in order to generate estimates of all-cause mortality, HIV incidence and AIDS mortality.

The Actuarial Society of South Africa's (ASSA) models have also been widely used to estimate all-cause and AIDS deaths nationally and provincially using a cohort component projection approach linked to assumptions about HIV free mortality and HIV infected transmission and survival [5]. The THEMBISA model developed by the Centre for Infectious Disease Epidemiology and Research at the University of Cape Town (UCT) is a demographic and epidemiological model that has been used to simulate paediatric HIV transmission and survival and concurrently estimate child mortality by province [32].

The United Nations Population Division (UNPOP) in its production of national estimates of mortality by country, generates mortality estimates for South Africa [33]. Although complete VR is the gold standard, in the absence of reliable VR, UNPOP child mortality estimates are derived from direct or indirect questions in surveys or censuses. Estimates of child mortality for the 2017 revision are based on collaboration with the UNICEF led United Nations Inter-agency Group for Mortality Estimation (UN-IGME) which uses a statistical model to predict child mortality [34]. UNPOP adult mortality estimates are also derived based on the available data. For countries with complete death registration, estimates are derived using the reported deaths by age and sex. In the case of incomplete registration; estimates are derived from questions on household deaths by age and sex, usually for a 12-month period before a census or survey; or from questions on the survival of the siblings of respondents in demographic surveys. In other cases, where available data on adult mortality are too sparse or inconsistent, life expectancy at birth is derived by using recent information about infant and child mortality together with model life tables. Furthermore, in countries with high levels of HIV prevalence, the demographic impact of the AIDS epidemic is accounted for using the Spectrum/EPP model [28].

The estimation methods vary across these different models with national all-cause mortality estimates comparable for adult mortality but varying widely for child mortality [35]. These modelling approaches do not produce district level estimates.

The Global Burden of Disease (GBD) Study uses a statistical modelling approach that makes use of a wide range of data sources including country-specific VR, survey and census data as well as regional and global data to estimate burden of disease. Estimating South Africa all-cause mortality was done by age, sex and province for GBD2015 [21], GBD2016 [36] and most recently GBD2017 [1]. These most recent iterations of the GBD built on the methodologies of GBD2010 [37] and GBD2013 [38] and with each iteration new data were added and methodologies were refined. Separate approaches were used to estimate child and adult mortality:

2.2.2.1 Estimating child mortality in the GBD

For South Africa, the GBD makes use of the same census, community survey and VR data used by the NBD. However, the study adjusts the biased VR and does not use the standard indirect method for analysing summary birth histories i.e. Brass's CEB/CD approach but rather improved methods developed and validated by Rajaratnam et al. [39]. An overview of the GBD child mortality estimation approach is provided below.

Estimates from summary birth history data

Rajaratnam et al. [39] point out three limitations to the standard indirect method that motivated their research. Firstly, the overestimation of child mortality for the most recent time period, a consequence of the higher risk profile of the youngest mothers, leads to the corresponding estimates being routinely discarded. Secondly, the standard method does not generate estimates of uncertainty in child mortality measures which limits their utility for accurately quantifying changes over time. Thirdly, the method has not been validated against VR or complete birth histories in a wide set of countries.

Rajaratnam et al. [39] used a large number of DHS complete birth history (CBH) datasets to extract observed mortality with child-level data on date of birth, survival status and age at death. Likewise, they extracted corresponding CEB/CD numbers by age of mother from summary birth history data (SBH). They used these data to develop four new child mortality estimation methods - the maternal-age-cohort (MAC), the maternal-age-period (MAP), the time-since-first-birth-cohort (TFBC) and time-since-first-birth-period (TFBP) derived methods:

- Maternal-Age-Cohort Derived Method (MAC): In the standard indirect method previously described (equation 2.26), $D_i = \frac{CD_i}{CEB_i}$ gives the proportion of children dead to mothers aged i. k_i correction factors related to parities P_1, P_2 and P_3 for women aged 15-19, 20-24 and 25-29, respectively, are estimated according to the relationship:

$$k_i = a_i + b_i \frac{P_1}{P_2} + c_i \frac{P_2}{P_3}$$

and used to convert the D_i into death probabilities according to the equation,

$$q_z = k_i D_i.$$

The q_z for $z \in [1:4]$ are mapped to $q_5 = {}_5q_0$ using model life tables. The MAC approach builds on this to predict reference times ($\hat{RT}$) and child mortality estimates (${}_5\hat{q}_0$) for each i using regression coefficients denoted by $\hat{\beta}_{.i}$ and estimated by Rajaratnam et al. [39] using the SBH and CBH data i.e.

$$\hat{RT}_i = \hat{\beta}_{0i} + \hat{\beta}_{1i} D_i + \hat{\beta}_{2i} CEB_i + \hat{\beta}_{3i} \frac{P_1}{P_2} + \hat{\beta}_{4i} \frac{P_2}{P_3}$$

$$\text{logit}\,({}_5\hat{q}_0)_i = \hat{\beta}_{0i} + \hat{U}_{ij} + \hat{\beta}_{1i} \text{logit}\,(D_i) + \hat{\beta}_{2i} CEB_i + \hat{\beta}_{3i} \frac{P_1}{P_2} + \hat{\beta}_{4i} \frac{P_2}{P_3}$$

where $\hat{U}_{ij}$ are age- and country-level random effects. The $\hat{\beta}_{.i}$ relate to the ${}_5q_0$ directly and so there is no need to use model life tables.

To improve estimation, the GBD version of this SBH method also includes region-level random effects and fits separate models for surveys that interview all women as compared to just ever-married women.

- Time since First Birth Cohort derived Method (TFBC) : The TFBC approach uses the same equations as the MAC but instead of i representing aggregation according to the mothers' age-group, aggregation is according to the time since first birth - a question included in some surveys such as the MICS-3.

- Maternal Age Period-Derived Method (MAP): The MAP approach estimates a CD/CEB ratio for each year prior to the survey by estimating the time distribution of births and deaths for mothers of a given age who have had a specific number of children. This allows for the derivation of the most recent estimates of under-five mortality using the experiences of all mothers rather than just the youngest as would be the case with the standard indirect approach.

  Although the MAC also corrects this, it is still vulnerable to the smaller sample size observed for the youngest cohort, something the MAP accounts for. Parameters $\hat{\beta}_{.t}$ were derived for each period t and are used to predict child mortality according to the equation

$$\text{logit}\left({}_5\hat{q}_0\right)_t = \hat{\beta}_{0t} + \hat{U}_{tj} + \hat{\beta}_{1t}\text{logit}\left(D_t\right)$$

- Time since First Birth Period derived Method (TFBP): As with the connection between the TFBC and MAC approaches, the TFBP approach uses the same equations as the MAP but instead of pooling estimates across age groups, estimates are pooled according to the time since first birth.

Estimates from VR data

Estimates of child mortality are also derived using bias-adjusted VR data. A Loess regression is applied to the non-VR ${}_5q_0$ estimates generated using the demographic techniques described above and this gives a set of estimates by year. The bias is estimated as the mean of the difference between the Loess predicted and the VR derived $\log_{10}({}_5q_0)$ summarized over the five-year period adjacent to the VR year. The VR estimates of ${}_5q_0$ are the corrected using the bias correction as shown in the equation:

$$ {}_5q_0^{corr.} = {}_5 q_0^{obs.} \times 10^{\hat{bias}} $$

where ${}_5q_0^{corr.}$ is the corrected estimate of ${}_5q_0$, ${}_5q_0^{obs.}$ is the ${}_5q_0$ estimate observed in VR and $10^{\hat{bias}}$ is the bias estimate described above.

Estimates of child mortality are thus derived using these improved demographic methods on the empirical data reported from censuses as well as from the adjusted VR. This estimation process results in numerous estimates by year which need to be summarized or "synthesized" for reporting, this is performed via a three stage process.

The first stage involves running hierarchical models to improve the estimates by making use of their association with lagged distributed income per person, maternal education and the under-5 HIV/AIDS death rate. In the second stage, the difference between the hierarchical model input and predicted estimates, are smoothed using spatio-temporal regression. In the third stage, the results from this smoothing of the residuals are used as priors in a Gaussian process regression (GPR). The GPR produces national and provincial child mortality estimates with 95% uncertainty intervals. However it does not produce estimates at the South Africa district level.

2.2.2.2 Estimating adult mortality in the GBD

As with the child mortality estimation, the GBD uses the same census, survey and VR data as used for the NBD but with a different strategy for correcting bias. As mentioned in the DDM review, optimal versions of DDMs are used to assess the completeness of VR [20]. A summary estimate of completeness is estimated using the median of the SEG with a 55-80 age-trim, the GGB with a 40-70 age-trim and the GGB+SEG with a 50-70 age-trim. Synthesis of the completeness estimates is a two stage process. The first stage predicts completeness based on the following mixed effects model:

$$\log_{10}\left(c_{i,s,t}^{adult}\right) = \alpha + \beta_1 \log_{10}\left(c_{i,s,t}^{child}\right) + \gamma_1^{SR} + \gamma_2^{SR}\log_{10}\left(c_{i,s,t}^{child}\right) + \gamma_1^{R} + \gamma_2^{R}\log_{10}\left(c_{i,s,t}^{child}\right) + \eta_{i,s} + \varepsilon_{i,s,t}$$

where for country i, source s, at time t, $\log_{10}\left(c_{i,s,t}^{adult}\right)$ is completeness of adult deaths registration, $\log_{10}\left(c_{i,s,t}^{child}\right)$ is completeness of child deaths registration, γ are random effects at the region R and super-region SR level, $\eta_{i,s}$ is a random effect at the country and child completeness source level, and $\varepsilon_{i,s,t}$ is an error term.

Second stage predictions are derived by calculating and then smoothing residuals before being added them back onto the first stage predictions. The variance in the distribution of completeness is estimated using the mean absolute deviation (MAD) of the completeness from stage 2 relative to stage 1. For South Africa, the completeness estimates are then applied to adjust the VR.

Once VR data are corrected, they are used to derive time-series of sex specific mortality rates for the broad 15 to 60 age-group (${}_{45}m_{15}$). Final estimates of ${}_{45}q_{15}$ are derived from the mortality estimates through a four stage process similar to that for children. In the first stage, mortality rates are modelled using a sex-specific non-linear mixed effects model with fixed effects for the log of lag distributed income (LDI), mean years of education in

age group 15 to 59 (Edu), crude death rate due to HIV/AIDS in age group 15 to 59 (HIV)[1] and a country level random effect(γ):

$$_{45}m_{15} = \exp(\beta_1 + \beta_2 Edu + \beta_3 \ln(LDI) + \gamma) + \beta_4 HIV + \varepsilon$$

In the second stage, residuals are calculated and then added back to the first stage predictions and the resultant estimates converted to probabilities. In the third stage, GPR is used to synthesize the probabilities providing estimates of underlying mortality. In the fourth stage, mortality shocks are added to produce a final time-series of $_{45}m_{15}$ estimates.

2.2.2.3 Empirical model life table system

The GBD also uses a database of over 16,000 empirical life tables for a model life table system that can be used to map the base probabilities $_5q_0$ and $_{45}q_{15}$ to age-specific estimates. Over 95% of these life tables are obtained from either the Human Mortality Database [41] or from VR data that have been evaluated and corrected using optimal death distribution methods [20, 42]. The observed base probabilities are related to the standard and used to estimate age-specific zero-AIDS mortality rates according to the equation:

$$_nQ_x^c = {}_n Q_x^s + \beta_x^1 ({}_5Q_0^c - {}_5 Q_0^s) + \beta_x^2 ({}_{45}Q_{15}^c - {}_{45} Q_{15}^s) + \varepsilon_x$$

where $_nQ_x^i = \text{logit}(_nq_x)$ for the standard $i = s$ or the zero-AIDS counter-factual $i = c$. The standard is calculated by first taking the empirical life tables with base probability values closest to the counter-factual based on the Mahalanobis distance. Next, these are summarized to a weighted average using empirical weights. After these counter-factual $_nQ_x$ have been derived, age-specific excess mortality due to HIV is added to the corresponding the death rate in the age interval x to $x+n$, denoted $_nM_x$, depending on whether or not the type of HIV epidemic is concentrated or generalized.

---

[1] HIV/AIDS estimates generated using versions of EPP and Spectrum developed for the GBD [40]

HIV/AIDS excess mortality is estimated relative to the 40 – 44 age-group, denoted ${}_nM_x^{HIV}$, and modelled in a Seemingly Unrelated Regression (SUR) to derive constants α_x and residuals ε_x. These are sampled from the variance and covariance matrix to get the mean and 95% uncertainty intervals of estimated relative risks by sex, age and types of epidemic. Once HIV mortality is added onto the counter-factual, a time-series of all-cause mortality estimates is generated. For South Africa, these estimates are by province, age, sex and year.

2.3 District all-cause mortality estimation

In this section, the methods used to estimate district-level all-cause mortality numbers, rates and demographic measures by sex, age and year are described. Figure 2.1 is a map South Africa's districts, colour-coded by province, to use as a visual geographic reference.

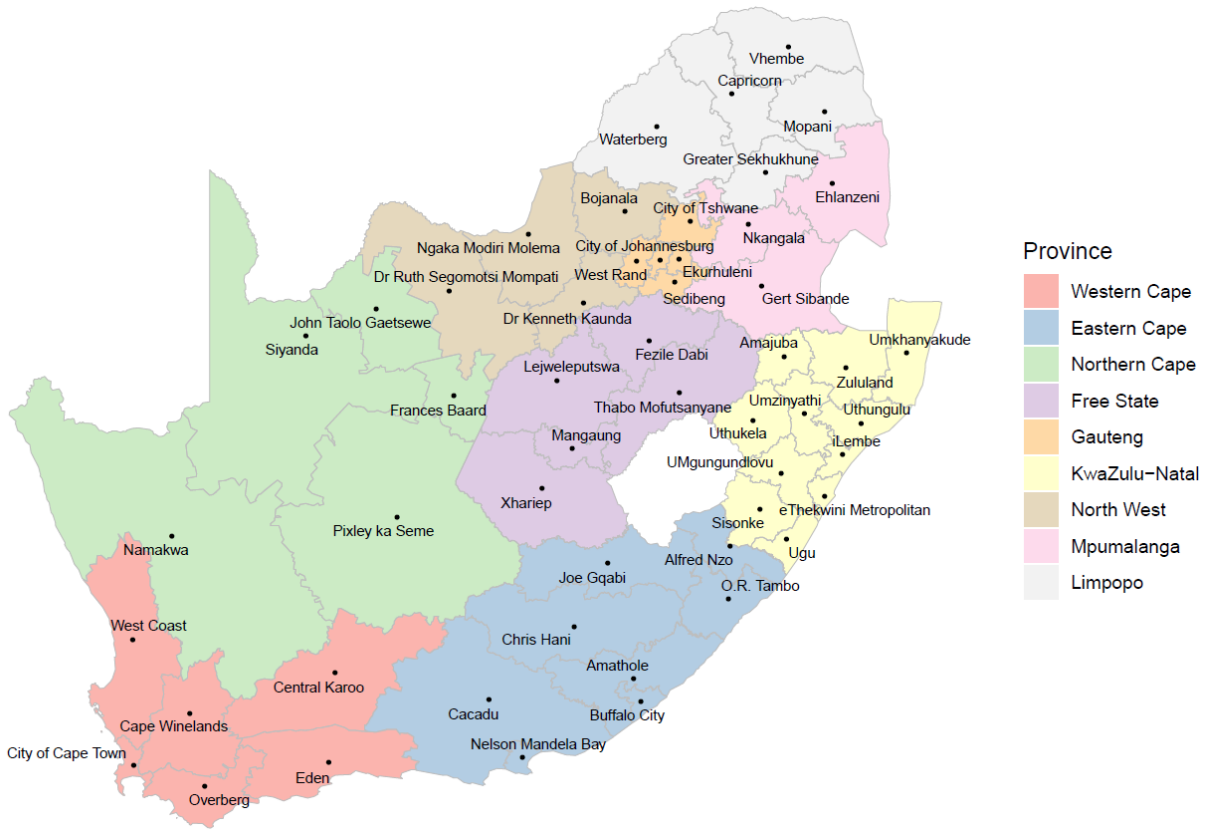

Figure 2.1: Map of South Africa's 52 health districts and 9 provinces

2.3.1 Methods

Assuming grouping by sex, the true complete deaths are by age $i = \{0, 1, \ldots, 95\}$, year $t \in \{1997 \ldots 2015\}$, district $d \in \{1 \ldots 52\}$ in province $p \in \{1 \ldots 9\}$ and can be represented by $D_{d,p,i,t}$. For each year t, the $D_{d,p,i}$ have corresponding rate schedules, $\mu_{d,p,i} = \frac{D_{d,p,i}}{N_{d,p,i}}$ where $N_{d,p,i}$ are the district d, province p numbers in the population aged i, and $\lambda_{d,p,i} = log(\mu_{d,p,i})$. Using a TOPALS (tool for projecting age-specific rates using linear splines) approach [43, 44, 45], to reduce the influence of erratic age patterns on our estimation, we consider a smoothed age pattern $\hat{\lambda}_{d,p,i}$ which is the sum of a province specific standard log-mortality $\lambda_p \in \mathbb{R}^{96}$ and district-specific deviations from this standard i.e.

$$\underset{96\times1}{\hat{\lambda}_{d,p}} = \underset{96\times1}{\lambda_p} + (\underset{96\times9}{B} \times \underset{9\times1}{\alpha_d})$$

In this relation, B is a cubic B-spline basis matrix for $K = 9$ knots at ages $i_0, \ldots, i_8 = (0, 1, 5, 10, 15, 25, 35, 55, 75)$ selected at potential turning points in the log-mortality rate. The α_d offsets quantify the deviation of a specific districts mortality pattern from that given by the standard. The mortality rate schedule for each district d in province p has:

$$\mu_{d,p} = \exp(\lambda_p + B\alpha_d) = \exp(\hat{\lambda}_{d,p})$$

resulting in age-specific death numbers:

$$D_{d,p,i} \sim Poisson(N_{d,p,i}, \mu_{d,p,i})$$

For $R_{d,p,i} \leq D_{d,p,i}$, reported deaths are assumed to follow a binomial distribution with age-specific parameters given by $D_{d,p,i}$ and $\pi_{d,p,i}$ where $\pi_{d,p,i}$ represents the completeness of death reporting for age i,

$$R_{d,p,i} \sim Binom(D_{d,p,i}, \pi_{d,p,i})$$

Schmertmann and Gonzaga [45] show that since the joint distribution $P(R, D)$ for each combination of d,p and i is the product of these two distributions, integrating out the marginal distribution of the unreported deaths $D - R$, enables us to determine the distribution of the reported deaths R which is also Poisson,

$$R_{d,p,i} \sim Poisson(N_{d,p,i}\mu_{d,p,i}\pi_{d,p,i})$$

This result can be generalised to accommodate the $R \geq D$ scenarios which arise due to a non-correspondence between reported place of death in VR and reported normal place of residence in census, as well as uncertainty in the number of people in the population when census are used for DDMs. For $R \geq D$, we define

$$U_{d,p,i} = R_{d,p,i} - D_{d,p,i} \sim Poisson(\delta_{d,p,i})$$

where $\delta_{d,p,i}$ is an unknown mean parameter for the difference between reported and true deaths. Defining $\pi = \frac{N\mu+\delta}{N\mu}$ gives us a similarly defined distribution as in the $R \leq D$ scenario i.e. $R \sim Poisson(N\mu\pi)$ for $\pi > 0$ such that π is not restricted to $0 \leq \pi \leq 1$. Within the Bayesian framework, we can use what prior beliefs we may have about α_d and $\pi_{d,p,i}$ to determine a posterior distribution for these parameters using this likelihood. For district d and year t, weakly informative priors are assumed for the offsets, with constraints assumed for them at adjacent knots and adjacent years i.e.

$$\begin{aligned} \alpha_{d,t} &\sim N(0, 4) \\ \alpha_{d,t}[2:K] - \alpha_{d,t}[1:(K-1)] &\sim N(0, \frac{1}{\sqrt{2}}) \\ \alpha_{d,t} - \alpha_{d,t-1} &\sim N(0, \frac{1}{\sqrt{2}}) \end{aligned}$$

used to borrow information across age-groups and over time based on the assumption that α_d values close to each other in distance are close to each other in magnitude.

Province and district coverage for the age-groups 0 and 1-4 are estimable using the ratio of the deaths in these age-groups according to vital registration versus the numbers of deaths in the same age-groups according to the high resolution study by Golding et al. [46]. Golding et al. [46] used the updated Brass-type techniques introduced by the GBD within a Bayesian geostatistical analytical framework to generate high-resolution estimates of under-5 and neonatal all-cause mortality across 46 countries in Africa, including the provinces and districts of South Africa, for the period 2000 to 2015. For the completeness of reporting of the deaths in the adult age-groups 15 and older, estimates of coverage are determined by comparing the age-sex-year-province specific VR numbers to the draws from GBD2017.

To determine district specific completeness of reporting, we assume five distinct age-groups $j \in 0, 1, 2, 3, 4$ for which district coverage is to be estimated, mapping our i indexing to j we now have $\pi_{d,p,j}$ where:

$$j = \begin{cases} 0 & \text{if } i = 0 \\ 1 & \text{if } i \in \{1 \dots 4\} \\ 2 & \text{if } i \in \{5 \dots 14\} \\ 3 & \text{if } i \in \{15 \dots 74\} \\ 4 & \text{if } i \in \{75+\} \end{cases}$$

As described above, $\pi_{d,p,0}$ and $\pi_{d,p,1}$ which represent the vital registration coverage estimates for the two youngest age-groups for district d in province p, can be estimated using the ratios of child mortality levels according to the VR and child mortality levels according to the local burden of disease (LBD) study by Golding et al. [46]:

$$\pi_{d,p,0} = \frac{{}_1q_{0,d,p}^{VR}}{{}_1q_{0,d,p}^{LBD}}$$

For all children under-5 we have:

$$\pi_{d,p,U5} = \frac{{}_5q_{0,d,p}^{VR}}{{}_5q_{0,d,p}^{LBD}}$$

We can solve for completeness of reporting for children aged 1–4 using:

$$\frac{R_{d,p,U5}}{\pi_{d,p,U5}} = \frac{R_{d,p,1}}{\pi_{d,p,1}} + \frac{R_{d,p,0}}{\pi_{d,p,0}}$$

The district coverage estimates for those aged 15 and older, represented by $\pi_{d,p,3}$, are estimated using the corresponding provincial completeness $\pi_{p,3}$ and the ratio of district to province for the child-mortality completeness estimates. The key assumption in determining adult completeness is that the ratio of district to province completeness for the adults follows a distribution related to the child completeness ratio. This ratio, represented by $\gamma_{d,p}$, is calculated:

$$\gamma_{d,p} = \frac{\pi_{d,p,U5}}{\pi_{p,U5}}$$

The $\gamma_{d,p}$ are estimated for all district-province-year combinations and the standard deviation calculated τ_γ across the estimated values. According to these assumptions, for age-groups $j \in (0,1)$ prior distributions for child completeness are based on the LBD study estimates and sampled as Gaussian i.e.

$$\hat{\pi}_{d,p,j,t} \sim N(\pi_{d,p,j,t}, \sigma_{\pi_{j,t}})$$

where $\sigma_{\pi_{j,t}}$ are the age-specific and year-specific standard deviations of the completeness estimates determined empirically using the age j distribution of completeness across all years and districts. For $j \in (3,4)$:

$$\hat{\pi}_{d,p,j,t} \sim N(\hat{\gamma}_{d,p,t}\pi_{p,j,t}, \sigma_{\pi_{j,t}}) \text{ where } \hat{\gamma}_{d,p,t} \sim N(\gamma_{d,p,t}, \tau_{\gamma})$$

Finally, for the age group $5-14$, estimated completeness $\hat{\pi}_{d,p,2}$ is assumed to be approximated by the average of the coverage in the two adjacent age-groups i.e. $\hat{\pi}_{d,p,1}$ and $\hat{\pi}_{d,p,3}$. Its is also assumed that on average, male and female completeness will similar with differences that can be modelled as Gaussian i.e.

$$\pi^{MALE}_{d,p,j} - \pi^{FEM}_{d,p,j} \sim N(0,1)$$

Sampling over all the prior possibilities using an MCMC approach allows us to sample the most likely estimates of α_d and $\pi_{d,p}$ that fit the observed death data conditional on the age-specific population numbers. This allows us to obtain posterior distributions for them to use in estimating true deaths.

To minimize the effect of the absence of identifiability inherent in this approach, certain constraints are imposed on the sampling. True national and provincial deaths are assumed known appriori from GBD2017 and can be represented using D_T and D_p, respectively. The values for α for the national and provincial predictions are chosen under the constraints:

$$D_T = N_T e^{\hat{\lambda}_T} \text{ and } D_p = N_p e^{\hat{\lambda}_p}$$

The true district deaths are constrained to sum to predicted true province i.e.

$$N_p e^{\hat{\lambda}_p} = \sum_d N_{d,p} e^{\hat{\lambda}_{d,p}}$$

Constraints are implemented by assuming $N(0,1)$ priors on the differences between the known true national and provincial deaths and estimated national and provincial deaths, respectively, as well as estimated district sum to province deaths.

Figure 2.2 summarizes the data and assumptions underlying the integrated coverage and mortality statistical model used in this research.

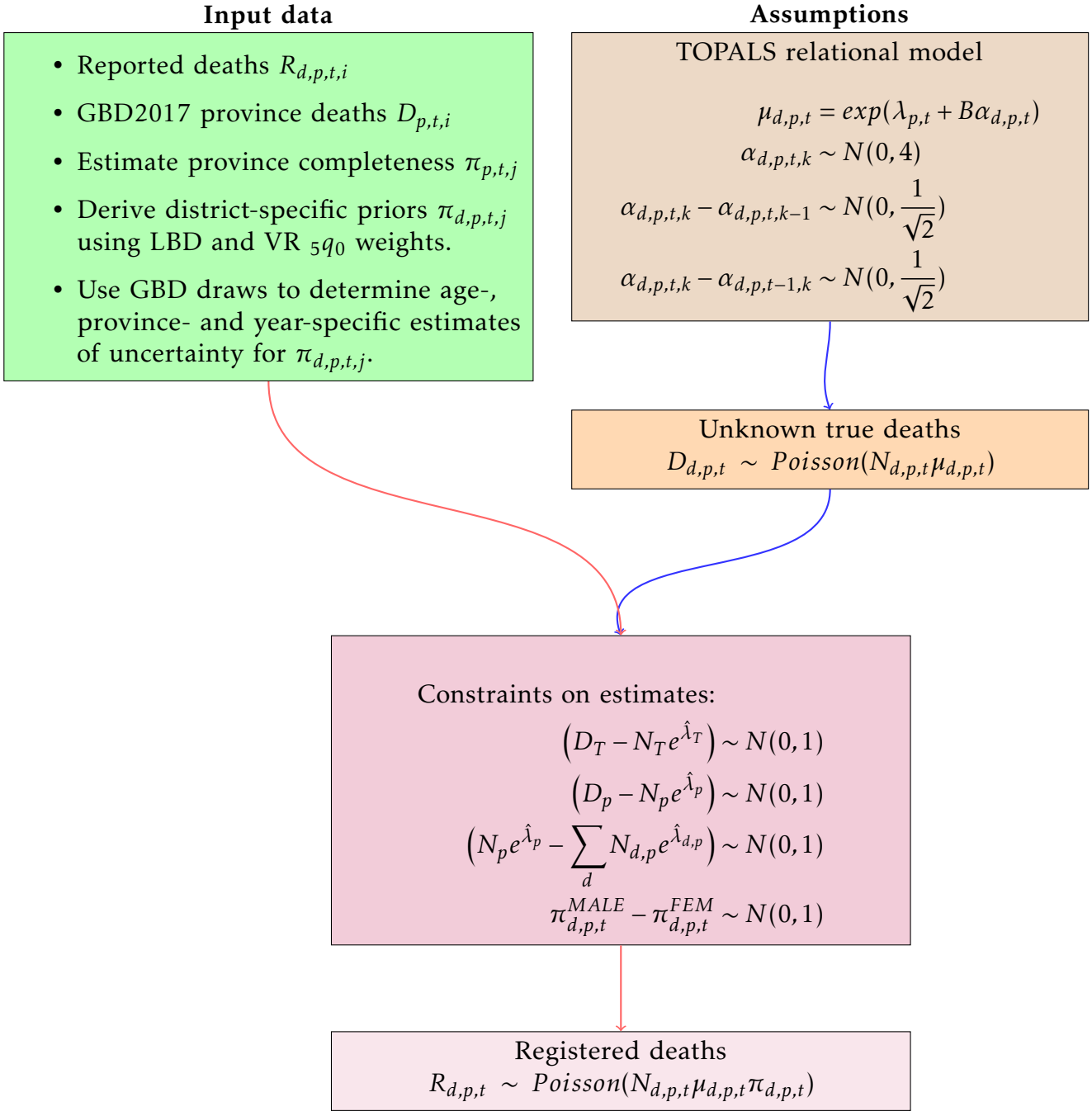

Figure 2.2: Integrated coverage and mortality model

2.3.2 Results

In this section, the results generated by the regression model described above are summarised. More detailed results are available in the accompanying appendix.

2.3.2.1 Estimated deaths

Over the 1997–2015 period, a total of 11.9 million deaths are estimated for South Africa (11.4–12.4) with 421 thousand of them estimated for 1997 (409–435), peaking at 747 thousand in 2006 (711–787) and falling to 522 thousand deaths in 2015 (504–544). The estimates are evenly split between males and females with 5.9 million deaths attributed to males (5.6–6.1 or 48.5%–50.3%). KwaZulu Natal province accounts for the largest number with an estimated 2.82 million total deaths (2.53–3.19), starting from a minimum of 98 thousand in 1997 (90–109), peaking at 185 thousand in 2006 (164–210) and falling to 102 thousand deaths in 2015 (93–116).

The numbers of deaths estimated for each health district vary widely depending on the population and geographic sizes of the district, if it is metropolitan and the province in which the district lies. The highest number of deaths are attributed to eThekwini Metropolitan district in KwaZulu Natal experiencing 884.7 thousand deaths between 1997 and 2015 (778.2–1016.8), approximately 7% of all of the deaths in the country. Unsurprisingly, the highest numbers of deaths are estimated for the most populous districts which are all metropolitan. From Gauteng are Johannesburg (673–849 thousand), Ekurhuleni (525–672 thousand) and the City of Tshwane (475–588 thousand) and from the Western Cape is the City of Cape Town (535–566 thousand). These metros are the leading districts in terms of total deaths and together account for approximately 30% of all of the deaths estimated for the country between 1997 and 2015. The five districts with the fewest deaths over the same period are found in the Northern Cape (Pixley ka Seme 49.0–52.6, John Taolo Gaetsewe 43.2–46.6, Namakwa 27.8–29.6) and also in the Western Cape (Overberg 37.5–39.9, Central Karoo 15.0–16.2) - for deaths in thousands.

Mortality rates allow for a more nuanced comparison than the numbers of deaths alone as they also consider the number of people exposed to mortality risks. Within each district we consider the general sex- and age-specific mortality rate trends. Figure 2.3 is derived from the ratios of deaths to population numbers by sex and year, and for select broad age-groups. It illustrates how often the minimum and maximum mortality rates for each district occur in each year for the selected sex and age-group.

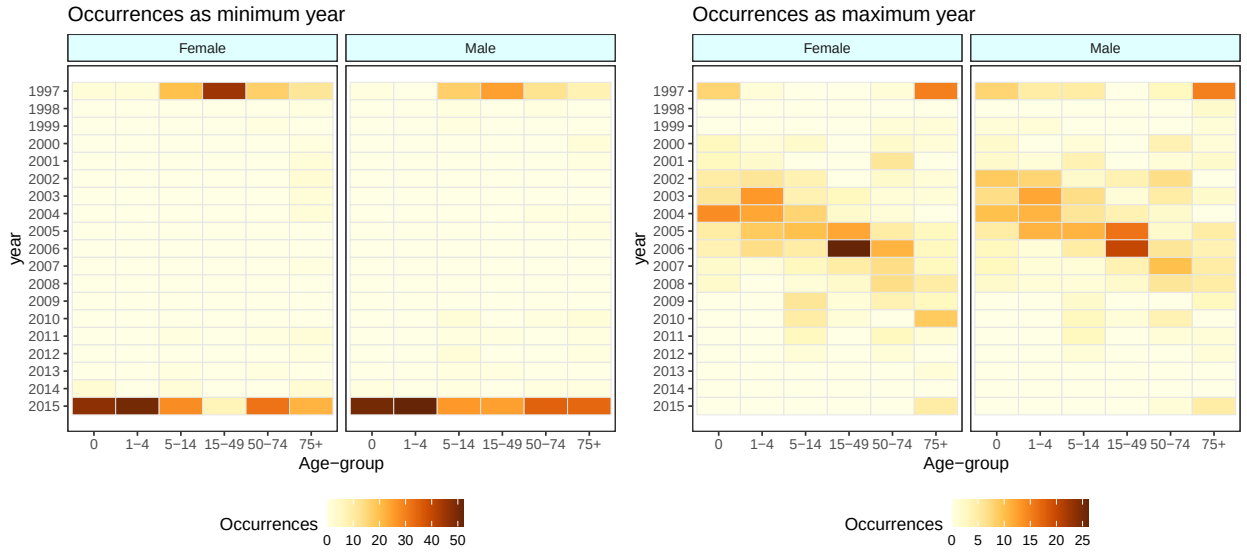

Figure 2.3: Occurrences as minimum/maximum year for age-specific mortality rates

We observe that for both males and females in the youngest age-groups, all districts had their minimum rates falling in the most recent year, 2015. For children aged 5-14 years as well as the older adults with ages above 50, the majority of districts had the minimum year also occurring in 2015, albeit there are a significant number in 1997. For ages 15-49, the minimum year in the majority of the districts is 1997 for females. There is a more even split for males between 1997 and 2015. This is in contrast to the years in which the maximum rates occur. Although there are some in the youngest and oldest age groups with 1997 as the year with most occurrences, the maximum is more widely spread for the two extreme age-groups as well as the age-groups 5-14 and 50-74. The maximum is

concentrated between years 2003 and 2005 for ages 1-4 and more emphatically so between years 2005 and 2006 for the age 15-49.

The time-series of each district-, sex- and age-specific mortality rate is shown in the appendix. From the age-specific rates, it is clear that apart from the very oldest age-groups, in general mortality peaked in the mid-2000s and has been falling since to minimums in 2015. Beyond this we would like to assess how the rates compare across the country as well as over time. There are sex-specific, spatial and temporal differences in the age compositions of the districts which can be accounted for in comparisons by estimating age standardized death rates (ASDR) [47]. Figure 2.4 shows the estimated ASDR by district (grouped by province), comparing females to males and for selected years: 1997 the beginning of the time-series, 2006 the peak of total deaths and 2015, the end of the series.

Firstly, we note that for almost all districts and years, the ASDR for males are higher than those for females. There are wide variations across the districts with the City of Cape Town, Overberg and Eden in the Western Cape and Waterberg district in Limpopo having the lowest ASDR in 1997. The highest ASDR for many of the districts are in 2006 where for some districts in the Eastern Cape, Free State, KwaZulu Natal and Mpumalanga, ASDR are double the 1997 levels with larger increases for females than males. There are also large increases for districts in the Northern Cape, North West and Gauteng between 1997 and 2006 but not as pronounced. The districts in the Western Cape and Limpopo province exhibit the smallest changes over the period. By 2015, many districts have reached or gone lower than their 1997 ASDR levels, although the reduction is larger in females than males. In 2015, the City of Cape Town remains the district with the lowest ASDR. It is important to note the significant mortality reductions in the previously extremely high mortality districts, particularly in Mpumalanga and KwaZulu Natal.

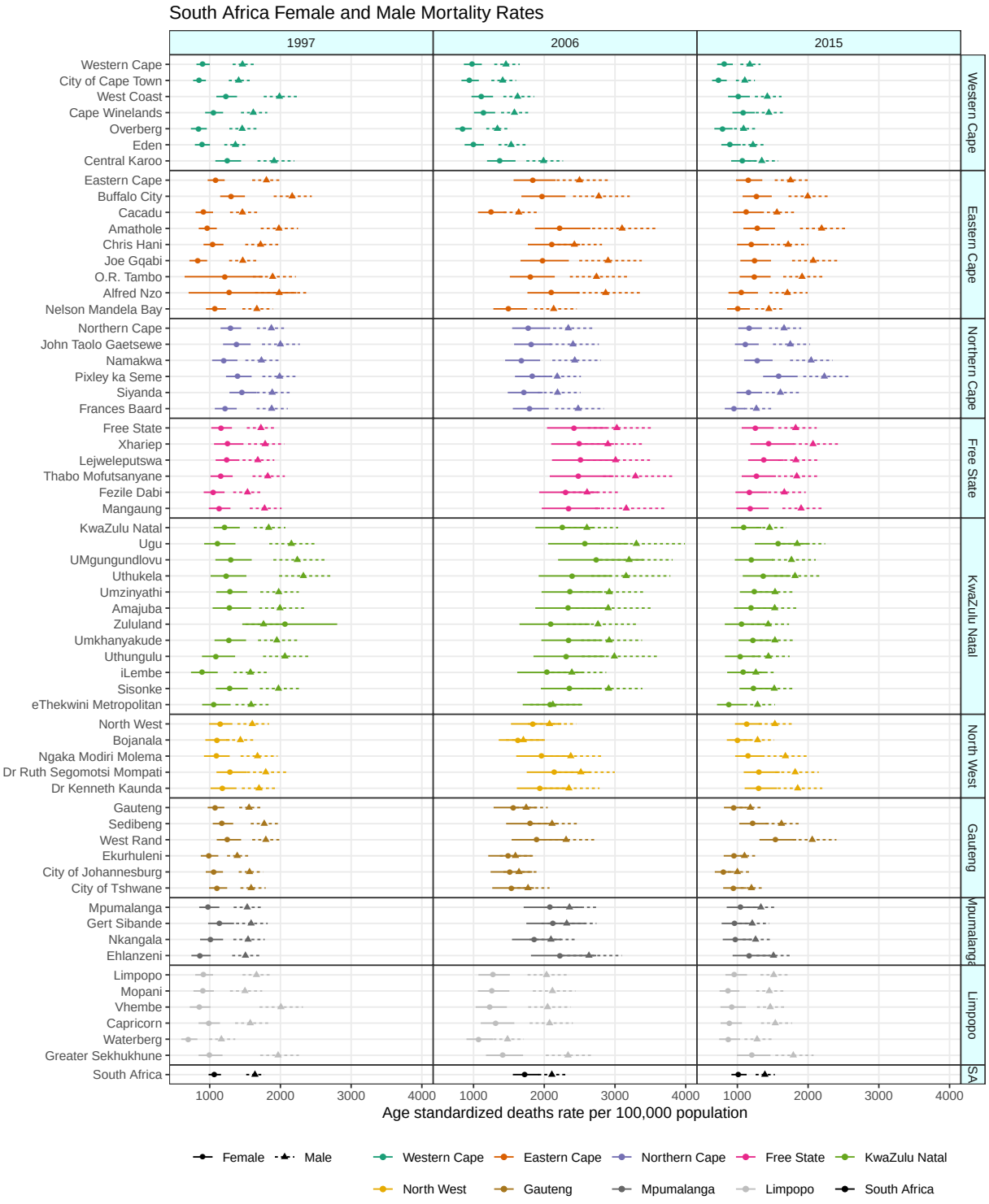

Figure 2.4: South Africa age standardized death rates by district, sex and year

2.3.2.2 Summary demographic measures

As with ASDR, there are several demographic measures that can be calculated to summarize the mortality information contained in the results. Figures 2.5 to 2.8 are plots of the estimated life-expectancy at birth (e_0) and selected probabilities of death between ages x and $x+n$, represented by ${}_nq_x$. Probabilities are derived for infants (${}_1q_0$), children (${}_5q_0$) and adults (${}_{45}q_{15}$) using abridged life tables, and calculated by draw, district, sex and year.

In 1997, female and male life-expectancy at birth had respective mean values of 64.9 years (63.3–66.3) and 57.3 years (55.7–58.8). On average, these initially fell by 1.27 years per year for females and 0.68 years per year for males to reach minimums in 2006 of 53.5 and 51.2, for females and males respectively (51–55.8 and 49.1–53.2). Since 2006, life-expectancy has been steadily increasing by an average of 1.43 per year for females and 1.13 for males to reach 2015 levels of 66.4 years (64.3–68.2) for females and 61.4 years for males (59.7–63.2).

In general, estimated life-expectancy has remained highest in the Western Cape and Limpopo provinces, although other provinces are reaching comparable life-expectancy levels in the most recent years. As with ASDR, Eastern Cape, Free State, KwaZulu Natal and Mpumalanga have the largest falls in life-expectancy between 1997 and 2006, but the same provinces also have the largest gains thereafter. For each sex, the districts with the highest and lowest life expectancies at birth are found and the years in which these levels are reached are noted to compare across districts. Between 1997 and 2015, UMgungundlovu district in KwaZulu Natal has the lowest estimated life-expectancy at birth for females at 43.3 years in 2004 (38.3–48.1). For males, Ugu district in KwaZulu Natal has the lowest life-expectancy of 41.2 in 2006 (37.4–44.7). Among females, City of Cape Town district in Western Cape has the highest life-expectancy of 72.8 in 2015 (70.4–74.7) and for males, Overberg district in Western Cape has the highest life-expectancy of 67.2 in 2015 (65–69.3).

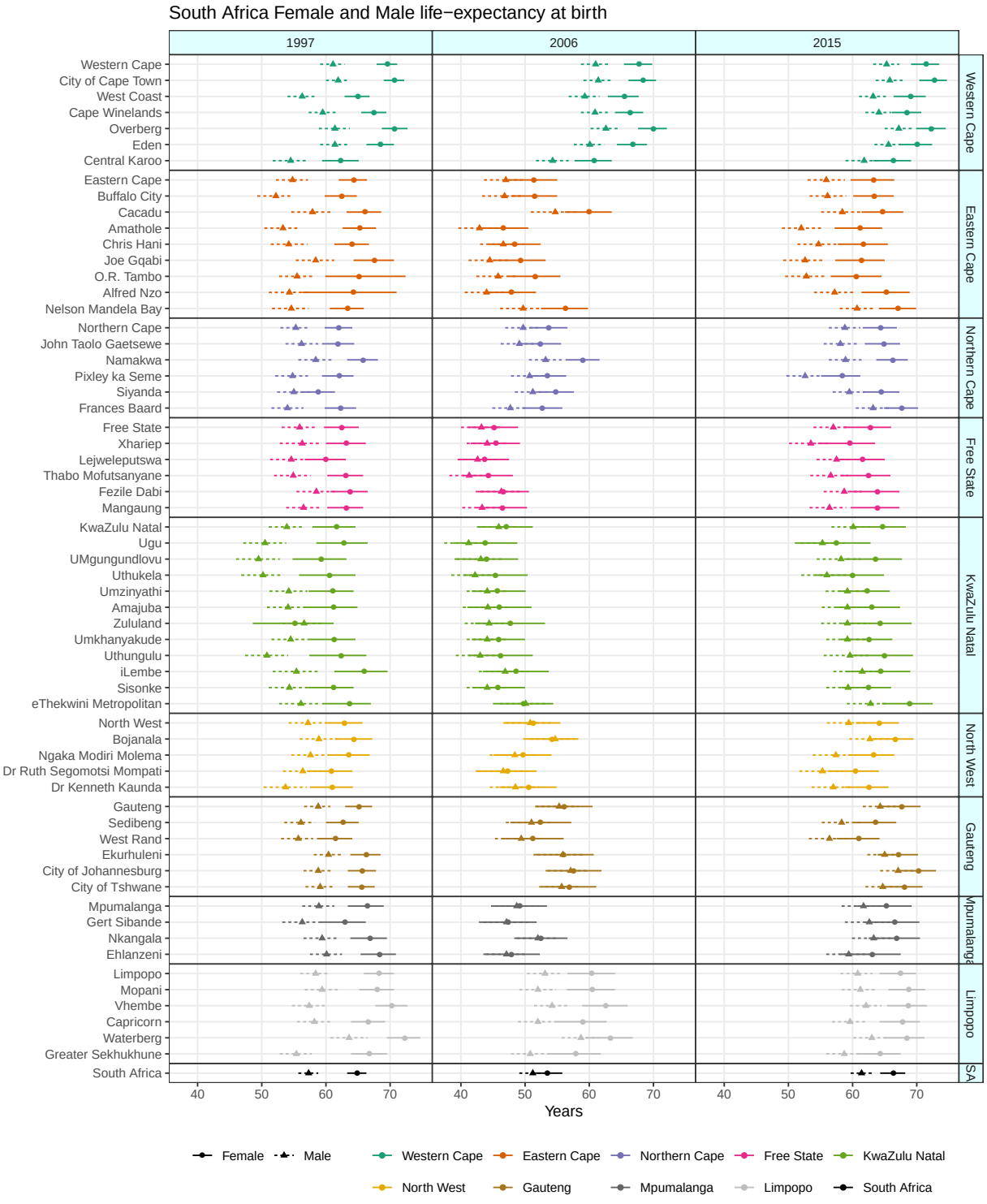

Figure 2.5: Life-expectancy at birth (e_0) by district, sex and year

Figure 2.6 illustrates the trends in the mean child mortality rates ($_1q_0$) for each district, grouped by province. Within each group, the province mean trend is shown using grey circles and the national trend is shown using black dashed lines, for both sexes combined.

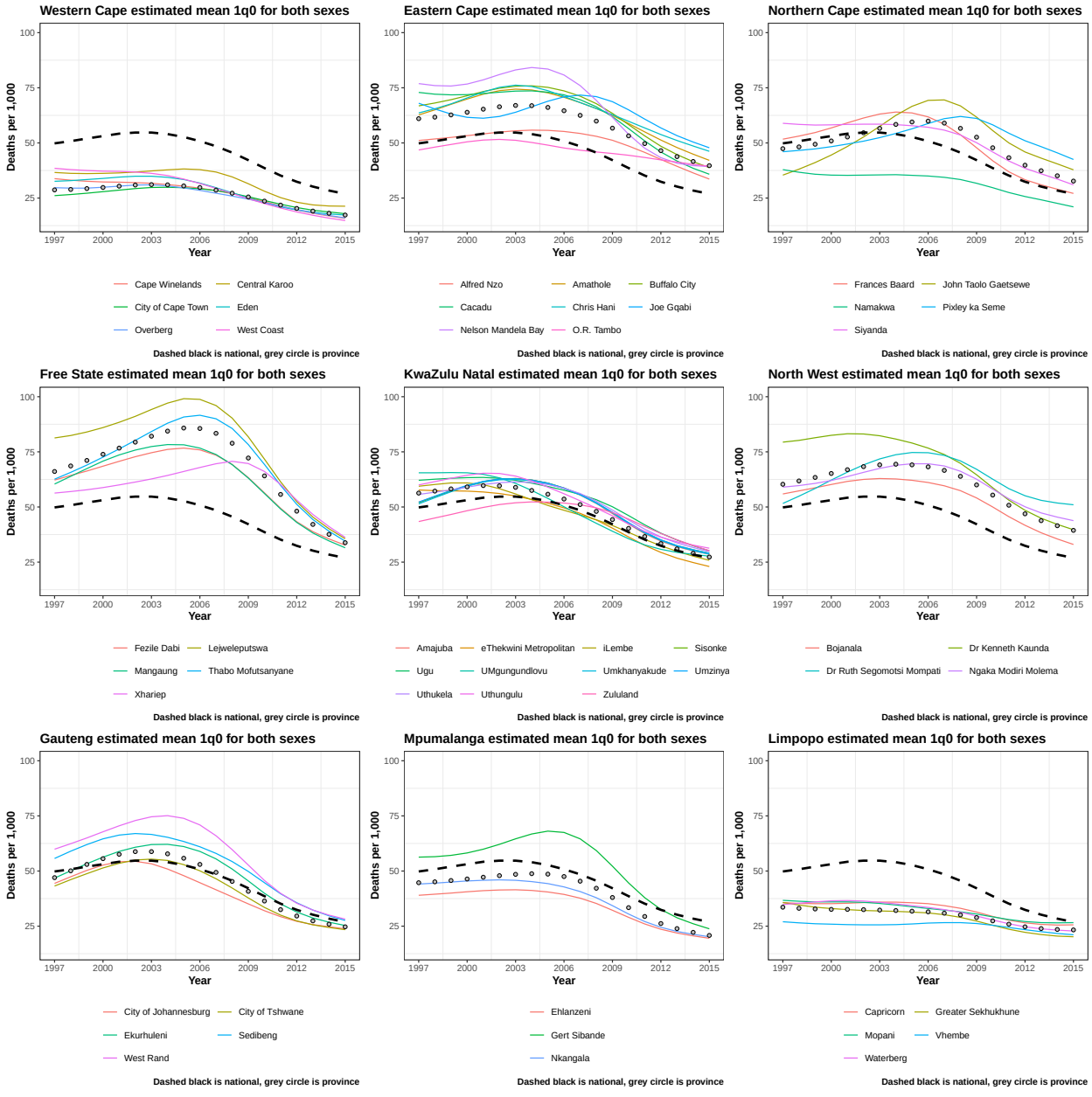

Figure 2.6: Infant mortality ($_1q_0$) by district and year, both sexes

Similarly, Figure 2.7 illustrates the trends in the mean child mortality rates ($_5q_0$) for each district within each province with province and national shown as in Figure 2.6.

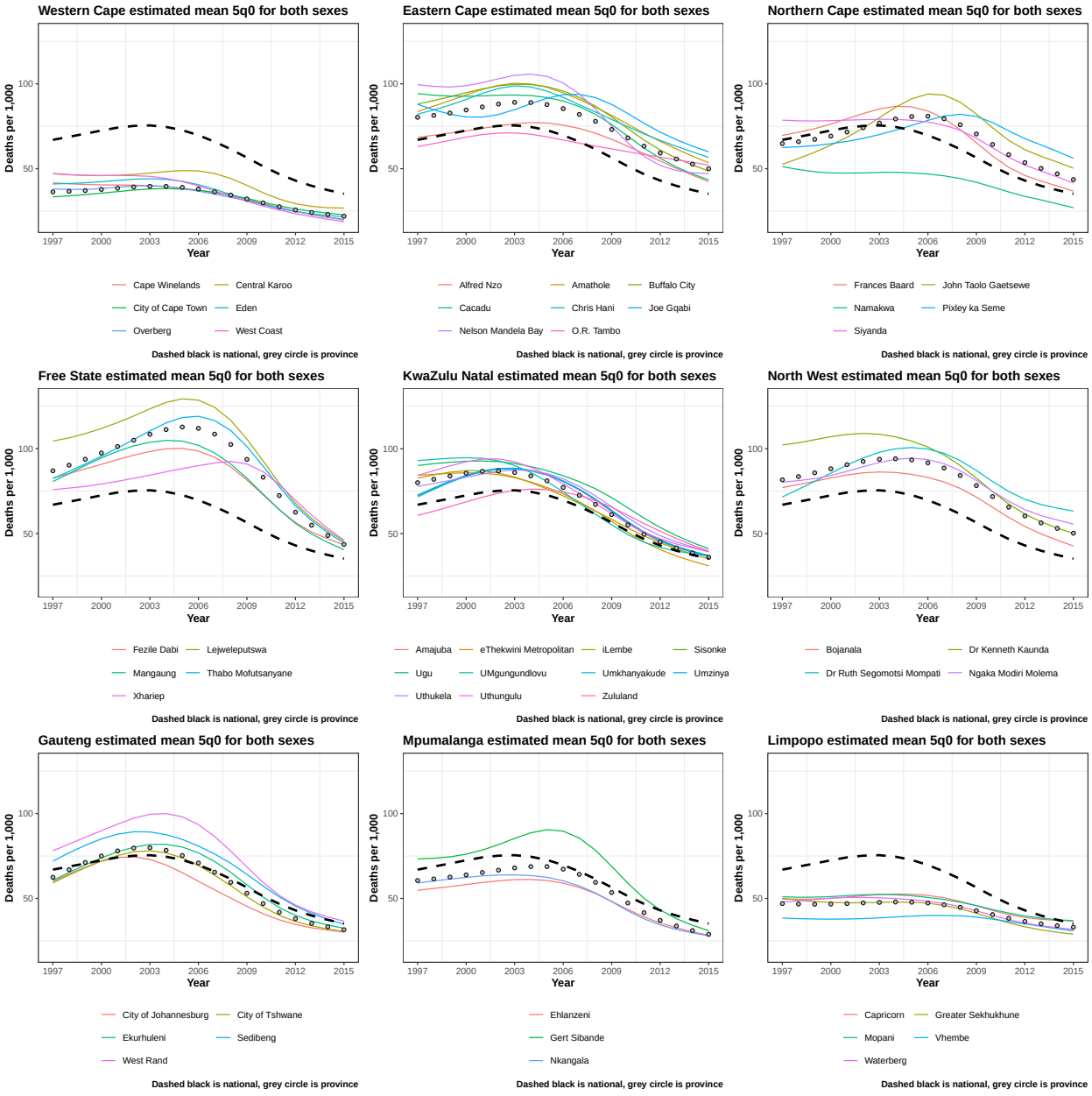

Figure 2.7: Child mortality ($_5q_0$) by district and year, both sexes

The ${}_5q_0$ and ${}_1q_0$ probabilities, shown for both sexes, are highly correlated and tell similar stories. In 1997, they have mean values of 67 and 49.8, respectively (60.6–74.2 and 45–55.3), reaching 75.5 and 54.7 maximum values in 2003 (67.5–84.8 and 49.1–61.6) and then falling to 35.2 and 26.9 (UI 31–39.9 and 23.7–30.6) by 2015. Districts in the Western Cape and Limpopo provinces have the lowest averages, significantly lower than national. There is wide variation in districts in Northern Cape, Gauteng and Mpumalanga where some districts lie above and others below national. There is also large within province variation across districts in Free State, Eastern Cape, North West and KwaZulu Natal for which districts and provincial averages are much higher than the national as well. Lejweleputswa district in the Free State province has the highest ${}_1q_0$ across the period reaching a highest value of 99.1 in 2005 (85.3–119.5). Running on an almost parallel trajectory, it also has the highest ${}_5q_0$ at 129.4 in 2005 (111.4–156.8). West Coast district in the Western Cape has the lowest ${}_1q_0$ of 14.8 in 2015 (11–19.9). It also has the lowest ${}_5q_0$ at 18.8 in 2015 (14.1–25).

Figure 2.8 provides a summary of the levels and trends in adult mortality (${}_{45}q_{15}$) by sex and district for select years 1997, 2006 and 2015. There are large differences between female and male ${}_{45}q_{15}$ with the latter being significantly higher. In 1997, female and male ${}_{45}q_{15}$ had mean values of 26.2 and 41.3, respectively (24.1–28.6 and 38.8–43.9), reaching maximums in 2006 of 52.4 and 57.3, for females and males respectively (48.2–57.2 and 53.6–61.4). Since 2006, ${}_{45}q_{15}$ has been steadily decreasing by an average of 2.52 per year for females and 2.15 for males to reach 2015 levels of 29.8 and 38 for females and males, respectively (26.6–33.4) and 34.9–41.3). As with ASDR and life-expectancy at birth, Eastern Cape, Free State, KwaZulu Natal and Mpumalanga have the largest changes in ${}_{45}q_{15}$. Between 1997 and 2015, Waterberg district in Limpopo has the lowest estimated ${}_{45}q_{15}$ for females at 17.9 in 1997 (15.1–21.5). For males, Overberg district in Western Cape has the lowest ${}_{45}q_{15}$ of 27.5 in 2015 (24.2–31.4). Among females, Ugu district in KwaZulu Natal has the highest ${}_{45}q_{15}$ of 72.4 in 2007 (62.8–81.8) and for males, Ugu district also has the highest ${}_{45}q_{15}$ of 79.1 in 2007 as well (73–86.2).

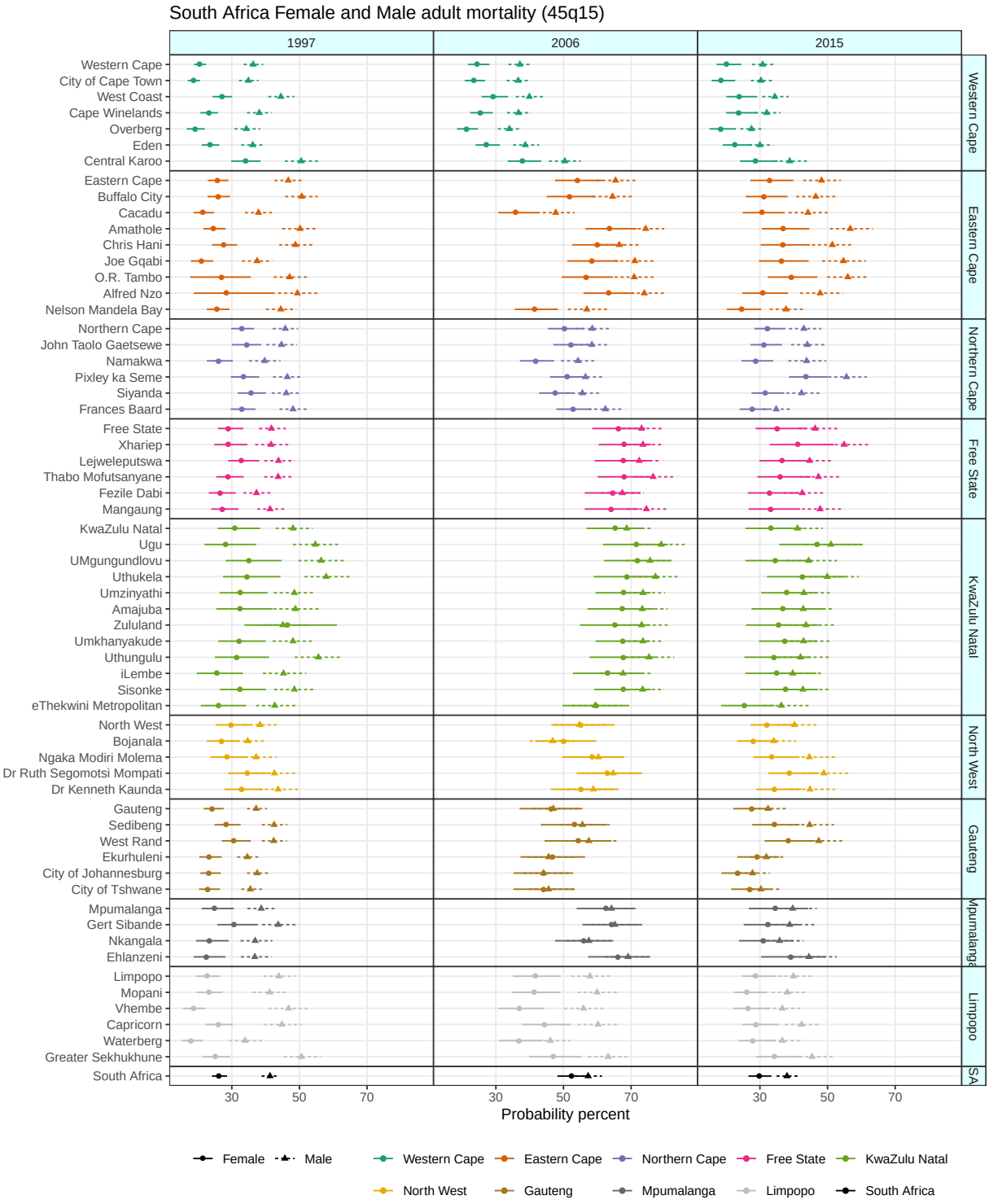

Figure 2.8: Adult mortality ($_{45}q_{15}$) by district, sex and year

2.4 Discussion

The results produced by this research echo those from the GBD and NBD studies. They show a South Africa mortality story of increasing death-rates between 1997 and the mid-2000s followed by very significant reversals leading to increases in life-expectancy and reductions in both child and adult mortality. In Aim 2 the cause-specific components of the age-specific mortality changes are explored in detail and show that most changes are attributable to post-1997 increasing HIV/AIDS deaths followed by ART roll-out and scale-up from 2003. This section has described how provincial all-cause death numbers are disaggregated to the district level by determining corrected district-, sex-and age-specific mortality profiles by year. The results are used to investigate which districts have had the worst mortality outcomes over the study period and which have seen the largest improvements. Detailed estimates of numbers, rates and summary demographic measures for each district are generated and these are available in the attached supplementary appendix. Having these results can contribute to the information at hand for the district for evaluating the success of their health systems at meeting the needs of the populations they serve when considering the levels and trends of age-specific mortality. In addition, the difference between the predicted and reported deaths gives a measure of the quality of death reporting as quantified by the level of completeness of reporting.

The Bayesian framework applied in this research innovatively adjusts the observed VR to not only give estimates of true district mortality, but measures of uncertainty as well. Results from the Local Burden of Disease and Global Burden of Disease studies are used to supplement the incomplete information that is derived using the VR. The model produces plausible age-specific estimates for each district that are based on assumptions about how the various available data sources are connected and how that connection can be extended to the district. Constraining the aggregates of the age-specific district numbers to the corresponding numbers for the provinces they lie within enhances the reliability of the estimates and the confidence we can have in them.

The proposed approach improves on using the raw district VR numbers proportionally which would introduce potential bias as this assumes uniform levels of under-reporting across the districts within a province. Although there are similarities in districts for many provinces, there are also a number of differences related to age-patterns, wealth, racial compositions and education which are expected to be factors impacting mortality risk and contributing to district mortality differentials. It also improves on applying the province completeness factors to the districts within it as this also potentially introduces error in its pushing or pulling estimates closer to the provincial mean. Ultimately, this method is designed to supplement the level of specification in the input data to give results that more correctly quantify the variation across the districts.

However, this study and the statistical model applied in it do have a number of limitations. Firstly, there is no gold-standard data source of true district numbers that can be used to determine the accuracy of the final results. Model validation or improvement in this case uses the observed mortality as a reference and the provincial mortality as a guide, under the assumption that the true district mortality must be related to both. Having a gold standard would also provide data that can be used to apply some post-estimation adjustments according to differences between the model and the gold-standard.

Secondly, as with any modelling exercise, the strength of the results is determined by the quality of the input data. There is uncertainty around the provincial estimates themselves and as stated previously, death distribution methods can be inaccurate depending on the level of migration and differential completeness of censuses. The provincial uncertainty is propagated to the districts which increases it for the district. Child completeness priors are obtained from the Local Burden of Disease study which uses an ensemble of child mortality estimation approaches but does not incorporate reported VR. Furthermore, together with estimates of death numbers, the death-rate incorporates the population numbers. In this study these have marginals taken from the census, interpolated using logistic age-specific growth rates for non-census years and scaled to sum to the province population numbers

by draw from the GBD. This gives smooth estimates of the population that may be more well behaved than actual numbers considering migration and other random or systematic factors and that may be affecting the age-patterns of the population numbers as well as the deaths for certain districts.

Thirdly is the regression model itself. There are a great many assumptions for priors that are considered in the model. Without direct estimates of district specific completeness of the type that the province obtains from DDMs, the model takes the district child completeness as a proxy for quality and uses it to determine a scaling factor on the provincial. This is less problematic where provincial completeness is close to 100% as in most of the years for the Western Cape, but it is more-so for provinces like Mpumalanga, Gauteng and the Northern Cape, which exhibit wide district variations in mortality experience. The standard mortality pattern is taken from province but the provincial boundary may play a weak role in determining mortality risks. The approach accounts for changes over time but assumes random fluctuations by age to be noise. This smoothing is problematic in the case of age-specific mortality shocks that are potentially lost.

Despite the limitations, the structure and data used for the model make for plausible and informative results that can be used to evaluate the health districts and historical trends. There are some patterns of mortality burden that go beyond the main analytical boundaries of district within province that emerge e.g. Figure 2.9 is a map of age standardized death rates for both sexes in 2006, the year with the highest estimated total deaths as well as the peak year for a number of the age-specific death-rates by sex and across all districts. It illustrates how the heaviest mortality burden follows a district-belt on the borders of Lesotho, with Xhariep, Mangaung, Lejweleputswa and Thabo Mafutsanyane in the Free State province, and extending to Amajuba, Umzinyathi, Uthukela, UMgungundlovu and Ugu in KwaZulu Natal province. Similarly, Namakwa which is of the Northern Cape has consistently lower levels of mortality than other districts in the province and is more akin to those in the Western Cape, which it borders.

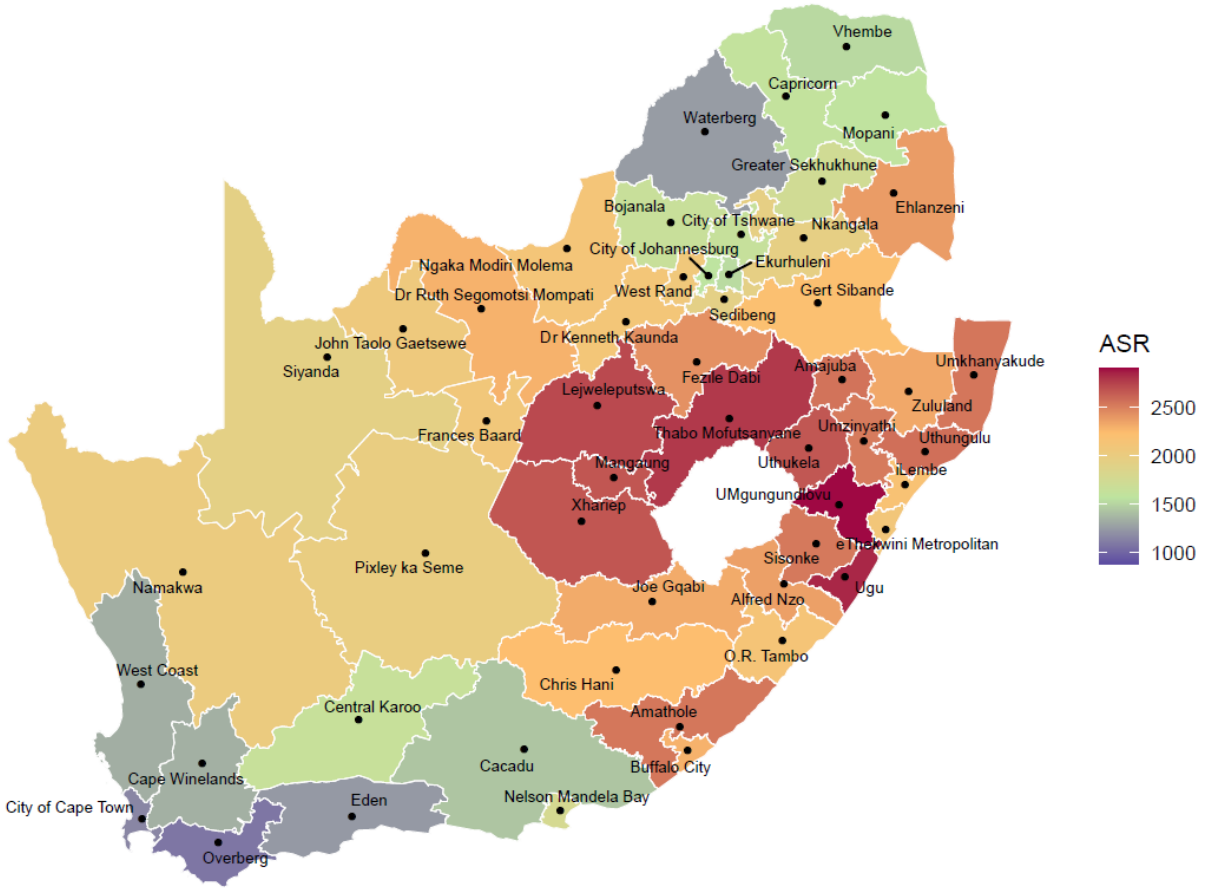

Figure 2.9: South Africa age standardized death rates map for both sexes, 2006

This would suggest that the approach used could be improved upon by using a model incorporating the geographic clustering beyond the province administrative boundaries along the lines of borrowing information based on geographic proximity. The question would be on how best to obtain priors that are informative and based on established data links in the same way that the current approach uses the links between the provinces, for which we have data, and the districts that lie within them.

REFERENCES

[1] Daniel Dicker, Grant Nguyen, Degu Abate, Kalkidan Hassen Abate, Solomon M Abay, Cristiana Abbafati, Nooshin Abbasi, Hedayat Abbastabar, Foad Abd-Allah, Jemal Abdela, et al. Global, regional, and national age-sex-specific mortality and life expectancy, 1950–2017: a systematic analysis for the global burden of disease study 2017. *The lancet*, 392(10159): 1684–1735, 2018.

[2] Victoria Pillay-van Wyk, William Msemburi, Ria Laubscher, Rob E Dorrington, Pam Groenewald, Tracy Glass, Beatrice Nojilana, Jané D Joubert, Richard Matzopoulos, Megan Prinsloo, et al. Mortality trends and differentials in South Africa from 1997 to 2012: second National Burden of Disease Study. *The Lancet Global Health*, 4(9):e642–e653, 2016.

[3] Neil G Bennett and Shiro Horiuchi. Estimating the completeness of death registration in a closed population. *Population Index*, pages 207–221, 1981.

[4] Kenneth Hill, Danzhen You, Yoonjoung Choi, et al. Death distribution methods for estimating adult mortality: sensitivity analysis with simulated data errors. *Demographic Research*, 21(9): 235–254, 2009.

[5] Actuarial Society of South Africa. ASSA2008 model. `aids.actuarialsociety.org.za/ASSA2008-Model-3480.htm`, 2012.

[6] Victoria Pillay-van Wyk, Ria Laubscher, William Msemburi, Rob E Dorrington, Pam Groenewald, Theo Vos, Richard Matzopoulos, Megan Prinsloo, Beatrice Nojilana, Nadine Nannan, et al. Second South African National Burden of Disease Study: Data cleaning, validation and SA NBD List. *Cape Town: Burden of Disease Research Unit, South African Medical Research Council*, 2014.

[7] William Brass. Uses of census or survey data for the estimation of vital rates.(e/cn. 14/cas. 4/v57). paper prepared for african seminar on vital statistics. *Addis Ababa*, 1964.

[8] William Brass et al. Methods for estimating fertility and mortality from limited and defective data. *Methods for estimating fertility and mortality from limited and defective data.*, 1975.

[9] Patrick Ward and Basia Zaba. The effect of HIV on the estimation of child mortality using the children surviving/children ever born technique. *Southern African Journal of Demography*, pages 39–73, 2008.

[10] Rob Dorrington, Tom A Moultrie, and Ian Timæus. *Estimation of mortality using the South African Census 2001 data*. Centre for Actuarial Research, University of Cape Town, 2004.

[11] Kenneth Hill. Methods for measuring adult mortality in developing countries: a comparative review. 2001.

[12] William Tinashe Msemburi. Simulation and sensitivity analysis of the choice of open interval, the methods of open interval, the methods of estimating life expectancy, completeness and δ in the seg method of estimating mortality. Master's thesis, University of Cape Town, 2010.

[13] William Brass et al. Methods for estimating fertility and mortality from limited and defective data. *Methods for estimating fertility and mortality from limited and defective data.*, 1975.

[14] Kenneth H Hill. Estimating census and death registration completeness. In *Asian and Pacific population forum/East-West Population Institute, East-West Center*, volume 1, pages 8–13, 1987.

[15] Populations Division of the United Nations. Methods for estimating adult mortality. *Department of Economic and Social Affairs*, ESA/P/WP.175:45–46, 2002.

[16] Neil G Bennett and Shiro Horiuchi. Estimating the completeness of death registration in a closed population. *Population index*, pages 207–221, 1981.

[17] Kenneth Hill, Danzhen You, and Yoonjoung Choi. Death distribution methods for estimating adult mortality: sensitivity analysis with simulated data errors. *Demographic Research*, 21: 235–254, 2009.

[18] RE Dorrington, Ian M Timæus, and Tom A Moultrie. Death distribution methods for estimating adult mortality: sensitivity analysis with simulated data errors, revisited. In *Abstract submitted to the 2007 UAPS Conference. UAPS Conference*, 2008.

[19] C. J. Murray, J. K. Rajaratnam, J. Marcus, T. Laakso, and A. D. Lopez. Reducing Ignorance about Adult Mortality: Improving Methods for Evaluating the Completeness of Death Registration. In *Population Association of America*, volume 7, pages 29–45, 2009.

[20] Christopher JL Murray, Julie Knoll Rajaratnam, Jacob Marcus, Thomas Laakso, and Alan D Lopez. What can we conclude from death registration? Improved methods for evaluating completeness. *PLoS Med*, 7(4):e1000262, 2010.

[21] Haidong Wang, Mohsen Naghavi, Christine Allen, Ryan M Barber, Zulfiqar A Bhutta, Austin Carter, Daniel C Casey, Fiona J Charlson, Alan Zian Chen, Matthew M Coates, et al. Global, regional, and national life expectancy, all-cause mortality, and cause-specific mortality for 249 causes of death, 1980–2015: a systematic analysis for the global burden of disease study 2015. *The Lancet*, 388(10053):1459–1544, 2016.

[22] T James Trussell. A re-estimation of the multiplying factors for the Brass technique for determining childhood survivorship rates. *Population studies*, 29(1):97–107, 1975.

[23] Kenneth Hill. Approaches to the measurement of childhood mortality: a comparative review. *Population Index*, pages 368–382, 1991.

[24] Douglas C Ewbank. The sources of error in Brass's method for estimating child survival: the case of Bangladesh. *Population studies*, 36(3):459–474, 1982.

[25] John Blacker and William Brass. The estimation of infant mortality from proportions dying among births in the past 24 months. *Southern African Journal of Demography*, pages 25–42, 2005.

[26] Mary Mahy and B Zaba. Measuring child mortality in AIDS-affected countries. In *Workshop on HIV/AIDS and Adult Mortality in Developing Countries. New York, United States of America*, pages 8–13. Citeseer, 2003.

[27] UNAIDS. Spectrum model. www.unaids.org/en/dataanalysis/tools/spectrumepp2011/, 2012.

[28] John Stover, Tim Brown, and Milly Marston. Updates to the Spectrum/Estimation and Projection Package (EPP) model to estimate HIV trends for adults and children. *Sexually transmitted infections*, 88(Suppl 2):i11–i16, 2012.

[29] Tim Brown, Le Bao, Adrian E Raftery, Joshua A Salomon, Rebecca F Baggaley, John Stover, and Patrick Gerland. Modelling HIV epidemics in the antiretroviral era: the UNAIDS Estimation and Projection package 2009. *Sexually transmitted infections*, 86(Suppl 2):ii3–ii10, 2010.

[30] Thomas M Rehle and Olive Shisana. Epidemiological and demographic HIV/AIDS projections: South Africa. *African Journal of AIDS Research*, 2(1):1–8, 2003.

[31] Eric O Udjo. A re-look at recent statistics on mortality in the context of HIV/AIDS with particular reference to South Africa. *Current HIV research*, 6(2):143–151, 2008.

[32] Leigh Johnson, Rob Dorrington, Thomas Rehle, Sean Jooste, Linda-Gail Bekker, Melissa Wallace, Landon Myer, and Andrew Boulle. THEMBISA version 1.0: A model for evaluating the impact of HIV/AIDS in South Africa. *Centre for Infectious Disease Epidemiology and Research Working Paper February*, 2014.

[33] United Nations. Department of International Economic and Social Affairs. Population Division. *World Population Prospects: The 2017 Revision*, *Methodology of the United Nations Population Estimates and Projections*, *Working Paper No. ESA/P/WP.250*. UN, 2017.

[34] Danzhen You, Lucia Hug, Simon Ejdemyr, Priscila Idele, Daniel Hogan, Colin Mathers, Patrick Gerland, Jin Rou New, Leontine Alkema, et al. Global, regional, and national levels and trends in under-5 mortality between 1990 and 2015, with scenario-based projections to 2030: a systematic analysis by the UN Inter-agency Group for Child Mortality Estimation. *The Lancet*, 386(10010):2275–2286, 2015.

[35] Kate J Kerber, Joy E Lawn, Leigh F Johnson, Mary Mahy, Rob E Dorrington, Heston Phillips, Debbie Bradshaw, Nadine Nannan, William Msemburi, Mikkel Z Oestergaard, et al. South

African child deaths 1990–2011: have HIV services reversed the trend enough to meet Millennium Development Goal 4? *Aids*, 27(16):2637–2648, 2013.

[36] Haidong Wang, Amanuel Alemu Abajobir, Kalkidan Hassen Abate, Cristiana Abbafati, Kaja M Abbas, Foad Abd-Allah, Semaw Ferede Abera, Haftom Niguse Abraha, Laith J Abu-Raddad, Niveen ME Abu-Rmeileh, et al. Global, regional, and national under-5 mortality, adult mortality, age-specific mortality, and life expectancy, 1970–2016: a systematic analysis for the global burden of disease study 2016. *The Lancet*, 390(10100):1084–1150, 2017.

[37] Rafael Lozano, Mohsen Naghavi, Kyle Foreman, Stephen Lim, Kenji Shibuya, Victor Aboyans, Jerry Abraham, Timothy Adair, Rakesh Aggarwal, Stephanie Y Ahn, et al. Global and regional mortality from 235 causes of death for 20 age groups in 1990 and 2010: a systematic analysis for the global burden of disease study 2010. *The Lancet*, 380(9859):2095–2128, 2013.

[38] M Naghavi, H Wang, R Lozano, A Davis, X Liang, M Zhou, et al. Gbd 2013 mortality and causes of death collaborators. global, regional, and national age-sex specific all-cause and cause-specific mortality for 240 causes of death, 1990-2013: a systematic analysis for the global burden of disease study 2013. *Lancet*, 385(9963):117–71, 2015.

[39] Julie Knoll Rajaratnam, Linda N Tran, Alan D Lopez, and Christopher JL Murray. Measuring under-five mortality: validation of new low-cost methods. *PLoS Med*, 7(4):e1000253, 2010.

[40] Haidong Wang, Tim M Wolock, Austin Carter, Grant Nguyen, Hmwe H Kyu, Emmanuela Gakidou, Simon I Hay, Edward J Mills, Adam Trickey, William Msemburi, et al. Estimates of global, regional, and national incidence, prevalence, and mortality of HIV, 1980–2015: the Global Burden of Disease Study 2015. *Lancet HIV*, 3(8):e361–e387, 2016.

[41] John R Wilmoth, Kirill Andreev, Dmitri Jdanov, Dana A Glei, C Boe, M Bubenheim, D Philipov, V Shkolnikov, and P Vachon. Methods protocol for the human mortality database. *University of California, Berkeley, and Max Planck Institute for Demographic Research, Rostock. URL: http://mortality. org [version 31/05/2007]*, 9:10–11, 2007.

[42] Haidong Wang, Chelsea A Liddell, Matthew M Coates, Meghan D Mooney, Carly E Levitz, Austin E Schumacher, Henry Apfel, Marissa Iannarone, Bryan Phillips, Katherine T Lofgren,

et al. Global, regional, and national levels of neonatal, infant, and under-5 mortality during 1990–2013: a systematic analysis for the Global Burden of Disease Study 2013. *The Lancet*, 384(9947):957–979, 2014.

[43] Joop De Beer. Smoothing and projecting age-specific probabilities of death by TOPALS. *Demographic Research*, 27:543–592, 2012.

[44] Marcos Roberto Gonzaga and Carl Paul Schmertmann. Estimating age-and sex-specific mortality rates for small areas with TOPALS regression: an application to brazil in 2010. *Revista Brasileira de Estudos de População*, 33(3):629–652, 2016.

[45] Carl Schmertmann and Marcos Roberto Gonzaga. Bayesian estimation of age-specific mortality and life expectancy for small areas with defective vital records. 2018.

[46] Nick Golding, Roy Burstein, Joshua Longbottom, Annie J Browne, Nancy Fullman, Aaron Osgood-Zimmerman, Lucas Earl, Samir Bhatt, Ewan Cameron, Daniel C Casey, et al. Mapping under-5 and neonatal mortality in africa, 2000–15: a baseline analysis for the sustainable development goals. *The Lancet*, 390(10108):2171–2182, 2017.

[47] Omar B Ahmad, Cynthia Boschi-Pinto, Alan D Lopez, Christopher JL Murray, Rafael Lozano, Mie Inoue, et al. Age standardization of rates: a new WHO standard. *Geneva: World Health Organization*, 9(10), 2001.

Chapter 3

SOUTH AFRICA CAUSE-SPECIFIC MORTALITY BY DISTRICT (1997–2015)

3.1 Introduction

Most of what is known about the spatial distribution of South Africa's cause-specific mortality is through the NBD and GBD projects. However, neither of these studies provide district-specific cause-of-death information and this research aims to fill this gap. The following sections outline historical cause-of-death patterns for the country and the methods used to derive them; summarise the shortcomings of current reported cause-of-death data and how they are adjusted for in the NBD and GBD; and finally give a detailed description of the cause-of-death estimation approach used for this research.

3.2 Review of national and provincial cause-of-death estimation

3.2.1 The journey to a "quadruple burden of disease"

Quantifying the number of South African deaths attributable to specific causes has been an active research area for decades. As early as 1940, there was a study looking at tuberculosis [1] and in the 1950s and 1960s a number of studies investigated cancers and cardiovascular diseases [2, 3, 4, 5]. A defining characteristic of early empirical studies is how they focused on the mortality of white South Africans to the exclusion of other races. Registration of deaths for non-whites was not prioritized and coverage was consequently very low. The national statistics office only began to make efforts to register deaths of all races in 1978 and of the estimated 50% of black South African deaths registered in the subsequent period, infectious and parasitic diseases were found to be leading causes [6].

The 1978 to 1994 period was one of technological advancement as well as extreme socio-political upheaval, culminating in the end of the apartheid era and South Africa's first democratic election in 1994. Infectious diseases began to decline in select segments of South African society whereas deaths due to trauma and violence increased [7]. Despite the injury increases, some parts of South Africa were following along the global path of epidemiological transition i.e. modernization, socio-economic progress, and mortality decline due to changing epidemiological conditions, primarily the decline in infectious disease [8]. Unfortunately, the post-1994 health potential was not realized for all as some poorer areas did not benefit from these advancements and their inhabitants were still experiencing high mortality levels attributable to infectious disease.

To exacerbate this, the advent of the HIV epidemic initiated significant increases in mortality in a very short period [9]. The public health response to the epidemic was not adequate and this was influenced by the relatively low numbers of deaths attributed to HIV/AIDS in the vital registration. Due to the stigma that was associated with HIV and AIDS, details completed on death certificates tended to focus on opportunistic infections or the mechanism of death rather than providing AIDS as the actual underlying cause-of-death [10]. In the two decades since 1994, the numbers of HIV/AIDS deaths have increased dramatically. This has not been observable directly from vital statistics. Rather it has been implied by the increase in the death numbers of unknown cause and of causes typically co-infecting AIDS patients [11, 12]. Increases in HIV incidence and prevalence as observed in antenatal clinics and prevalence studies has also been clear evidence of the scope of the epidemic [13, 14, 15]. The UNAIDS-Spectrum [16] and ASSA [17] models have used the prevalence estimates with assumptions on fertility, survival and transmission, to derive estimates of HIV/AIDS mortality.

Despite the relatively high levels of mortality due to infectious diseases and HIV/AIDS, there have been some specific health improvements. Medical advancements and investment into maternal and child health have seen reduced child mortality [18]. Now a greater

number of the population are surviving into middle and older ages and face the risk of dying from non-communicable diseases if management of such conditions does not improve [19].

Although the government has made significant strides at reducing wealth inequity, previous educational and economic marginalization has left large proportions of the populous unskilled and unemployable. Many have turned to gangs and criminal behaviour which tend to be violent in nature and lead to numerous deaths [20]. Added to this is a scourge of alcohol abuse which has contributed to the violence and has also led high numbers of transport related fatalities [21]. All of these different societal, demographic and epidemiological components contribute to the quadruple burden characterizing South Africa's mortality landscape; HIV/AIDS, persistent infectious diseases, violence and transport related injuries, as well as increasing non-communicable diseases.

The challenge for the health district is obtaining accurate estimates of cause-specific burden from the national VR system. VR data is regarded as the most timely and accurate source of COD information [22, 23]. However, due to under-reporting and the large proportions of reported deaths that are not well specified, South African VR has been regarded as being of poor quality [24, 25]. Deaths reported in VR are grouped according to ICD-10 codes. An ideal situation would have complete coverage and accurate reporting of the underlying COD. These deaths could then be aggregated into a mutually exclusive, collectively exhaustive cause list quite directly [26].

VR data for South Africa are not in this ideal state. The issue of overall completeness being below 100% has already been discussed and the problem of inaccurate COD has been mentioned in the context of HIV; however, it extends to other causes. Some deaths are coded to causes termed "garbage codes", constituting of intermediate, immediate, or otherwise inapplicable cause-of-death [27]. Districts report varying numbers of deaths that are coded to the ICD code R99 which denotes ill-defined or unknown cause, a grouping

entirely uninformative for public policy [28]. Other deaths are coded to causes that are imprecise but that provide some information on the correct applicable cause family e.g. malignant neoplasms or cancers, but with no specification provided for site or type.

The 2nd National Burden of Disease study (NBD) [29] and the Global Burden of Disease study (GBD2017) [30] used contrasting methods to account for the errors in VR and determine COD estimates for South Africa. The NBD also provides the data reported in the district health barometer (DHB) [31]. The DHB reports unadjusted causes-of-death that have been cleaned and grouped according to the NBD's COD list, without any adjustments for misclassified HIV and under-reporting. I review the COD estimation methods of the NBD and GBD studies in more detail.

3.2.2 The National Burden of Disease Study

Following adjusting the all-cause numbers for under-reporting in the NBD, the three main components of deriving age and sex specific cause of death profiles for South Africa and its provinces are estimating the numbers of HIV/AIDS deaths, determining the numbers of injuries by cause and then redistributing ill-defined and garbage codes to remain with a mutually exclusive and exhaustive list of 139 causes. The HIV/AIDS approach was according to the following rationale:

(a) AIDS deaths were being systematically misallocated to target causes and the increase in mortality in these causes before ART roll out in 2003 was strongly associated with the increase in lagged antenatal prevalence [32]. By taking advantage of this association and regressing target cause mortality against prevalence, the estimated model intercept could be taken as the zero-HIV mortality level;

(b) The target cause mortality pattern over time for the oldest age groups least affected by HIV/AIDS, provided a valid counter-factual for what would have happened in the cause-specific trends of the younger age-groups if they had not experienced HIV.

Projecting the zero-HIV level according to the derived counter-factual provided cause-specific zero-HIV trends for the target causes and the difference between these and the observed was attributed to misallocated HIV/AIDS. This approach is similar to that by Birnbaum et al. [12] but using in country older age mortality data to derive the non-AIDS trends for the target causes rather than global trends and within age groups.

For injuries, empirical data from the 2009 Injury Mortality Survey (IMS) [33] and the 2001 National Injury Mortality Surveillance System (NIMSS) [34] were used to determine cause fractions. The IMS used post-mortem injury data and any additional information available from accompanying police reports and hospital records for the year 2009. In the IMS, mortuaries were taken as primary sampling units for a multi-stage stratified cluster sample design stratified by metro and non-metro area and mortuary size. This was done for all provinces except for the Western Cape for which records were obtained from the Provincial Injury Mortality Surveillance System [35]. The IMS assessed whether a death was from natural, external or undetermined cause and recorded the date of death, circumstances of death and the apparent manner of death (homicide, suicide, transport-related, or other unintentional or undetermined intent). The study was designed to be nationally representative and captured 99% of its intended sample [33].

NIMSS annually collected cause of death information for deaths due to external causes with different years having differing levels of funding and correspondingly different sample sizes and representativity. The specific report used by the NBD was for the year 2001 and had data obtained from 15 forensic pathology service (FPS) laboratories covering five provinces. The primary cause of death was classified according to the International Classification of Disease version-9 (ICD-9) [36].

The IMS and NIMSS studies were used to estimate trends in the external cause profiles according to five broad injury categories (homicide with a firearm, homicide without a firearm, suicide', transport', and other unintentional). A multinomial logistic regres-

sion model was applied to the 2009 Injury Mortality Survey data by age, sex, province, and population group, to smooth out sampling fluctuations in the cause fractions. The predicted "other intentional" was further broken down into single causes based on the observed injury proportions from the surveys. Once 2009 and 2001 injury proportions were estimated, a linear interpolation on these proportions was used to generate estimates by year. Finally the estimates were normalized to provide injury cause fractions summing up to 1 for each age-sex-year combination.

The NBD built upon algorithms applied in GBD2010 [37] to deal with causes that were not well specified. Garbage and ill-defined causes were proportionally distributed by age, sex, race and province. This was done in sequence, starting with the ill-defined conditions for which there was some information and ending with the very vague conditions with no information at all [38]. For instance, ill-defined cancers were proportionally redistributed to fully-defined cancers exclusively, whereas ill-defined natural deaths without any additional information were proportionally redistributed to all natural deaths. In the NBD the sequence of steps to determining COD profiles had the numbers of HIV and cause-specific injuries estimated first, followed by the proportional redistribution of garbage and ill-defined natural causes.

The NBD approach is predominantly empirical with VR patterns guiding correction factors. An alternative would be to adjust VR based on statistical models. There is a long history of generating COD estimates in this way. Preston's work in 1976 [39] used a regression-based approach to assess trends in mortality and causes of death taking into account misclassification of deaths. Hakulinen et al. [40] continued on from this work deriving age-sex-specific regression equations for major causes of death through 1980 for different regions of the world. More recently, the GBD2017 applied a statistical framework.

3.2.3 The Global Burden of Disease Study

The first Global Burden of Disease (GBD) Study generated comprehensive estimates of cause-specific mortality and morbidity by age, sex and region for eight regions of the world in 1990 [27, 41]. Subsequent iterations of the GBD [30, 37, 42, 43] have sought to improve the estimation process and accuracy with an approach that comprises of identification of data sources, application of demographic and statistical methods to adjust the empirical data for biases, and data synthesis through statistical methods.

The underlying algorithm for allocating garbage codes to target causes combines using statistical models, expert judgement and predefined proportions, as suggested by Naghavi et al. [26]. Before GBD2013, GBD calculated these predefined fractions solely based on the observed proportions of the underlying target causes [37]. However, from GBD2013 onwards, some of these proportions are estimated using a regression model based on research by Ahern et al. [44]. For specific COD families i.e. cancer sites, external causes of injury, stroke, heart failure, hypertension and atherosclerosis; the association between proportions attributed to well specified target groups and proportions of ill-defined or garbage codes are estimated using the following regression model for each family:

$$TG_{crt} = \alpha + \beta_1 Gar_{crt} + \beta_2 Age_{crt} Gar_{crt} + \theta_r Gar_{crt} + \gamma_r + \varepsilon_{ct}$$

where subscripts are for country c, countries categorized into regions r and year t, TG and Gar are the percentages of deaths of a specific COD family allocated to particular target groups and garbage codes, respectively, and β_1 is a slope coefficient describing the association between Gar_{crt} and TG_{crt}. β_2 measures the associations between the Age and Gar interaction and TG whereas γ and θ are random intercept and random slope, respectively. ε is a Gaussian error term derived through bootstrap. Unlike proportional redistribution, this approach effectively smooths out extreme allocations that are based on bias because of small numbers of deaths or large garbage proportions.

Notwithstanding the application of this model, for some targets proportional redistribution is applied as a cap on proposed reallocations and for a few, further adjustments are made on a case-by-case basis per country, age, sex, and target group based on existing epidemiological evidence and expert judgement.

In addition to the garbage code corrections, the GBD also performs VR corrections for specific causes where the country- and cause-specific mortality trends do not match what is expected based on either what is known about the prevalence of the cause in the country or based on the observed global mortality trends attributable to that cause. In the particular case of HIV/AIDS mortality, for many country-years, causes of death known to be co-morbid with HIV/AIDS (e.g., tuberculosis, other infectious diseases) exhibit HIV patterns indicating misallocation of AIDS deaths to these causes. In the GBD, correction factors for these causes are determined by first obtaining cause- and age-specific relative mortality ratios in countries with low HIV prevalence. Once derived, these factors are used to estimate cause-specific expected death numbers, assuming similar ratios in the high prevalence setting, such that any excess between observed and expected is reallocated to HIV/AIDS. For South Africa, HIV death numbers are derived using a version of Spectrum that was coded in python specifically for the GBD and that aligns assumptions used to determine HIV incidence in the EPP module with assumptions about all-cause mortality and population numbers, for each GBD modelling draw [45].

With garbage codes redistributed and HIV deaths correctly estimated, causes of death are determined within the Cause of Death Ensemble modelling (CODEm) framework [46]. CODEm uses mortality data from numerous countries and several source types to build prediction models linking cause-specific estimates to covariate combinations. Five core principles guide the CODEm approach:

1. identify and use all available data in the modelling process;
2. develop diverse set of plausible models according to established associations;

3. assess predictive validity of each individual model;
4. create an ensemble of models from the pool of plausible models;
5. select best model and ensemble using out-of-sample predictive validity.

This means that for South Africa, it is not only in-country covariate values being used to estimate cause-of-death, but in-country supplemented by global and regional effects as estimated using this comprehensive database.

In addition to CODEm, negative binomial models are also run for rare causes and natural history models are run for causes that are rarely recorded in vital registration or verbal autopsy data, albeit occurring in the population. For particular causes such as Alzheimer's disease and other dementias, mortality trends have been influenced by changes in certification practice. Consequently, adjustment is made for these causes based on prevalence surveys and estimates of excess mortality from deaths certified in countries with good quality data and the level of coding to dementia as an underlying cause of death in the most recent year. These approaches are used to estimate numbers for almost all causes-of-death; Cancers are approached differently. Cancer mortality-to-incidence (MI) models are derived using cancer registries and VR data. After all cause-specific estimates have been derived, the CodCorrect step is taken. CodCorrect involves rescaling age-sex-year-cause-specific estimates to ensure that their sum is equal to the all-cause value.

In dealing with ill-defined and garbage codes, a key difference in these two studies is what is assumed to be a valid source for the true cause profile. The NBD approach essentially assumes the poorly classified are data in which the correct cause is missing completely at random (MCAR) [47], and that the well specified provide a valid template to use to impute the true cause. The GBD2017 approach takes the true cause profile to be associated with key variables such that if one can determine what these variables are and estimate the effects linking them to the cause profile, one can predict it. If the MCAR assumption is applicable and the distributions of the well specified and poorly specified

are indistinguishable, then the strength of the NBD approach is that the external data does not influence what may be unique country specific cause patterns; something which can potentially happen with the GBD2017. However, data are rarely MCAR and it is highly likely that the poorly specified are not specified well because of the cause, which makes this a missing not at random (MNAR) scenario. The strength of the GBD2017 is thus being able to model cause independently of the observed missings to produce a substantiated cause profile based on established associations.

3.3 District cause-of-death estimation

In this section, the methods used to estimate district-level cause-specific mortality numbers and rates by sex, age and year are described.

3.3.1 Methods

The approach to estimate district cause-specific mortality relies on reported cause-specific data by district and province, corrected cause-specific mortality by province, and predicted all-cause mortality by district and province. The ratio of observed to predicted deaths provides completeness factors by district, age and sex. Completeness of reporting is not assumed to be constant across all causes. Instead, we assume completeness to depend on cause-type and race, contrasting three broad grouping combinations i.e. all-races non-natural, black natural and non-black natural deaths. The levels of completeness of reporting of non-natural deaths are impacted by South African law which requires a medico-legal investigation (an inquest) and post-mortem examination to be held for all non-natural deaths [29]. To estimate province-specific injury completeness, the estimated number of injury deaths for 2009 according to the IMS study [33] are compared to the injury deaths reported in VR for that year. Assuming the relative change in injury-completeness is the same as that for all-cause mortality, we can derive estimates for years 1997-2008 and 2010 to 2015 based on the derived 2009 estimate.

For natural deaths, the highest levels of under-reporting are assumed to occur in the rural areas where racial composition of the population is predominantly black [48]. The apartheid system deprived these communities of the socio-economic development that urban areas benefited from [49] and the ramifications on the rural areas are evident in the poor health-outcomes they still experience [50].

The previously disenfranchised rural communities have also had to endure mismanagement and corruption by those in government office [51, 52]. A consequence of such factors are resource limitations which have meant death registration is not prioritised. In addition, the legal enforcement of certification requirements that are followed more rigidly in urban areas, such as a death certificate being a burial order pre-requisite, is more lax in the rural areas [53].

Province p and cause-type-specific completeness adjustment factors are determined by finding the solution to the relationship

$$S_{p,tot}R_{p,tot} = S_{p,bn}R_{p,bn} + S_{p,inj}R_{p,inj} + R_{p,nbn}$$

where $S_{p,tot}$ is the reciprocal of age-specific completeness for province p that is determined in Aim 1, $R_{p,tot}$ are the total age-specific reported deaths, the bn index represents black-natural, inj represents injuries with $S_{p,inj}$ derived from the IMS, and nbn represents non-black natural. With $S_{d,p,tot}$ estimated in Aim 1, a raking procedure is applied to determine district-level cause-type and race-specific scaling factors $\hat{S}_{d,p,bn}$ using:

$$\begin{pmatrix} \hat{S}_{1,p,bn}R_{1,p,bn} & \hat{S}_{1,p,inj}R_{1,p,inj} \\ \vdots & \cdots \\ \hat{S}_{d,p,bn}R_{d,p,bn} & \hat{S}_{d,p,inj}R_{d,p,inj} \\ \vdots & \cdots \\ \hline S_{p,bn}R_{p,bn} & S_{p,inj}R_{p,inj} \end{pmatrix} = \begin{pmatrix} S_{1,p,tot}R_{1,p,tot} - R_{1,p,nbn} \\ \vdots \\ S_{d,p,tot}R_{d,p,tot} - R_{d,p,nbn} \\ \vdots \\ \hline S_{p,tot}R_{p,tot} - R_{p,nbn} \end{pmatrix}$$

We assume the vector of reported deaths indexed by reported cause k is a function of the vector of true deaths indexed by true underlying cause c, completeness of reporting and some latent effects related to province, age, sex and year i.e.

$$\{R_1, \ldots, R_k\} = f(\{D_1, \ldots, D_c\} | prov, sex, age, year, completeness)$$

To build a model quantifying the inverse of this process involves a number of steps and assumptions:

Derive estimates of deaths by reported cause k for a shorter list:

- Reported deaths, having been adjusted for completeness, are aggregated to a short list of $k = 10$ mutually exclusive and collectively exhaustive reported cause-of-death categories that summarize the reported data and can be used as covariates in a statistical model. These causes are listed in Table 3.1:

Table 3.1: List of reported cause-of-death groupings

1.	Infectious and parasitic diseases	6.	Cardiovascular
2.	HIV/AIDS and TB	7.	Other non-communicable
3.	Other communicable diseases	8.	Injuries
4.	Cancers	9.	Ill-defined (R99)
5.	Diabetes	10.	Other garbage

The goal is to determine the function that maps these $k = 10$ causes to the true causes and essentially reverses the data generating process that attributed the reported causes-of-death to them in the first place. Although many more distinct groupings are possible, these 10 are chosen to maximize the amount of variation in the input data that is explained by them while minimizing the occurrence of sparse zero-valued categories in the input data matrices.

Table 3.2 gives the ICD-10 categories of the VR data used to generate the reported cause groups for this research. To simplify identifying which exact causes are contained in each of the reported cause-of-death categories and to facilitate comparisons with other burden-of-disease lists using cause-names, the ICD-10 causes are also mapped to the single-cause labels used by the NBD [38] in their cleaning of the Stats-SA data.

Table 3.2: Reported cause-of-death grouping by ICD-10

Reported cause	**Single-cause labels**	**ICD-10 categories**
Cancers	Mouth and oropharynx, Nasopharynx cancer and other pharynx cancer, Oesophagus, Stomach, Colo-rectal, Liver, Gallbladder and biliary tract, Pancreas, Larynx, Trachea/bronchi/lung, Melanoma, Other skin cancer, Breast, Cervix, Corpus uteri, Ovary, Prostate, Testis cancer, Bladder, Kidney, Brain, Thyroid, Hodgkin's lymphoma, Non-Hodgkins lymphoma, Multiple myeloma, Leukaemia, Other malignant neoplasms, Other neoplasms, Malignant neoplasm without specification of site, Malignant neoplasm of other and ill-defined sites in the lip, oral cavity and pharynx, Malignant neoplasm of other and ill-defined digestive organs, Malignant neoplasm of other and ill-defined sites in the respiratory system and intrathoracic organs, Haematemesis and melaena/other diseases of GIT	C00-C16, C18-C25, C32-C34, C43, C44, C50, C53-C56, C61, C62, C67, C64-C66, C68, C70-C73, C81-C85, C88, C90-C96, C17, C30, C31, C37, C38, C40, C41, C45, C47-C49, C51, C52, C57, C58, C60, C63, C69, C74, C75, D00-D07, D09-D48, C76, C80, C14, C26, C39, K92
Cardiovascular	Rheumatic heart disease, Hypertensive heart disease, Ischaemic heart disease, Pericarditis, endocarditis and myocarditis, Cardiomyopathy, Cerebrovascular disease, Conduction disorders and other dysrythmias, Aortic aneurism, Peripheral vascular disorders, Other circulatory diseases, Ill defined descriptions of heart disease and unspecified disorders of circulatory system, Hypertension, Atrioventricular and left bundle-branch block, Other conduction disorders, Arterial embolism and thrombosis, Pulmonary oedema, Hemiplegia, Other cardiac arrhythmias, Heart failure, Secondary hypertension, Atherosclerosis	I00, I01, I02, I05-I09, E10-E14, I11, I20-I22, I24, I25, I30, I31, I33, I38, I40, I42, I60-I64, I67, I69, P52, I47, I48, I71, I73, I27, I28, I34, I35, I36, I37, I72-I78, I80, I82, I83, I86-I89, I95, I51, I99, I10, I44, I45, I74, J81, G81, I49, I50, I15, I70
Diabetes	Diabetes mellitus	E10-E14
HIV/AIDS and TB	Tuberculosis, HIV/AIDS, Pleural effusion, not elsewhere classified, Other pleural conditions, Extrapulmonary TB, Miliary TB, HIV Pseudonyms	A15, A16, B90, U51, U52, B20-B24, P35, J90, J94, A17, A18, A19, P37, B33, B45, B59, C46, D84

Ill-defined	Ill defined natural, Pulmonary embolism, Pneumonitis due to solids and liquids, Adult respiratory distress syndrome, Pneumothorax, Other inflammatory liver diseases, Osteomyelitis, Gangrene, not elsewhere classified, Ascites, Disseminated intravascular coagulation [defibrination syndrome], Cardiac arrest	E14, E86, E87, F10, F16, F19, F99, G20, G21, G30, G43, G44, H25, H26, H40, H90, H91, I01, I05, I09, I10, I20-I22, I25-I28, I30, I42, I46, I50, I70, I78, I80, I82, I88, I89, I95, I99, J61-J65, J80, K70, M05, M06, M30, M32, N40, O00-O03, O06, O07, O10-O16, O20, O22-O26, O29, O32-O36, O40, O41, O43, O46, O47, O60, O62-O64, O67, O71, O72, O74, O75, O85, O88-O90, O95, P00-P04, P07, P10-P12, P14, P15, P20, P21, P26, P27, P38, P39, P50, P51, P53-P60, P71, P72, P74, P76, P80, P81, P83, P90-P96, Q03, Q05, Q35-Q45, Q86, R00-R99, J69, J93, K75, M86, D65
Infectious and parasitic diseases	STDs excluding HIV, Diarrhoeal disease, Vaccine preventable childhood, Malaria, Intestinal parasites, other parasitic and vector diseases, Meningitis, Hepatitis, Other infectious diseases, Lower respiratory infections, Upper respiratory infections, Otitis media, Unspecified sexually transmitted disease, Septicaemia, Pyothorax, Sequelae of other and unspecified infectious and parasitic diseases, Sequelae of inflammatory diseases of central nervous system, Other disorders of brain (encaphalitis), Encephalitis	A50-A60, A63, N70-N73, A00-A09, K52, P77, P78, A33-A37, A80, B01, B05, B06, B26, B91, B50-B54, A82, A95, B55-B57, B65, B67-B81, A39, A87, G00, G03, B15-B19, A20-A28, A30-A32, A38, A42-A44, A46, A48, A49, A65-A71, A74, A75, A77-A79, A81, A88, A89, A92-A94, A96-A99, B00, B02-B04, B07-B09, B25, B27, B30, B34, B37,-B44, B46-B49, B58, B60, B64, B66, B75, B83, B92, B99, J09, J10-J16, J18, J20-J22, P22, P23, P28, J00-J06, H65, H66, A64, A40, A41, P36, J86, B94, G09, G93, A83-A86, G04
Injuries	Road injuries, Rail injury, Poisonings (including herbal), Falls, Fires, heat and hot substances, Drowning, Other threats to breathing, Mechanical forces: machinery, Exposure to natural forces, Adverse effects of medical and surgical treatment, Animal contact, Other unintentional injuries, Self-inflicted injuries, Interpersonal violence with firearm	V01-V04, V06, V09-V35, V38-V51, V53, V54, V56, V58-V60, V63, V65, V67-V70, V73, V74, V76, V78-V80, V82-V85, V87, V89, V05, V81, X40-X49, W01-W23, X00-X04, X06, X08-X19, V90, V92, W65-W70, W73-W81, W83, W84, W24, W30, W31, X30-39, Y40-Y65, Y69-Y71, Y73, Y74, Y78-Y84, Y88, W53-W59, X20-X26, X29, W35-W44, W49-W51, W64, W85-W87, W89-W94, W99, X28, X50-X95
Other communicable	Maternal haemorrhage, Maternal sepsis, Hypertension in pregnancy, Obstructed labour, Abortion, Other maternal, Preterm birth complications, Birth asphyxia, Sepsis and other infectious conditions of the newborn, Other perinatal conditions, Protein-energy malnutrition, Vitamin A deficiency, Iron deficiency anaemia, Other nutritional disorders, Perinatal death unspecified cause, Peritonitis, Other disorders of peritoneum, Sequelae of malnutrition and other nutritional deficiencies, Indirect maternal	O44-O46, O67, O72, O10-O16, O64-O66, O00-O07, O20-O36, O40-O43, O47, O48, O60-O63, O68-O71, O73-O75, O85-O92, O95, O96, I61-I64, P01, P07, P20-P29, P52, P61, P77, P80, P02, P03, P10-P15, P50, P90, P91, A33, A50, A54, P35-P39, P60, F10, F12, P00, P04, P05, P08, P51, P53-P59, P70, P71, P72, P74, P76, P78, P81, P83, P93, P94, E40-E46, D50-D53, E00-E02, E50-E63, D00, D02, D03, D07, D13, D15, D18, D21-D30, D33, D35, D36-D39, D43, D45, D48, F99, G40, G41, G43, G80, H66, J60, J64, J84, J86, K35, K37, M17-M19, P92, P96, K65, K66, E64, O98, O99

Other Garbage	Other transport accidents, Mechanical forces; firearm, Mechanical forces: sharp object, Interpersonal violence without firearm, Homicide unspecified means, Unspecified intestinal parasitism, Unspecified parasitic disease, Unspecified transport accident, Exposure to unspecified factor, Injuries with Undetermined intent, Toxic encephalopathy, Paraplegia and tetraplegia, Other paralytic syndromes, Sequelae of transport accidents, Sequelae of other accidents, Sequelae of intentional self-harm, assault and events of undetermined intent, Sequelae of other external causes, Legal intervention and acts of war	V86, V88, V93-V98, W32-W34, W25-W29, X85-X92, X96-X99, Y00-Y09, Y36, B82, B89, V99, X59, Y10-Y34, G92, G82, G83, Y85-Y87, Y89, Y35
Other non-communicable	Endocrine nutritional,blood and immune disorders, Unipolar, Bipolar, Schizophrenia, Alcohol dependence, Drug use, Anxiety disorders, Eating disorders, Development disorders, Childhood behaviour disorders, Mental retardation not included as sequelae elsewhere, Other mental and behavioural disorders, Alzheimer and other degenerative diseases of nervous system, Parkisons disease, Multiple sclerosis, Epilepsy, Other neurological conditions, Other vision loss, Other sense organ disorders, Copd, Pneumoconiosis, Asthma, Other interstitial lung disease, Other respiratory, Peptic ulcer, Appendicitis, Intestinal obstruction and strangulated hernia, Noninfective inflammatory bowel disease, Cirrhosis and liver disease, Gall bladder and bile duct disease, Pancreatitis, Other digestive, Renal disease, Benign prostatic hypertrophy, Other urinary and gynaecological diseases, Skin diseases, Rheumatoid arthriis, Osteoarthritis, Back and neck pain, Other muculo-skeletal, Neural tube defects, Cleft lip/palate, Congenital heart anomalies, Congenital disorders of GIT, Urogenital malformations, Fetal alcohol syndrome, Down syndrome and other chromosomal anomalies, Other chromosomal abnormalities, Other congenital abnormalities, Dental caries, Periodontal disease, Other oral diseases, Mental disorder, not otherwise specified, Seqence of hyperalimentation, Portal vein thrombosis, Oesophageal varices, Toxic liver disease, Hepatic failure, not elsewhere classified, Acute renal failure, Chronic renal failure, Unspecified renal failure, Cerebral palsy, Respiratory failure, not elsewhere classified	D55-D76, D80-D83, D86, D89, E03-E07, E15, E16, E20-E34, E65-E67, E70-E80, E83-E85, E88, P61, P70, F01-F25, F28-F33, F38-F45, F50, F79-F84, F89-F92, F34, F48, F51-F55, F59-F65, F68, F69, F93-F95, F98, G30, G31, G20, G21, G40, G41, G06, G08, G10-G12, G22-G25, G35-G37, G45, G47, G50-G72, G90, G91, G95, G96, G98, H30, H33-H35, H49-H54, H00-H02, H04, H05, H10, H11, H15-H18, H20, H21, H27, H43, H44, H46, H47, H57, H60, H61, H68-H73, H81, H83, H92, H93, J40-J44, J60-J65, J45-J47, J84, J30-J39, J66-J68, J70, J82, J85, J92, J95, J98, J99, P24, P25, K25-K27, K35-K37, K40-K46, K56, K50, K51, K70, K73, K74, K80-K83, K85, K86, K20-K22, K28-K31, K38, K55, K57-K64, K76, K90, E10-E12, E14, I12, I13, N00-N07, N10-N15, N20-N36, N39, N41-N50, N60-N64, N75, N76, N80-N98, B35, B36, B85-B88, L00-L05, L08, L10-L13, L20-L30, L40-L44, L50-L60, L63-L67, L70, L72-L75, L80-L85, L87-L95, L97, L98, M05, M06, M15-M19, M47, M48, M50-M54, M00, M02, M08, M10-M13, M20-M25, M30-M35, M40-M46, M60-M62, M65-M67, M70-M72, M75-M77, M79, M80, M81, M83-M85, M87-M95, M99, P29, Q20-Q28, Q35-Q45, Q50-Q56, Q00-Q07, Q10-Q18, Q30-Q34, Q60-Q99, K00-K14, F99, E68, I81, I85, K71, K72, N17N19, G80, J96

The age-specific and province-specific levels of these reported cause-of-death categories are assumed to be a function of the true underlying cause-of-death numbers.

Derive estimates of deaths by true cause c:

- The true underlying causes of death by province, age, sex and year are assumed known based on GBD2017. To reduce the complexity and increase the robustness of estimation, the true cause-of-death list is also shortened to only include the causes that have inflicted the heaviest burden over time as well as causes known to be particularly relevant for health policy. Figure 3.1 lists the top causes of year-of-life-lost (YLLs) in 2017 according to GBD2017 and the percent change in that number for all ages comparing 2017 to 2007[1]. The target true cause list includes the eleven 2017 top causes-of-YLLs shown in Figure 3.1 as well as the four below:
  - COPD - listed in GBD2017 top 10 COD list for South Africa;
  - Cancers - the aggregate of all malignant neoplasms (policy relevant [54]);
  - Congenital birth defects - significant cause of under-5 deaths;
  - Hypertensive heart diseases - listed in NBD top 10 COD list for South Africa;

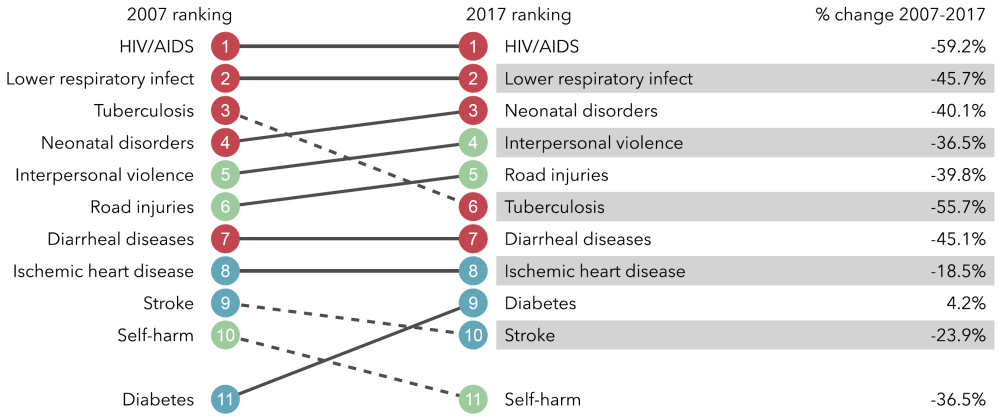

Figure 3.1: Top causes-of-YLLs in 2017 and percent change for 2007-2017

As shown in Table 3.3, this list accounts for over 85% of the deaths that occurred in the country over the study period.

[1] Available at `http://www.healthdata.org/south-africa`, accessed on 1 April 2019

Table 3.3: Age-specific deaths (%) attributed to cause in GBD2017 (South Africa 1997–2015)

age	Sum of 15[a]	COPD	Congen	Diab	Diarr	HIV/AIDS	Hypert	Viol	Ischem	LRI	Neon	Canc	Road	Self-harm	Stroke	TB
< 1 year	90.8	0.0	3.5	0.0	11.8	27.7	0.0	0.5	0.0	11.9	33.6	0.1	0.5	0.0	0.0	1.2
1–4	77.0	0.1	2.1	0.1	19.1	31.1	0.0	2.8	0.0	11.3	0.3	0.9	4.7	0.0	0.1	4.4
5–9	79.8	0.1	1.2	0.1	6.8	36.9	0.0	5.6	0.0	6.6	0.0	2.0	15.4	0.0	0.3	4.8
10–14	75.5	0.1	1.9	0.5	5.6	24.6	0.0	10.1	0.0	6.9	0.0	2.9	16.2	0.3	0.5	5.9
15–19	81.0	0.3	0.5	0.5	3.2	21.3	0.1	18.6	0.3	5.0	0.0	2.2	14.4	5.8	1.0	7.8
20–24	85.8	0.2	0.3	0.3	2.3	39.3	0.1	14.4	0.3	4.1	0.0	1.4	10.7	4.5	0.7	7.2
25–29	89.7	0.1	0.2	0.2	1.4	59.6	0.1	8.0	0.4	3.1	0.0	1.5	6.6	2.7	0.6	5.2
30–34	90.1	0.2	0.1	0.2	1.2	63.7	0.2	6.1	0.7	2.9	0.0	2.1	4.8	2.4	0.7	4.8
35–39	90.7	0.2	0.1	0.3	1.1	64.5	0.3	5.0	1.1	2.9	0.0	3.0	4.3	2.1	0.9	4.9
40–44	91.1	0.3	0.1	0.6	1.1	64.1	0.6	3.8	1.7	2.8	0.0	4.4	3.7	1.7	1.3	4.9
45–49	90.1	0.6	0.1	1.3	1.3	57.3	0.9	2.9	3.1	3.2	0.0	7.0	3.2	1.5	2.1	5.6
50–54	87.7	1.3	0.1	2.8	1.5	41.5	1.7	2.7	5.3	4.1	0.0	11.4	3.3	1.5	3.5	7.0
55–59	85.4	2.5	0.1	4.9	1.8	26.5	2.5	2.0	7.9	4.8	0.0	15.7	2.7	1.2	5.1	7.7
60–64	85.7	3.2	0.1	8.7	1.7	18.0	2.6	1.3	10.4	6.8	0.0	15.6	1.9	0.7	8.6	6.1
65–69	84.7	4.7	0.1	9.4	2.0	12.6	3.0	0.9	11.5	6.3	0.0	15.8	1.4	0.5	10.1	6.4
70–74	82.6	7.3	0.0	9.2	2.8	8.2	3.3	0.7	12.1	6.2	0.0	15.3	1.2	0.4	11.2	4.7
75–79	79.4	6.9	0.0	8.3	3.0	5.2	3.8	0.5	13.4	6.6	0.0	14.2	0.9	0.3	12.6	3.7
80–84	75.7	6.9	0.0	6.6	3.7	0.9	4.4	0.1	15.2	7.7	0.0	12.9	0.8	0.3	13.1	3.1
85–89	72.4	6.5	0.0	5.7	4.2	0.4	4.8	0.1	15.8	8.3	0.0	10.2	0.7	0.2	13.2	2.3
90–94	67.5	5.9	0.0	4.6	4.5	0.3	5.2	0.0	16	8.5	0.0	7.5	0.6	0.2	12.6	1.6
95+	66.5	5.3	0.0	3.6	6.8	0.2	5.2	0.1	15.8	9.7	0.0	5.1	0.8	0.2	12.1	1.6
All Ages	85.8	2.2	0.4	3.1	3.4	36.1	1.6	3.6	5.4	5.5	2.8	7.4	3.5	1.4	4.5	4.9

[a]Respectively: Chronic obstructive pulmonary disease; Congenital birth defects; Diabetes mellitus; Diarrheal diseases; HIV/AIDS; Hypertensive heart disease; Interpersonal violence; Ischemic heart disease; Lower respiratory infections; Neonatal disorders; Cancers; Road injuries; Self-harm

Determine an appropriate model for the inverse function:

- We assume a Dirichlet-multinomial (DM) regression model for grouped count data to estimate the true cause-of-death distribution. DM regression has been used for modelling categorical count or compositional data from diverse fields such as econometrics [55], bioinformatics [56], topic modelling [57] and ecology [58]. Although the standard multinomial distribution has been used for cause-of-death detection [59, 60, 61], applications of the model have either been working with individual-level data or grouped for a specific age range, not accounting for the effect of over-dispersion that characterizes grouped age-specific cause-of-death data. The DM distribution is particularly useful for such data as it includes an over-dispersion parameter when marginalizing over the standard multinomial parameters [62].

Consider a matrix of death counts D, with rows representing G groups (where each group is a sex-specific combination of province p, age j, year t) and C columns representing the true underlying cause-of-death. Each cell $D_{gc}, g = 1;\ldots;G$ and $c = 1;\ldots;C$, represents the number of times group g deaths are attributed to cause c. It is assumed that the count data follow a multinomial distribution consisting of row probability vectors $\boldsymbol{p_g} = \{p_{g1},\ldots,p_{gC}\}$ with $p_{gc} \approx \frac{D_{gc}}{\sum_c D_{gc}}$. In our DM regression model, we define a $G \times (V+1)$ array containing covariate information represented by x_{gv}, where V are the number of independent variables. The logits of the probabilities p_{gc} are modelled as a function of covariates using:

$$\theta_{gc} = log\left(\frac{p_{gc}}{1-p_{gc}}\right) = \boldsymbol{x_g}\boldsymbol{\beta_c} + \eta_g$$

where $\boldsymbol{\beta}$ is a $(V+1) \times C$ matrix of unknown regression coefficients associated with the covariates x_{gv} and η_g is a random group effect that accounts for group g unobservable heterogeneity. It can be assumed that the $exp(\eta_g)$'s follow independent gamma distributions with both shape and scale parameters $\delta_g\lambda_g$, $\delta_g > 0$, where the δ_g are used to quantify the overdispersion [58].

We assume that the probability vector $\boldsymbol{p}_g$ is a random variable that follows a Dirichlet distribution with corresponding parameter vectors $\boldsymbol{\alpha}_g = \{\alpha_{g1}, \ldots, \alpha_{gC}\}$ and probability mass function,

$$f_{Dir}(\boldsymbol{p}_g; \boldsymbol{\alpha}_g) = \frac{\Gamma(\alpha_g^*)}{\prod_{c=1}^{C} \Gamma(\alpha_{gc})} \prod_{c=1}^{C} p_{gc}^{\alpha_{gc}-1}, g = 1, \ldots, G. \tag{3.1}$$

where $\alpha_g^* = \sum_{c=1}^{C} \alpha_g c$. As mentioned previously, the count data follow a multinomial distribution. Defining $\boldsymbol{D}_g = \sum_c D_{gc}$, the probability matrix of the count data has row vectors $\boldsymbol{p}_g$ and probability mass function:

$$f_{MN}(\boldsymbol{D}_g; \boldsymbol{p}_g) = \frac{\boldsymbol{D}_g!}{\prod_{c=1}^{C} D_{gc}!} \prod_{c=1}^{C} p_{gc}^{D_{gc}}, g = 1, \ldots, G. \tag{3.2}$$

The resultant compound DM probability mass function (PMF) can be derived as:

$$\begin{aligned} f_{DM}(\boldsymbol{D}_g; \boldsymbol{\alpha}_g) &= \int_p f_{MN}(\boldsymbol{D}_g; \boldsymbol{p}_g) f_{Dir}(\boldsymbol{p}_g; \boldsymbol{\alpha}_g) \mathrm{d}\boldsymbol{p} \\ &= \frac{\boldsymbol{D}_g! \Gamma(\alpha_g^*)}{\Gamma(\alpha_g^* + \boldsymbol{D}_g)} \prod_{c=1}^{C} \frac{\Gamma(\alpha_{gc} + D_{gc})}{\Gamma(\alpha_{gc}) D_{gc}!}, g = 1, \ldots, G. \end{aligned} \tag{3.3}$$

The derivation of the DM likelihood function is necessary for the Bayesian implementation of the DM regression model in the R-Stan statistical package [63]. R-Stan does not include the compound PMF as one of its in-built distributions but is chosen to conduct this analysis because even for custom distributions, it allows for a full Bayesian inference with posterior draws for effects and covariances. Consequently, the R-Stan output is considered to be more informative for this research when compared to other R packages that can conduct a grouped data DM regression e.g. MGLM [64]. The latter uses a maximum-likelihood-estimation approach and was also found to be prohibitively slow when attempting to run on a large dataset with as many parameters as must be estimated for this scenario.

The prediction of true cause-of-death by district within province, age and year is conducted using a mixed effects DM regression model. The model predicts θ_c which represents the logit of the probability of deaths being attributable to true cause c using:

$$\theta_c = \beta_c^{(0)} + \beta_{c,j}^{(1)} I_j + \beta_{c,p}^{(2)} I_p + \sum_{k=1}^{10} \beta_{c,z_k}^{(3)} z_k + w(t,3) + \eta \tag{3.4}$$

where θ_c is the logit of p_c and the other terms in Equation 3.4 are defined as:

- $\beta_c^{(0)}$ is a cause c specific intercept,
- I_j are age-specific dummy variable for 5 year age-groupings

  $$j \in \{0-4, 5-9, 10-14, \ldots, 85+\}$$

  The $\beta_{c,j}^{(1)}$ are age j and cause c specific regression coefficients.
- Similarly, the I_p are province p specific dummy variable for p given by 1 Western Cape, 2 Eastern Cape, 3 Northern Cape, 4 Free State, 5 KwaZulu Natal, 6 North West, 7 Gauteng, 8 Mpumalanga and 9 Limpopo. The $\beta_{c,p}^{(2)}$ are province and cause c specific regression coefficients.
- The z_k represent the mortality rate z-scores for the reported cause-grouping $k \in 1, \ldots, 10$ shown in Table 3.1 i.e.

  $$z_{k,d,p,t,j} = \frac{D_{k,d,p,t,j} - mean(D_{k,\bullet})}{sd(D_{k,\bullet})}$$

  where sd represents the standard-deviation. Correspondingly, the $\beta_{c,z_k}^{(3)}$ are the true cause c and reported cause-grouping k regression coefficients.
- The $w(t,3)$ is a 3-parameter cubic polynomial on t representing time since 1997 e.g. $t = 1$ corresponding to 1998, with the t variables also standardised.

- The η is a random effect to adjust for over-dispersion.

The compound PMF given in Equation 3.3 is used to sample the mixed effects assuming

$$D_c \sim DirichletMultinomial(\theta_c)$$

Standard-normal non-informative priors are assumed for all fixed-effects and log-normal priors are assumed for η. These are used to derive posterior distributions for the coefficients and their estimated covariances. District- and province-specific values for the covariates and draws from the derived posterior of the random and fixed effects are used to derive initial district-level and province-level cause-of-death estimates which when normalised give the corresponding first stage cause-fraction estimates $\theta_{d,p,j,t,c}$ for district d within province p, at age j, in year t and for cause c.

The residuals for the implied age-specific cause-fractions by year are smoothed over time and summarised as Gaussian i.e.

$$e_{p,j,t,c} = f(\theta_{p,j,t,c} - \hat{\theta}_{p,j,t,c}) \sim N(\epsilon_{p,j,t,c}, \sigma^2_\epsilon)$$

where $f(\dot{)}$ is the spline smoother applied and ϵ is the mean year, age and cause-specific residual quantifying the variation unexplained by the model. Samples of these residuals are then drawn and added back to the stage 1 district-specific cause-fractions. The results are normalised and we can refer to them as the second stage estimates.

Final district-level cause-of-death estimates are derived by applying a three-dimensional iterative proportional fitting procedure with the province-specific seed for each year and sex provided by the second stage district cause- and age-specific numbers and target totals given by the age-specific district numbers from Aim 1, scaled to sum to province exactly for each draw as well as the cause- and age-specific province numbers from GBD2017, also scaled to sum to Aim 1 province. The data structure is depicted in Figure 3.2:

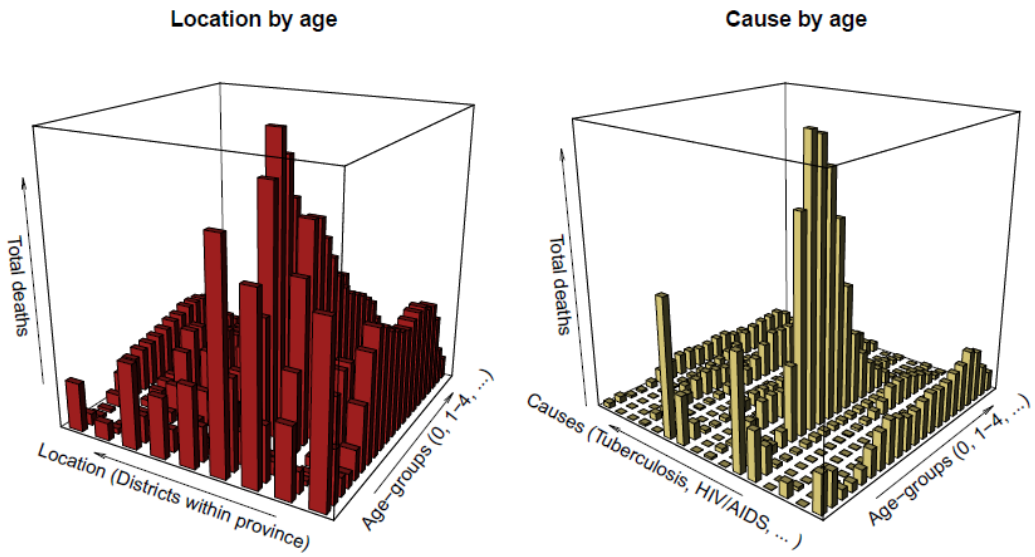

Figure 3.2: Data structure for 3D iterative proportional fitting

3.3.2 Results

Figures 3.3 and 3.4 show the crude cause-fractions by year based on the total deaths aggregated across all ages and for both sexes combined. The circles in the first plot are calculated using the province-specific means of total deaths and cause-specific deaths as estimated in GBD2017. The values illustrated using the fitted lines and uncertainty bounds on the same plot are derived by aggregating the district cause-specific deaths estimated using the approach described above to province. As can be seen in Figure 3.3, the formulated model predicts the input GBD cause-specific proportions well. Figure 3.4 is of the same predicted data and stacks the proportions to illustrate the relative proportions attributed to each cause and to also show that for all districts, 75% to 90% of deaths are attributed to the chosen 15 causes with the remainder attributed to the rest category "All Other". The plots do not provide any new insights for the country but establish that the statistical model works well at predicting cause-fractions in-sample and that the cause-list used covers most of the deaths in all of the provinces for the entire period.

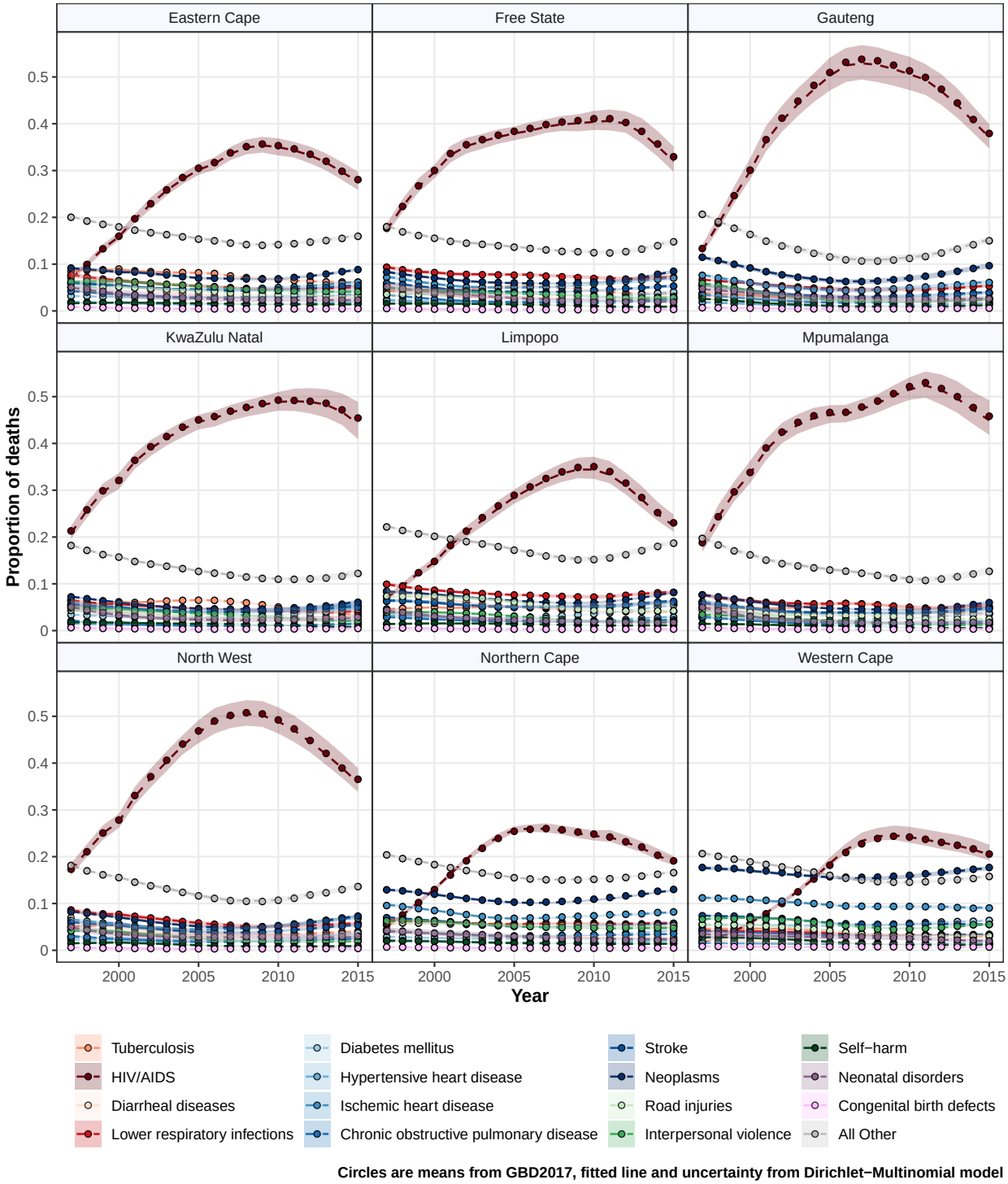

Figure 3.3: Predicted and GBD2017 cause-fractions by province and year

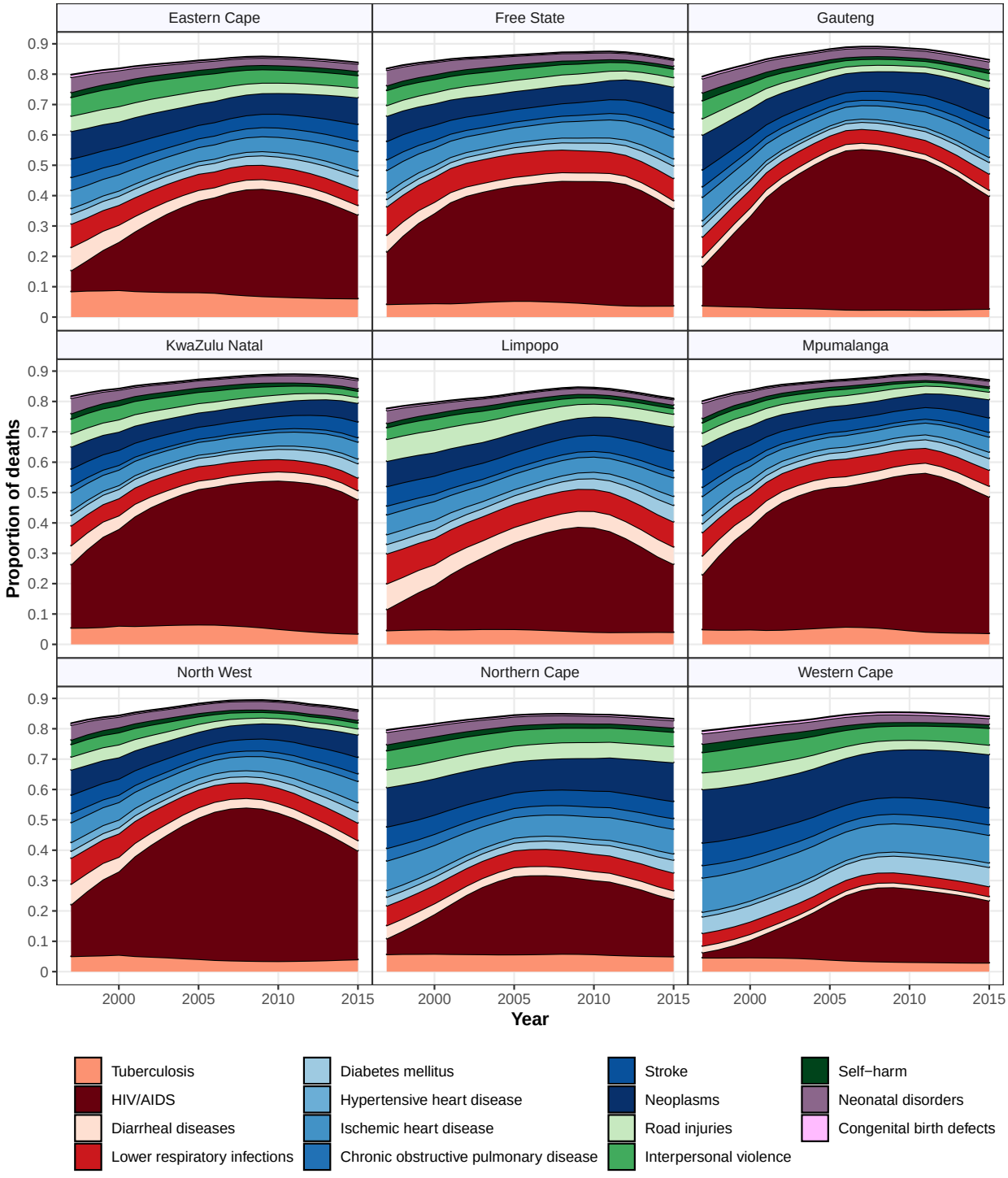

Figure 3.4: Stacked predicted cause-fractions by province and year

Table 3.4 shows the 2015 cause-specific mortality rates per 100,000 by district for ages 0-4. The highest rate of 392 is estimated for Joe Gqabi district in Eastern Cape, attributed to HIV/AIDS. Neonatal disorders are responsible for the greatest burden in general with highest rates estimated for districts in the North West, Eastern Cape and Northern Cape. Districts in the Western Cape have lowest rates across infectious diseases and Mpumalanga districts are also low for Neonatal disorders and Congenital birth defects.

Table 3.4: Heatmap of cause-specific mortality rates by district, ages 0-4

Location		Tuberculosis	HIV/AIDS	Diarrheal diseases	Lower respiratory infections	Diabetes mellitus	Hypertensive heart disease	Ischemic heart disease	COPD	Stroke	Neoplasms	Road injuries	Interpersonal violence	Self-harm	Neonatal disorders	Congenital birth defects	All Other
Western Cape	Central Karoo	9.2	24.2	55.0	57.9	0.5	0.0	0.0	0.0	0.4	5.3	18.7	11.8	0.0	215.2	59.8	102.2
	Eden	6.8	25.1	42.4	44.0	0.4	0.0	0.0	0.0	0.3	4.0	14.2	9.0	0.0	188.2	48.1	78.7
	Overberg	5.9	25.2	36.8	38.2	0.3	0.0	0.0	0.0	0.3	3.5	12.9	8.2	0.0	160.9	40.2	68.9
	Cape Winelands	6.9	23.5	41.5	42.7	0.4	0.0	0.0	0.0	0.3	4.1	14.5	9.3	0.0	150.6	43.1	78.8
	West Coast	6.2	22.2	39.5	40.1	0.3	0.0	0.0	0.0	0.3	3.7	13.3	8.4	0.0	155.6	42.2	74.3
	City of Cape Town	7.7	29.0	48.3	49.4	0.4	0.0	0.0	0.0	0.4	4.5	16.3	10.3	0.0	181.6	52.6	89.6
Eastern Cape	Nelson Mandela Bay	18.2	251.3	96.3	94.7	0.3	0.0	0.0	0.0	0.3	2.2	13.7	11.3	0.0	314.0	54.1	104.5
	Alfred Nzo	24.4	282.7	127.2	120.8	0.4	0.0	0.0	0.0	0.4	2.9	14.9	12.6	0.0	140.9	29.4	142.4
	O.R. Tambo	28.6	327.1	134.3	133.3	0.5	0.0	0.0	0.0	0.5	3.8	20.5	15.9	0.0	274.6	47.6	164.5
	Joe Gqabi	35.3	392.1	179.1	173.4	0.5	0.0	0.0	0.0	0.5	4.2	21.6	16.8	0.0	222.6	43.5	194.6
	Chris Hani	26.3	328.3	132.2	129.9	0.4	0.0	0.0	0.0	0.4	3.3	17.9	13.3	0.0	268.7	42.5	146.9
	Amathole	25.6	273.7	118.6	116.7	0.4	0.0	0.0	0.0	0.4	3.4	19.1	14.7	0.0	272.7	45.8	144.9
	Cacadu	19.3	225.8	96.4	99.8	0.3	0.0	0.0	0.0	0.3	2.4	14.0	11.7	0.0	269.1	48.7	115.6
	Buffalo City	19.9	244.4	94.3	95.6	0.4	0.0	0.0	0.0	0.3	2.7	16.1	12.5	0.0	379.9	64.0	114.7
Northern Cape	Frances Baard	18.9	28.0	137.3	114.3	0.4	0.0	0.0	0.0	0.7	4.5	22.7	14.5	0.0	209.1	44.7	152.6
	Siyanda	19.8	43.2	142.7	117.5	0.4	0.0	0.0	0.0	0.8	4.8	24.4	15.4	0.0	288.6	45.1	158.2
	Pixley ka Seme	29.1	59.0	214.8	183.2	0.6	0.0	0.0	0.0	1.0	6.6	32.6	20.6	0.0	312.3	72.1	225.0
	Namakwa	12.1	23.4	89.4	76.6	0.3	0.0	0.0	0.0	0.5	2.8	14.4	9.8	0.0	167.3	35.9	99.4
	John Taolo Gaetsewe	27.0	56.2	203.4	174.4	0.6	0.0	0.0	0.0	1.0	5.7	30.4	20.0	0.0	357.5	54.4	211.7
Free State	Mangaung	19.9	74.8	143.4	168.5	0.4	0.0	0.0	0.0	0.6	4.1	14.2	10.4	0.0	230.7	39.8	153.7
	Fezile Dabi	20.7	106.3	140.3	159.7	0.5	0.0	0.0	0.0	0.6	4.6	16.3	11.3	0.0	247.6	31.7	157.7
	Thabo Mofutsanyane	20.7	93.7	140.5	165.8	0.5	0.0	0.0	0.0	0.6	4.4	15.4	11.0	0.0	270.7	34.3	159.9
	Lejweleputswa	21.1	112.8	144.8	168.0	0.5	0.0	0.0	0.0	0.6	4.6	16.0	11.3	0.0	246.8	31.1	162.7
	Xhariep	22.1	79.8	153.1	183.2	0.5	0.0	0.0	0.0	0.6	4.7	16.1	11.7	0.0	241.3	38.8	172.1
KwaZulu Natal	eThekwini	13.4	131.8	81.8	63.7	0.4	0.0	0.0	0.0	0.4	3.3	8.8	6.3	0.0	204.1	32.4	113.5
	Sisonke	15.0	177.5	97.6	77.4	0.4	0.0	0.0	0.0	0.5	3.5	9.5	7.0	0.0	270.6	36.9	133.9
	iLembe	14.9	135.9	87.7	66.3	0.5	0.0	0.0	0.0	0.5	3.7	10.1	7.1	0.0	237.4	35.9	122.6
	Uthungulu	14.3	164.7	91.0	70.1	0.4	0.0	0.0	0.0	0.4	3.5	9.4	6.6	0.0	248.6	35.5	122.7
	Umkhanyakude	15.2	164.1	94.0	77.1	0.4	0.0	0.0	0.0	0.4	3.5	9.6	6.9	0.0	253.7	33.9	132.0
	Zululand	16.9	177.9	102.8	81.5	0.5	0.0	0.0	0.0	0.5	4.0	10.8	7.6	0.0	244.6	35.2	142.1
	Amajuba	14.0	143.8	87.4	68.8	0.4	0.0	0.0	0.0	0.4	3.4	9.2	6.6	0.0	257.5	38.0	121.5
	Umzinyathi	14.2	176.4	84.3	66.7	0.4	0.0	0.0	0.0	0.4	3.5	9.4	6.3	0.0	243.9	31.7	121.3
	Uthukela	16.3	154.0	94.3	74.5	0.5	0.0	0.0	0.0	0.5	4.0	10.9	7.6	0.0	257.6	36.7	135.6
	UMgungundlovu	15.6	150.9	93.5	73.8	0.5	0.0	0.0	0.0	0.5	3.8	10.1	7.2	0.0	260.3	38.7	131.2
	Ugu	17.7	166.1	103.0	80.4	0.5	0.0	0.0	0.0	0.5	4.4	11.8	8.1	0.0	259.1	39.6	145.4
North West	Dr Kenneth Kaunda	21.6	160.0	157.8	140.8	0.4	0.0	0.0	0.0	0.5	3.5	12.6	11.5	0.0	352.5	41.3	136.0
	Dr Ruth Segomotsi	26.9	227.1	198.7	175.9	0.5	0.0	0.0	0.0	0.6	4.2	15.5	14.0	0.0	372.7	41.4	163.5
	Ngaka Modiri Molema	24.2	222.3	178.6	158.6	0.4	0.0	0.0	0.0	0.6	3.9	14.1	12.9	0.0	301.7	37.6	152.2
	Bojanala	18.9	142.3	134.9	121.7	0.3	0.0	0.0	0.0	0.5	3.1	11.1	10.3	0.0	304.2	34.6	122.2
Gauteng	City of Tshwane	10.8	52.5	74.0	78.5	0.5	0.0	0.0	0.0	0.3	5.9	11.1	10.2	0.0	215.8	42.0	141.9
	City of Johannesburg	10.5	56.3	73.4	77.9	0.5	0.0	0.0	0.0	0.3	5.6	10.4	9.7	0.0	204.8	40.8	138.4
	Ekurhuleni	11.9	79.5	86.3	91.6	0.5	0.0	0.0	0.0	0.3	6.1	11.4	10.7	0.0	235.7	45.1	159.7
	West Rand	13.7	72.6	95.5	103.3	0.6	0.0	0.0	0.0	0.3	7.3	13.6	12.3	0.0	229.1	46.4	177.8
	Sedibeng	11.8	74.2	83.2	87.4	0.5	0.0	0.0	0.0	0.3	6.2	11.7	10.7	0.0	248.0	41.3	156.5
Mpumalanga	Ehlanzeni	14.3	87.8	106.7	79.4	0.5	0.0	0.0	0.0	0.4	4.3	9.9	5.2	0.0	151.8	23.9	110.0
	Nkangala	14.1	69.7	109.1	83.1	0.5	0.0	0.0	0.0	0.4	4.0	9.2	4.9	0.0	150.1	24.4	109.8
	Gert Sibande	14.6	88.1	117.3	91.0	0.5	0.0	0.0	0.0	0.4	3.9	9.2	5.0	0.0	160.9	24.3	115.9
Limpopo	Waterberg	11.1	209.1	79.0	80.1	0.3	0.0	0.0	0.0	0.3	2.3	11.3	5.7	0.0	174.3	22.3	84.8
	Capricorn	13.5	243.1	99.7	99.4	0.4	0.0	0.0	0.0	0.3	2.8	13.6	6.7	0.0	182.6	27.4	102.4
	Vhembe	12.0	201.7	92.0	88.2	0.3	0.0	0.0	0.0	0.3	2.6	12.1	6.0	0.0	108.9	20.0	92.5
	Mopani	12.9	237.5	94.3	93.4	0.4	0.0	0.0	0.0	0.3	2.7	13.1	6.3	0.0	177.2	24.6	97.1

Likewise, Table 3.5 is for ages 5-14 and indicates that comparing levels across all causes, HIV/AIDS leads in general and districts in the Eastern Cape and KwaZulu-Natal are the highest, led by districts O.R Tambo at 83.7 and Ugu 88.4 in the respective districts. It is important to note this age-group has the lowest rates compared to other age-groups with a highest rate less than a quarter of the highest rates in the under-5 age-group. Other than for HIV/AIDS, rates are more or less comparable across districts and causes.

Table 3.5: Heatmap of cause-specific mortality rates by district, ages 5-14

Location		Tuberculosis	HIV/AIDS	Diarrheal diseases	Lower respiratory infections	Diabetes mellitus	Hypertensive heart disease	Ischemic heart disease	COPD	Stroke	Neoplasms	Road injuries	Interpersonal violence	Self-harm	Neonatal disorders	Congenital birth defects	All Other
Western Cape	Central Karoo	1.5	21.8	1.6	1.7	0.3	0.0	0.0	0.0	0.2	2.9	12.0	6.2	0.1	0.0	1.7	12.4
	Eden	1.1	15.4	1.1	1.3	0.2	0.0	0.0	0.0	0.1	2.0	8.6	4.4	0.1	0.0	1.2	8.8
	Overberg	1.2	14.9	1.2	1.3	0.2	0.0	0.0	0.0	0.1	2.1	9.4	4.6	0.1	0.0	1.2	9.3
	Cape Winelands	1.0	13.4	1.1	1.2	0.1	0.0	0.0	0.0	0.1	1.9	8.4	4.1	0.1	0.0	1.1	8.4
	West Coast	1.1	15.1	1.2	1.3	0.2	0.0	0.0	0.0	0.1	2.1	9.4	4.7	0.1	0.0	1.2	9.4
	City of Cape Town	1.2	16.4	1.3	1.4	0.2	0.0	0.0	0.0	0.1	2.3	10.5	5.3	0.1	0.0	1.3	10.4
Eastern Cape	Nelson Mandela Bay	2.6	43.7	3.3	2.1	0.1	0.0	0.0	0.0	0.1	1.2	7.7	4.2	0.1	0.0	0.7	11.1
	Alfred Nzo	2.6	46.4	3.2	2.1	0.1	0.0	0.0	0.0	0.1	1.2	7.4	4.2	0.1	0.0	0.7	11.0
	O.R. Tambo	4.9	83.7	5.9	3.9	0.3	0.0	0.0	0.0	0.2	2.3	13.8	7.6	0.1	0.0	1.3	20.5
	Joe Gqabi	3.6	60.0	4.3	2.9	0.2	0.0	0.0	0.0	0.1	1.7	10.1	5.7	0.1	0.0	0.9	15.0
	Chris Hani	3.1	51.6	3.8	2.5	0.2	0.0	0.0	0.0	0.1	1.5	8.9	5.1	0.1	0.0	0.8	13.2
	Amathole	4.5	74.4	5.4	3.6	0.2	0.0	0.0	0.0	0.2	2.1	12.6	6.9	0.1	0.0	1.2	18.8
	Cacadu	2.7	45.9	3.3	2.2	0.1	0.0	0.0	0.0	0.1	1.3	7.8	4.3	0.1	0.0	0.7	11.5
	Buffalo City	4.2	70.2	5.2	3.4	0.2	0.0	0.0	0.0	0.2	2.0	12.2	6.4	0.1	0.0	1.1	17.9
Northern Cape	Frances Baard	0.9	39.3	2.3	1.1	0.1	0.0	0.0	0.0	0.1	1.7	5.2	2.4	0.0	0.0	0.5	7.5
	Siyanda	0.9	39.9	2.4	1.2	0.2	0.0	0.0	0.0	0.1	1.7	5.4	2.5	0.0	0.0	0.5	7.7
	Pixley ka Seme	1.3	49.9	3.0	1.6	0.2	0.0	0.0	0.0	0.1	2.2	6.9	3.2	0.1	0.0	0.6	10.0
	Namakwa	0.7	26.4	1.6	0.8	0.1	0.0	0.0	0.0	0.1	1.2	3.5	1.7	0.0	0.0	0.4	5.2
	John Taolo Gaetsewe	1.0	39.2	2.4	1.2	0.1	0.0	0.0	0.0	0.1	1.7	5.5	2.6	0.0	0.0	0.5	7.7
Free State	Mangaung	1.9	54.3	2.4	3.7	0.1	0.0	0.0	0.0	0.1	1.6	6.8	3.2	0.0	0.0	0.6	9.8
	Fezile Dabi	1.7	51.6	2.2	3.4	0.1	0.0	0.0	0.0	0.1	1.4	6.1	2.9	0.0	0.0	0.6	8.9
	Thabo Mofutsanyane	1.5	45.7	1.9	3.0	0.1	0.0	0.0	0.0	0.1	1.3	5.6	2.7	0.0	0.0	0.5	8.0
	Lejweleputswa	1.5	43.7	1.9	2.9	0.1	0.0	0.0	0.0	0.1	1.2	5.4	2.6	0.0	0.0	0.5	7.6
	Xhariep	2.0	58.2	2.5	3.9	0.2	0.0	0.0	0.0	0.2	1.7	7.2	3.3	0.1	0.0	0.7	10.6
KwaZulu Natal	eThekwini	3.9	68.0	5.8	4.9	0.2	0.0	0.0	0.0	0.2	2.1	9.3	4.4	0.1	0.0	1.1	17.0
	Sisonke	3.1	57.3	4.5	3.8	0.2	0.0	0.0	0.0	0.2	1.7	7.4	3.6	0.1	0.0	0.9	13.4
	iLembe	4.2	69.5	6.1	5.2	0.3	0.0	0.0	0.0	0.3	2.2	9.6	4.5	0.1	0.0	1.1	17.8
	Uthungulu	3.4	62.4	5.1	4.3	0.2	0.0	0.0	0.0	0.2	1.9	8.1	4.0	0.1	0.0	1.0	14.9
	Umkhanyakude	3.0	57.0	4.5	3.8	0.2	0.0	0.0	0.0	0.2	1.7	7.3	3.6	0.1	0.0	0.9	13.4
	Zululand	3.6	65.2	5.3	4.5	0.2	0.0	0.0	0.0	0.2	2.0	8.5	4.2	0.1	0.0	1.0	15.6
	Amajuba	2.9	56.0	4.3	3.7	0.2	0.0	0.0	0.0	0.2	1.6	7.1	3.5	0.1	0.0	0.9	12.9
	Umzinyathi	3.1	57.0	4.5	3.9	0.2	0.0	0.0	0.0	0.2	1.7	7.3	3.6	0.1	0.0	0.9	13.6
	Uthukela	3.4	63.5	5.0	4.2	0.2	0.0	0.0	0.0	0.2	1.9	8.1	4.0	0.1	0.0	1.0	14.7
	UMgungundlovu	3.6	63.0	5.3	4.5	0.2	0.0	0.0	0.0	0.2	2.0	8.6	4.0	0.1	0.0	1.0	15.8
	Ugu	5.1	88.4	7.4	6.3	0.3	0.0	0.0	0.0	0.3	2.7	11.8	5.6	0.1	0.0	1.4	21.9
North West	Dr Kenneth Kaunda	1.5	69.0	2.9	2.1	0.1	0.0	0.0	0.0	0.1	1.1	3.9	2.3	0.0	0.0	0.4	6.8
	Dr Ruth Segomotsi	1.2	55.1	2.3	1.6	0.1	0.0	0.0	0.0	0.1	0.9	3.0	1.8	0.0	0.0	0.3	5.3
	Ngaka Modiri Molema	1.0	54.4	2.0	1.4	0.1	0.0	0.0	0.0	0.1	0.8	2.7	1.7	0.0	0.0	0.3	4.8
	Bojanala	1.2	61.2	2.4	1.7	0.1	0.0	0.0	0.0	0.1	0.9	3.2	1.9	0.0	0.0	0.3	5.6
Gauteng	City of Tshwane	1.5	33.3	1.8	3.0	0.1	0.0	0.0	0.0	0.1	1.9	5.5	3.8	0.0	0.0	0.9	9.8
	City of Johannesburg	1.5	32.7	1.8	3.0	0.1	0.0	0.0	0.0	0.1	1.9	5.4	3.7	0.0	0.0	0.9	9.6
	Ekurhuleni	1.5	33.6	1.8	3.0	0.1	0.0	0.0	0.0	0.1	1.9	5.5	3.8	0.0	0.0	0.9	9.8
	West Rand	2.2	47.2	2.6	4.3	0.2	0.0	0.0	0.0	0.2	2.8	8.1	5.5	0.1	0.0	1.3	14.3
	Sedibeng	1.9	41.0	2.2	3.6	0.2	0.0	0.0	0.0	0.1	2.4	6.6	4.6	0.1	0.0	1.1	11.8
Mpumalanga	Ehlanzeni	2.8	51.7	5.0	4.5	0.2	0.0	0.0	0.0	0.2	1.5	6.9	2.5	0.1	0.0	0.8	11.9
	Nkangala	2.5	43.0	4.4	4.0	0.2	0.0	0.0	0.0	0.2	1.3	6.0	2.1	0.0	0.0	0.7	10.5
	Gert Sibande	2.3	41.5	4.1	3.7	0.2	0.0	0.0	0.0	0.1	1.2	5.6	2.0	0.1	0.0	0.6	9.8
Limpopo	Waterberg	1.9	40.0	5.3	3.7	0.2	0.0	0.0	0.0	0.1	1.3	7.3	2.4	0.1	0.0	0.6	9.5
	Capricorn	2.4	50.6	6.7	4.7	0.2	0.0	0.0	0.0	0.1	1.6	9.2	3.0	0.1	0.0	0.8	12.1
	Vhembe	1.8	38.9	5.1	3.5	0.1	0.0	0.0	0.0	0.1	1.2	6.9	2.2	0.0	0.0	0.6	9.0
	Mopani	2.0	42.1	5.7	3.9	0.2	0.0	0.0	0.0	0.1	1.4	7.9	2.5	0.1	0.0	0.6	10.2

Ages 15-49 mortality in 2015 is dominated by HIV/AIDS as shown in Table 3.6. Highest rates are concentrated in KwaZulu-Natal where the highest rate of 793 is estimated for Ugu and 741 for Uthukela. HIV/AIDS rates for districts in the Eastern Cape, Free State, North West and Mpumalanga are also high but less so for Limpopo, Northern Cape and the Western Cape. Categories like Interpersonal violence, Road injuries and Cancers begin to increase in this age-group albeit they are still overshadowed by HIV/AIDS mortality.

Table 3.6: Heatmap of cause-specific mortality rates by district, ages 15-49

Location		Tuberculosis	HIV/AIDS	Diarrheal diseases	Lower respiratory infections	Diabetes mellitus	Hypertensive heart disease	Ischemic heart disease	COPD	Stroke	Neoplasms	Road injuries	Interpersonal violence	Self-harm	Neonatal disorders	Congenital birth defects	All Other
Western Cape	Central Karoo	21.7	321.1	4.9	9.0	6.3	1.8	11.7	2.4	7.1	41.6	41.5	99.1	18.2	0.0	0.0	61.2
	Eden	14.1	246.6	3.2	5.6	4.4	1.3	8.3	1.6	4.9	28.2	26.9	63.3	12.2	0.0	0.0	39.6
	Overberg	11.9	208.9	2.8	4.7	3.6	1.0	7.1	1.3	4.1	23.4	23.3	56.7	10.9	0.0	0.0	33.9
	Cape Winelands	15.0	228.8	3.4	6.0	4.7	1.3	8.7	1.7	5.2	30.1	27.6	64.3	12.8	0.0	0.0	41.5
	West Coast	17.7	254.6	3.9	7.0	5.3	1.5	10.1	2.0	5.9	34.8	32.1	75.1	14.9	0.0	0.0	48.2
	City of Cape Town	13.8	216.7	3.1	5.4	3.9	1.1	7.7	1.5	4.5	25.7	27.8	69.1	13.0	0.0	0.0	38.8
Eastern Cape	Nelson Mandela Bay	29.1	387.2	5.8	8.5	3.0	1.6	6.2	1.7	4.4	16.6	31.7	51.6	17.5	0.0	0.0	49.8
	Alfred Nzo	30.1	451.8	6.9	8.8	2.7	1.3	4.8	1.6	3.8	15.9	38.7	64.3	21.1	0.0	0.0	55.9
	O.R. Tambo	56.7	557.9	11.8	16.9	4.4	2.3	7.8	2.6	6.4	26.1	64.4	106.9	33.5	0.0	0.0	95.3
	Joe Gqabi	50.4	518.4	10.0	14.4	4.1	2.2	7.9	2.5	6.1	24.7	56.1	93.5	29.9	0.0	0.0	82.8
	Chris Hani	53.6	503.1	10.6	15.8	4.5	2.4	8.4	2.7	6.6	26.3	57.3	95.4	30.2	0.0	0.0	87.0
	Amathole	55.8	513.9	10.9	16.4	4.7	2.5	8.9	2.8	6.9	28.2	60.2	100.3	32.0	0.0	0.0	91.0
	Cacadu	41.7	481.9	8.1	12.2	3.9	2.1	8.0	2.3	5.8	22.6	43.6	69.5	23.7	0.0	0.0	69.0
	Buffalo City	41.2	470.3	8.1	12.3	4.0	2.3	8.3	2.3	6.0	23.3	42.8	68.4	23.0	0.0	0.0	69.0
Northern Cape	Frances Baard	30.5	241.0	6.0	17.6	4.6	2.8	11.0	3.1	7.8	32.5	55.2	57.6	16.2	0.0	0.0	68.8
	Siyanda	38.4	282.1	7.2	21.6	5.2	3.2	13.0	3.7	9.1	38.4	69.4	72.6	20.3	0.0	0.0	84.1
	Pixley ka Seme	69.4	351.9	12.9	38.3	9.2	6.0	23.5	6.5	16.2	70.2	112.8	117.9	32.1	0.0	0.0	145.4
	Namakwa	37.3	268.3	6.6	21.0	5.7	3.6	14.9	4.1	9.8	41.5	60.1	59.0	17.7	0.0	0.0	80.1
	John Taolo Gaetsewe	37.8	263.8	7.1	20.8	4.9	3.0	12.0	3.5	8.5	35.2	71.1	77.9	20.8	0.0	0.0	81.7
Free State	Mangaung	29.4	513.3	7.9	24.3	3.6	3.3	8.5	2.2	7.0	24.2	42.8	50.0	14.8	0.0	0.0	67.9
	Fezile Dabi	24.0	503.1	6.4	18.9	3.0	2.7	6.7	1.8	5.6	19.5	37.1	44.0	12.6	0.0	0.0	54.8
	Thabo Mofutsanyane	28.2	508.8	7.9	23.0	3.4	3.1	7.6	2.0	6.3	22.8	42.3	51.1	14.5	0.0	0.0	65.7
	Lejweleputswa	26.6	555.4	7.3	21.8	3.5	3.2	7.8	2.0	6.6	23.5	39.5	44.7	13.2	0.0	0.0	62.4
	Xhariep	45.6	620.2	12.4	39.2	5.4	5.0	12.9	3.3	10.4	36.1	60.5	67.3	21.4	0.0	0.0	103.0
KwaZulu Natal	eThekwini	11.6	513.3	5.4	5.6	1.5	0.6	2.4	0.4	2.0	8.4	14.2	20.8	7.5	0.0	0.0	24.6
	Sisonke	14.4	591.5	6.7	7.3	1.9	0.8	2.7	0.5	2.5	10.7	17.8	26.3	9.0	0.0	0.0	31.9
	iLembe	21.2	589.4	8.8	11.1	2.6	1.1	3.8	0.7	3.6	13.1	21.8	29.8	11.3	0.0	0.0	43.5
	Uthungulu	17.2	609.9	7.6	8.9	2.2	0.9	3.3	0.6	2.9	12.0	19.7	28.6	9.9	0.0	0.0	37.2
	Umkhanyakude	15.2	589.1	6.9	7.9	2.0	0.8	2.9	0.5	2.6	11.0	18.4	27.1	9.3	0.0	0.0	34.1
	Zululand	19.2	591.7	8.1	9.8	2.2	0.9	3.1	0.6	3.0	11.7	21.7	31.1	10.9	0.0	0.0	40.2
	Amajuba	15.3	641.4	6.9	7.7	2.0	0.8	3.1	0.5	2.6	11.4	18.1	26.4	9.1	0.0	0.0	33.0
	Umzinyathi	16.3	584.3	7.3	8.5	2.3	1.0	3.2	0.6	2.9	12.1	18.5	26.4	9.3	0.0	0.0	35.6
	Uthukela	25.0	741.9	10.0	12.6	3.2	1.4	4.8	0.8	4.3	16.7	25.5	36.0	12.6	0.0	0.0	50.5
	UMgungundlovu	16.5	641.3	7.3	8.3	2.2	0.9	3.5	0.6	2.9	12.3	18.8	26.7	9.6	0.0	0.0	35.3
	Ugu	37.1	793.0	13.7	19.4	4.5	2.0	6.6	1.2	6.3	22.3	33.3	45.0	16.7	0.0	0.0	72.2
North West	Dr Kenneth Kaunda	28.1	584.9	9.0	17.7	3.1	3.2	7.1	1.6	5.5	19.7	26.5	31.3	13.6	0.0	0.0	49.9
	Dr Ruth Segomotsi	32.8	610.2	10.6	20.6	3.4	3.4	7.5	1.8	6.0	21.6	33.1	40.6	16.6	0.0	0.0	59.1
	Ngaka Modiri Molema	20.5	571.3	6.9	12.5	2.1	2.0	4.3	1.1	3.6	14.0	22.2	27.3	11.4	0.0	0.0	37.0
	Bojanala	15.3	474.2	5.3	9.4	1.8	1.6	3.6	0.9	2.9	11.0	16.1	19.4	8.6	0.0	0.0	27.7
Gauteng	City of Tshwane	13.0	356.0	3.6	11.8	2.4	1.3	5.4	1.4	4.0	16.0	19.2	21.6	10.5	0.0	0.0	38.9
	City of Johannesburg	11.7	333.1	3.2	10.5	2.1	1.1	4.7	1.2	3.5	13.6	18.0	20.4	10.0	0.0	0.0	34.6
	Ekurhuleni	16.0	411.8	4.4	14.4	2.9	1.5	6.3	1.6	4.7	19.2	23.9	27.0	13.1	0.0	0.0	47.4
	West Rand	28.5	598.4	7.3	25.3	5.6	3.0	12.6	3.1	8.6	36.8	38.3	42.0	21.0	0.0	0.0	81.7
	Sedibeng	23.8	528.1	6.3	21.1	4.4	2.3	9.4	2.4	6.8	28.6	35.8	40.1	19.6	0.0	0.0	69.3
Mpumalanga	Ehlanzeni	23.2	650.8	11.1	15.3	2.7	1.8	4.4	0.9	3.7	17.1	30.5	17.2	7.0	0.0	0.0	51.9
	Nkangala	15.5	489.6	8.0	10.7	2.1	1.4	3.3	0.7	2.7	12.5	20.0	10.4	4.7	0.0	0.0	35.5
	Gert Sibande	19.1	560.1	9.2	12.5	2.3	1.4	3.8	0.8	3.1	13.6	25.8	14.9	6.2	0.0	0.0	42.2
Limpopo	Waterberg	30.6	327.5	17.4	25.1	5.6	3.7	7.1	1.6	5.7	25.4	53.1	28.9	16.5	0.0	0.0	71.9
	Capricorn	30.9	334.8	18.2	26.0	5.7	3.8	7.1	1.6	5.8	27.0	53.8	29.2	16.6	0.0	0.0	74.7
	Vhembe	23.0	283.9	14.5	20.0	4.5	3.0	5.4	1.2	4.5	22.2	40.0	21.3	12.4	0.0	0.0	57.7
	Mopani	25.5	288.4	15.5	21.8	5.0	3.3	6.0	1.4	5.0	23.6	44.7	24.2	13.9	0.0	0.0	62.6

Mortality rates per 100,000 for ages 50-74 are presented in Table 3.7 and exhibit the widest amount of variation across districts and causes. High NCD rates are evident in places like the Western and Northern Capes e.g. cancers at 821.1 in Northern Cape's Pixley ka Seme, and high HIV/AIDS mortality is also estimated particularly for KwaZulu-Natal and less so for districts in Free State, North West, Gauteng and Mpumalanga. A significant proportion of all deaths is attributed to the rest category "All Other".

Table 3.7: Heatmap of cause-specific mortality rates by district, ages 50-74

	Location	Tuberculosis	HIV/AIDS	Diarrheal diseases	Lower respiratory infections	Diabetes mellitus	Hypertensive heart disease	Ischemic heart disease	COPD	Stroke	Neoplasms	Road injuries	Interpersonal violence	Self-harm	Neonatal disorders	Congenital birth defects	All Other
Western Cape	Central Karoo	93.1	261.9	17.8	67.5	240.1	41.3	247.8	103.5	151.1	660.0	44.9	41.2	17.6	0.0	0.0	327.8
	Eden	79.1	217.9	15.2	58.8	205.8	35.1	223.8	91.7	134.5	542.7	38.5	35.1	15.3	0.0	0.0	289.6
	Overberg	68.7	206.9	13.7	51.8	181.6	30.7	202.0	81.8	120.7	474.2	33.3	29.8	13.7	0.0	0.0	258.4
	Cape Winelands	97.1	237.2	17.0	70.1	232.6	40.9	251.2	103.0	149.9	654.6	44.2	38.3	17.1	0.0	0.0	331.6
	West Coast	100.5	233.1	16.9	70.2	230.5	40.1	248.2	103.9	148.6	675.9	42.9	36.3	16.7	0.0	0.0	327.3
	City of Cape Town	68.1	204.8	13.0	48.6	169.4	29.0	183.8	73.8	110.9	466.7	33.1	29.9	13.5	0.0	0.0	240.8
Eastern Cape	Nelson Mandela Bay	178.1	357.2	39.3	101.6	157.4	47.6	162.7	80.6	143.3	311.9	51.8	40.4	21.1	0.0	0.0	328.3
	Alfred Nzo	185.8	394.4	50.9	99.7	182.7	50.8	172.3	98.0	162.6	318.7	53.0	44.6	21.8	0.0	0.0	337.7
	O.R. Tambo	235.2	394.8	56.0	124.2	212.7	61.0	205.4	113.4	189.6	389.4	62.2	48.6	24.3	0.0	0.0	406.5
	Joe Gqabi	284.7	383.4	62.9	145.5	239.5	68.2	231.1	134.2	212.9	461.3	69.9	54.7	27.0	0.0	0.0	460.6
	Chris Hani	231.5	392.2	54.7	128.2	214.6	61.6	209.6	113.9	191.1	397.1	64.3	51.9	25.3	0.0	0.0	413.3
	Amathole	293.1	394.5	62.1	157.5	254.2	73.3	246.9	140.6	224.3	493.3	72.6	54.4	26.9	0.0	0.0	485.4
	Cacadu	216.7	392.9	48.6	122.8	194.8	57.6	197.0	102.1	175.4	370.7	61.8	49.8	24.5	0.0	0.0	391.9
	Buffalo City	263.8	344.9	51.9	147.8	215.9	67.3	226.2	111.3	194.8	442.1	70.3	50.7	27.4	0.0	0.0	462.2
Northern Cape	Frances Baard	119.0	241.4	30.4	117.0	151.8	56.8	239.2	101.2	165.0	399.8	67.0	44.6	19.4	0.0	0.0	333.9
	Siyanda	159.3	279.8	36.2	151.7	186.2	70.5	296.5	130.0	201.0	528.1	82.8	51.0	22.7	0.0	0.0	419.2
	Pixley ka Seme	245.5	296.9	48.4	225.7	267.0	104.3	410.6	186.3	277.9	821.1	116.5	68.7	29.2	0.0	0.0	593.3
	Namakwa	195.7	256.1	37.9	196.1	217.0	85.4	355.7	161.2	235.2	677.6	87.2	47.8	22.7	0.0	0.0	500.9
	John Taolo Gaetsewe	157.8	298.7	35.2	137.1	174.1	63.5	262.6	122.8	184.8	495.5	83.8	56.7	23.4	0.0	0.0	377.9
Free State	Mangaung	161.7	419.7	46.3	256.1	208.7	97.6	303.2	108.2	227.5	413.8	69.4	37.9	20.5	0.0	0.0	481.1
	Fezile Dabi	127.0	561.8	39.0	205.8	181.6	81.9	249.8	92.8	194.8	350.3	59.8	34.7	17.6	0.0	0.0	390.0
	Thabo Mofutsanyane	145.1	537.1	43.8	230.2	204.6	92.0	271.0	103.1	214.8	406.8	63.3	36.5	18.3	0.0	0.0	425.4
	Lejweleputswa	149.6	590.7	45.5	231.4	204.5	92.9	274.8	101.5	215.0	406.1	70.1	40.3	20.7	0.0	0.0	439.2
	Xhariep	184.8	533.7	55.3	286.7	250.6	113.1	339.8	128.1	261.4	492.6	80.3	45.8	23.2	0.0	0.0	537.0
KwaZulu Natal	eThekwini	102.9	533.4	36.7	83.3	156.6	36.5	147.5	36.5	130.3	200.0	30.9	23.0	13.9	0.0	0.0	236.5
	Sisonke	141.7	668.1	53.6	120.2	248.2	57.3	208.9	55.3	198.8	301.6	39.3	29.2	16.0	0.0	0.0	330.9
	iLembe	110.8	546.5	41.7	93.0	185.7	43.0	164.3	40.7	151.5	226.7	32.7	24.7	14.4	0.0	0.0	261.8
	Uthungulu	114.8	565.9	41.8	94.2	182.3	42.5	167.0	41.5	150.7	225.3	34.1	25.9	14.9	0.0	0.0	266.1
	Umkhanyakude	151.7	623.3	57.3	127.0	260.2	60.0	223.7	60.1	211.9	308.2	41.6	32.0	17.0	0.0	0.0	352.1
	Zululand	117.6	581.0	43.4	95.9	189.6	43.6	169.6	44.3	156.0	234.5	34.0	26.0	14.6	0.0	0.0	268.1
	Amajuba	136.2	727.8	47.4	112.4	217.9	50.9	192.9	49.1	175.1	278.3	40.5	30.2	17.1	0.0	0.0	309.4
	Umzinyathi	133.9	698.3	54.0	115.8	252.7	57.5	203.7	53.9	198.1	296.8	39.4	30.0	16.1	0.0	0.0	322.9
	Uthukela	164.5	784.4	53.6	132.1	254.0	59.6	217.8	58.1	201.0	340.7	44.5	31.5	18.0	0.0	0.0	353.0
	UMgungundlovu	152.8	645.8	49.4	126.4	230.1	54.9	208.1	54.1	187.1	315.2	40.3	27.7	16.8	0.0	0.0	336.7
	Ugu	168.7	681.8	59.0	139.8	273.9	64.3	232.1	62.0	217.7	361.7	43.4	29.7	17.7	0.0	0.0	375.6
North West	Dr Kenneth Kaunda	210.7	405.3	59.5	209.3	193.9	112.2	294.3	99.4	216.2	387.4	59.3	41.9	27.5	0.0	0.0	457.9
	Dr Ruth Segomotsi	198.5	528.1	59.8	192.8	198.3	107.8	280.9	101.3	214.7	375.0	57.8	43.6	26.5	0.0	0.0	429.8
	Ngaka Modiri Molema	173.8	609.9	53.6	167.0	173.2	91.8	239.0	93.1	186.6	350.8	48.3	34.6	22.7	0.0	0.0	368.7
	Bojanala	128.8	506.9	41.9	127.8	133.4	71.2	189.4	68.5	146.5	257.8	38.4	28.3	18.7	0.0	0.0	289.2
Gauteng	City of Tshwane	73.3	414.2	22.0	119.6	144.9	47.8	191.8	85.0	122.5	347.8	35.9	25.0	17.4	0.0	0.0	329.0
	City of Johannesburg	56.0	382.4	18.5	90.7	113.6	37.3	150.6	65.6	97.2	261.7	29.2	21.2	14.5	0.0	0.0	258.4
	Ekurhuleni	68.1	438.4	21.4	105.8	131.3	42.8	171.4	75.4	110.7	311.2	35.0	25.9	17.2	0.0	0.0	296.2
	West Rand	145.1	512.9	34.5	208.4	228.3	76.9	301.4	135.2	187.1	629.3	61.8	39.9	28.7	0.0	0.0	539.1
	Sedibeng	104.9	541.5	28.9	161.1	194.2	63.6	247.0	113.0	158.6	494.0	49.6	34.1	23.2	0.0	0.0	431.3
Mpumalanga	Ehlanzeni	141.0	642.5	59.9	156.1	180.6	74.4	187.5	58.7	167.7	265.6	45.9	19.8	12.6	0.0	0.0	335.4
	Nkangala	121.3	603.0	53.0	131.7	154.1	61.6	156.5	49.8	140.2	230.6	40.2	17.1	11.6	0.0	0.0	283.1
	Gert Sibande	112.0	580.0	50.0	121.8	144.1	58.1	149.1	45.1	133.1	205.8	39.0	17.7	11.2	0.0	0.0	267.8
Limpopo	Waterberg	120.9	235.8	84.9	175.7	184.1	68.7	153.8	52.5	140.8	243.0	82.7	30.3	22.6	0.0	0.0	345.2
	Capricorn	144.8	208.1	97.6	210.6	215.2	80.8	177.4	63.7	164.4	302.0	86.7	29.1	23.1	0.0	0.0	398.8
	Vhembe	125.0	216.7	94.9	184.9	200.8	73.8	159.7	59.4	153.6	277.7	75.5	25.9	20.3	0.0	0.0	357.3
	Mopani	132.0	217.1	91.7	187.9	199.7	73.6	162.0	56.9	150.4	269.4	86.9	31.7	23.3	0.0	0.0	361.3

For the rates of the oldest 75+ age-group, shown in Table 3.8, Cancers at 4,100 per 100,000 for West Rand in Gauteng, 3,700 for Namakwa in the Northern Cape and 3,300 for the Cape Winelands of the Western Cape are the highest. Ischemic heart disease, Stroke and are also relatively high and a significant number of deaths are attributed to causes in the class "All Other". As expected, rates for this terminal age are the highest across all ages. This is the only age with a relatively low HIV/AIDS mortality burden.

Table 3.8: Heatmap of cause-specific mortality rates by district, ages 75+

	Location	Tuberculosis	HIV/AIDS	Diarrheal diseases	Lower respiratory infections	Diabetes mellitus	Hypertensive heart disease	Ischemic heart disease	COPD	Stroke	Neoplasms	Road injuries	Interpersonal violence	Self-harm	Neonatal disorders	Congenital birth defects	All Other
Western Cape	Central Karoo	109.5	280.6	183.4	392.7	878.9	258.6	1512.3	649.1	1068.8	1739.0	102.5	35.1	51.5	0.0	0.0	2245.7
	Eden	123.4	77.5	123.7	519.4	854.6	288.8	1589.9	677.0	1011.7	2161.8	48.9	18.2	21.6	0.0	0.0	2469.8
	Overberg	115.0	91.8	158.3	468.2	833.5	256.8	1558.3	657.7	995.6	1884.2	51.8	28.1	23.3	0.0	0.0	2369.6
	Cape Winelands	218.8	82.2	130.1	835.5	1027.2	394.9	1953.9	850.2	1175.7	3322.6	53.7	13.8	20.2	0.0	0.0	3304.8
	West Coast	154.8	95.5	133.5	609.7	1001.0	350.9	1705.3	774.0	1110.2	2798.1	55.7	17.1	20.5	0.0	0.0	2980.9
	City of Cape Town	86.1	68.1	118.6	372.9	718.1	230.2	1545.9	519.1	956.2	1404.8	44.9	17.8	22.1	0.0	0.0	2225.8
Eastern Cape	Nelson Mandela Bay	415.4	84.5	255.4	905.9	786.6	518.9	1405.6	749.9	1214.4	1454.8	48.0	15.7	20.1	0.0	0.0	2789.4
	Alfred Nzo	586.7	112.8	636.0	606.5	670.1	371.4	1216.4	1005.4	1172.1	1034.6	61.4	23.3	27.9	0.0	0.0	2516.6
	O.R. Tambo	366.4	102.2	414.0	514.3	613.5	331.9	1205.7	676.7	1106.5	782.6	68.5	29.7	32.3	0.0	0.0	2334.8
	Joe Gqabi	525.9	105.3	502.9	698.9	757.2	431.7	1412.5	927.9	1309.2	1183.0	71.9	26.9	28.9	0.0	0.0	2870.1
	Chris Hani	344.8	110.4	393.3	562.8	665.4	367.0	1325.2	684.0	1178.3	903.6	73.7	25.8	37.5	0.0	0.0	2504.4
	Amathole	549.5	86.6	394.1	880.3	856.1	521.7	1611.4	989.8	1378.3	1367.5	91.5	29.7	29.6	0.0	0.0	3103.5
	Cacadu	399.2	104.3	314.9	808.8	777.2	517.3	1600.0	744.4	1339.3	1093.7	81.1	25.9	32.1	0.0	0.0	3247.6
	Buffalo City	703.0	37.3	278.2	1451.4	927.3	674.1	1793.3	1041.2	1406.5	2285.5	64.0	19.0	22.8	0.0	0.0	3466.8
Northern Cape	Frances Baard	116.4	67.4	223.2	488.9	506.9	360.0	1517.3	546.9	1046.7	853.0	69.6	23.7	22.6	0.0	0.0	2193.2
	Siyanda	190.1	110.9	298.7	694.7	673.0	493.6	1783.7	859.0	1263.8	1313.8	84.9	32.3	24.0	0.0	0.0	2617.1
	Pixley ka Seme	267.1	85.4	272.7	916.7	783.0	615.3	2104.6	957.0	1421.3	1877.6	98.6	28.0	22.8	0.0	0.0	3200.8
	Namakwa	370.2	71.7	244.0	1346.0	782.8	601.9	2029.1	927.0	1391.4	3785.2	82.5	22.7	24.5	0.0	0.0	2731.1
	John Taolo Gaetsewe	160.1	119.2	293.9	505.4	680.8	425.9	1469.3	789.0	1196.4	1335.0	105.9	30.7	29.6	0.0	0.0	2096.0
Free State	Mangaung	190.9	73.6	336.1	1080.3	698.3	546.3	1896.6	665.4	1313.8	1122.1	64.2	20.6	20.6	0.0	0.0	2999.6
	Fezile Dabi	138.2	224.8	281.1	985.0	681.9	532.0	1705.0	584.0	1229.7	1113.3	68.2	21.5	21.6	0.0	0.0	2705.5
	Thabo Mofutsanyane	166.7	169.9	352.0	1038.1	773.8	589.2	1815.6	681.6	1336.9	1204.4	78.0	20.9	23.0	0.0	0.0	2857.8
	Lejweleputswa	213.4	194.6	345.1	1188.3	833.2	623.4	1868.6	780.4	1382.6	1704.4	73.6	24.2	22.5	0.0	0.0	2869.9
	Xhariep	173.1	257.1	358.5	1053.0	777.3	552.1	1855.4	669.7	1343.0	1182.6	82.4	31.5	27.7	0.0	0.0	3035.7
KwaZulu Natal	eThekwini	225.2	161.0	367.3	570.4	795.1	365.9	1336.5	350.9	1245.0	716.2	49.6	16.5	22.6	0.0	0.0	2247.8
	Sisonke	306.2	142.8	492.6	680.7	995.9	435.7	1530.9	424.8	1521.8	981.1	57.4	16.0	23.6	0.0	0.0	2528.6
	iLembe	209.5	142.0	362.3	516.8	759.3	336.1	1236.4	305.3	1199.3	635.2	44.8	16.2	22.8	0.0	0.0	2026.5
	Uthungulu	215.7	136.7	361.9	547.0	725.2	345.7	1383.1	318.7	1247.5	610.0	48.2	16.0	22.4	0.0	0.0	2196.7
	Umkhanyakude	302.5	194.2	513.4	626.1	972.1	425.7	1590.3	450.2	1517.8	880.8	66.9	23.0	29.8	0.0	0.0	2708.9
	Zululand	198.0	161.4	394.9	492.2	723.6	321.2	1287.4	308.4	1221.9	573.4	48.4	17.4	26.1	0.0	0.0	2088.1
	Amajuba	271.1	288.4	426.8	633.2	973.8	426.5	1545.0	404.5	1464.5	976.7	67.3	20.1	31.2	0.0	0.0	2449.3
	Umzinyathi	270.4	248.2	482.4	658.6	1056.5	462.6	1572.2	409.3	1547.2	1011.1	58.5	18.0	24.8	0.0	0.0	2564.0
	Uthukela	288.0	358.3	391.0	756.2	1055.2	490.0	1569.5	435.8	1509.4	1123.7	60.5	17.9	25.4	0.0	0.0	2696.3
	UMgungundlovu	421.1	133.1	375.2	1196.1	1100.5	556.9	1586.8	536.8	1509.0	1848.7	50.5	15.4	19.1	0.0	0.0	2737.9
	Ugu	400.7	150.2	421.2	1015.2	1044.7	514.1	1532.9	540.1	1426.9	1630.7	56.5	18.5	21.9	0.0	0.0	2688.5
North West	Dr Kenneth Kaunda	378.5	23.0	319.9	1177.1	793.3	965.1	2012.9	766.5	1456.2	1563.1	67.4	19.6	25.1	0.0	0.0	3287.8
	Dr Ruth Segomotsi	224.0	311.5	353.8	705.7	707.1	799.5	1773.7	585.6	1389.6	934.2	78.7	23.1	34.3	0.0	0.0	2889.3
	Ngaka Modiri Molema	245.9	160.5	520.7	701.2	679.1	712.1	1710.8	639.6	1376.7	986.8	59.5	18.2	27.9	0.0	0.0	2778.4
	Bojanala	212.7	139.6	410.6	770.7	641.1	744.8	1697.4	591.3	1325.0	1013.8	50.4	16.1	23.8	0.0	0.0	2702.1
Gauteng	City of Tshwane	107.8	147.7	164.8	786.5	668.6	422.1	1452.3	632.4	917.0	1380.8	51.5	15.4	23.4	0.0	0.0	2619.9
	City of Johannesburg	76.9	116.0	168.0	571.3	517.4	317.6	1239.9	481.4	771.0	940.5	40.3	15.3	22.4	0.0	0.0	2138.7
	Ekurhuleni	80.0	149.4	161.1	571.2	549.7	325.0	1243.5	495.7	788.6	998.8	47.5	18.7	27.5	0.0	0.0	2143.2
	West Rand	285.4	83.3	146.9	1734.6	1079.9	751.0	1657.5	1162.1	1068.5	4105.0	52.4	16.8	16.8	0.0	0.0	3368.2
	Sedibeng	131.3	207.3	186.9	886.2	820.8	496.1	1541.8	752.1	1013.6	1711.5	61.6	18.4	26.6	0.0	0.0	2838.6
Mpumalanga	Ehlanzeni	222.8	148.7	352.7	725.4	628.5	512.9	1083.3	374.6	1113.8	783.8	50.2	12.1	13.7	0.0	0.0	2173.6
	Nkangala	206.5	206.3	405.2	656.9	649.7	497.4	1058.0	361.6	1133.4	793.7	52.4	11.5	17.0	0.0	0.0	2050.7
	Gert Sibande	164.4	139.6	317.9	509.2	502.4	377.1	919.3	274.7	930.7	579.0	44.4	10.7	16.5	0.0	0.0	1674.6
Limpopo	Waterberg	121.3	69.7	573.5	791.5	621.9	444.2	1109.6	320.6	1148.8	521.5	92.6	16.7	30.2	0.0	0.0	2623.5
	Capricorn	153.4	38.5	701.7	795.6	626.8	434.3	1116.2	361.4	1202.8	622.8	72.5	12.7	25.4	0.0	0.0	2733.4
	Vhembe	315.3	22.4	1093.6	1372.5	787.6	589.3	1251.0	608.9	1440.5	1129.4	68.6	13.9	19.8	0.0	0.0	3409.1
	Mopani	159.4	45.8	656.2	923.8	705.2	505.0	1220.0	381.9	1272.9	715.3	86.7	15.7	26.5	0.0	0.0	2832.3

Figures 3.5 to 3.7 illustrate trends in the age-standardised death-rates per 100,000 for HIV/AIDS, Ischemic heart disease and Interpersonal violence, respectively. The grey dots represent the provinces and lines are colour coded by district. Although scales differ across provinces, the plots illustrate the within province and across district variation.

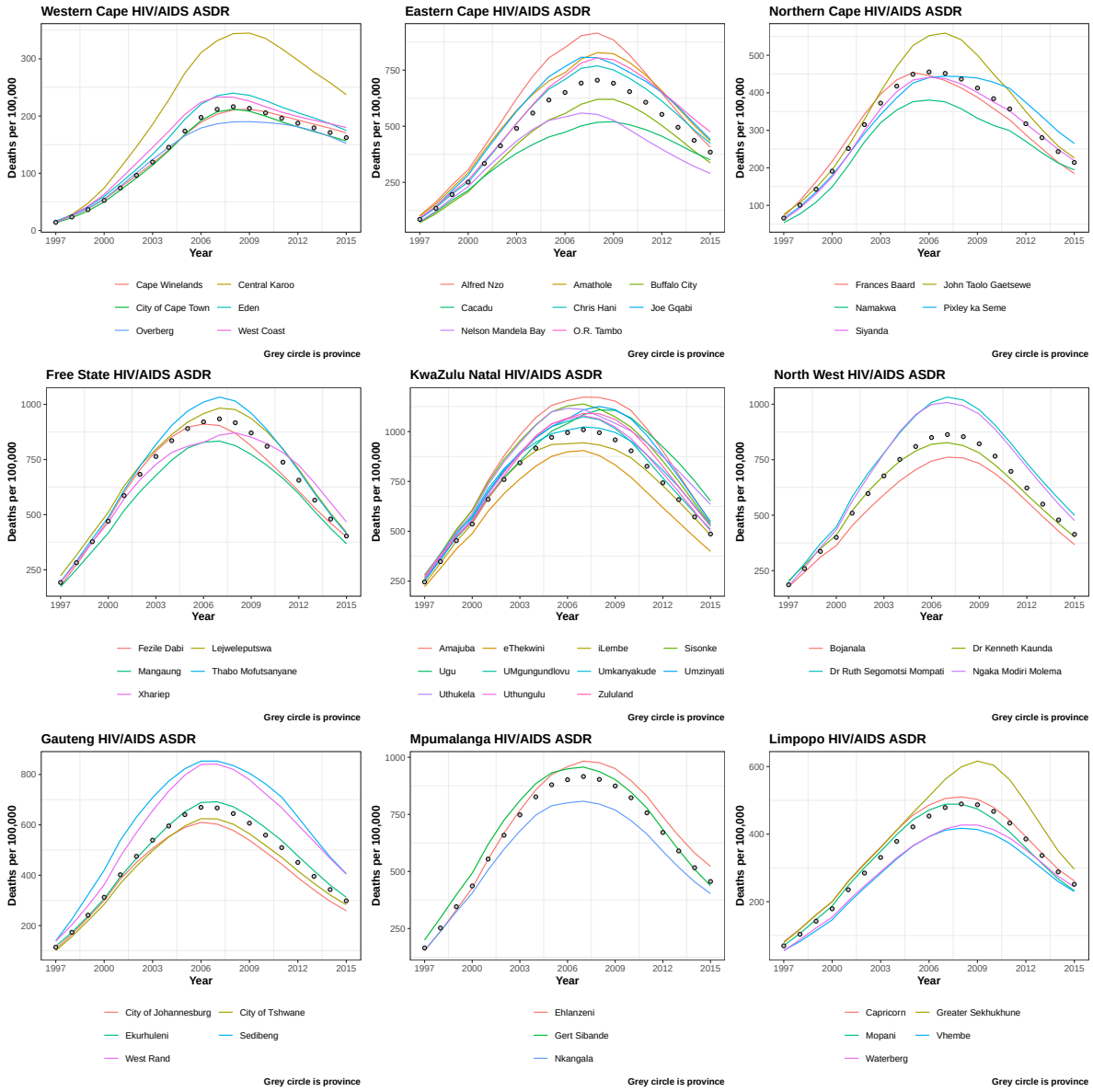

Figure 3.5: HIV/AIDS ASR by district

As with the HIV, there is significant variation across districts for Ischemic heart disease, but unlike for HIV, by 2015, the levels for most districts have not changed significantly from the 1997 levels. Furthermore, most provinces have a pattern dominated by largest district e.g. City of Cape Town in Western Cape which influences other district patterns.

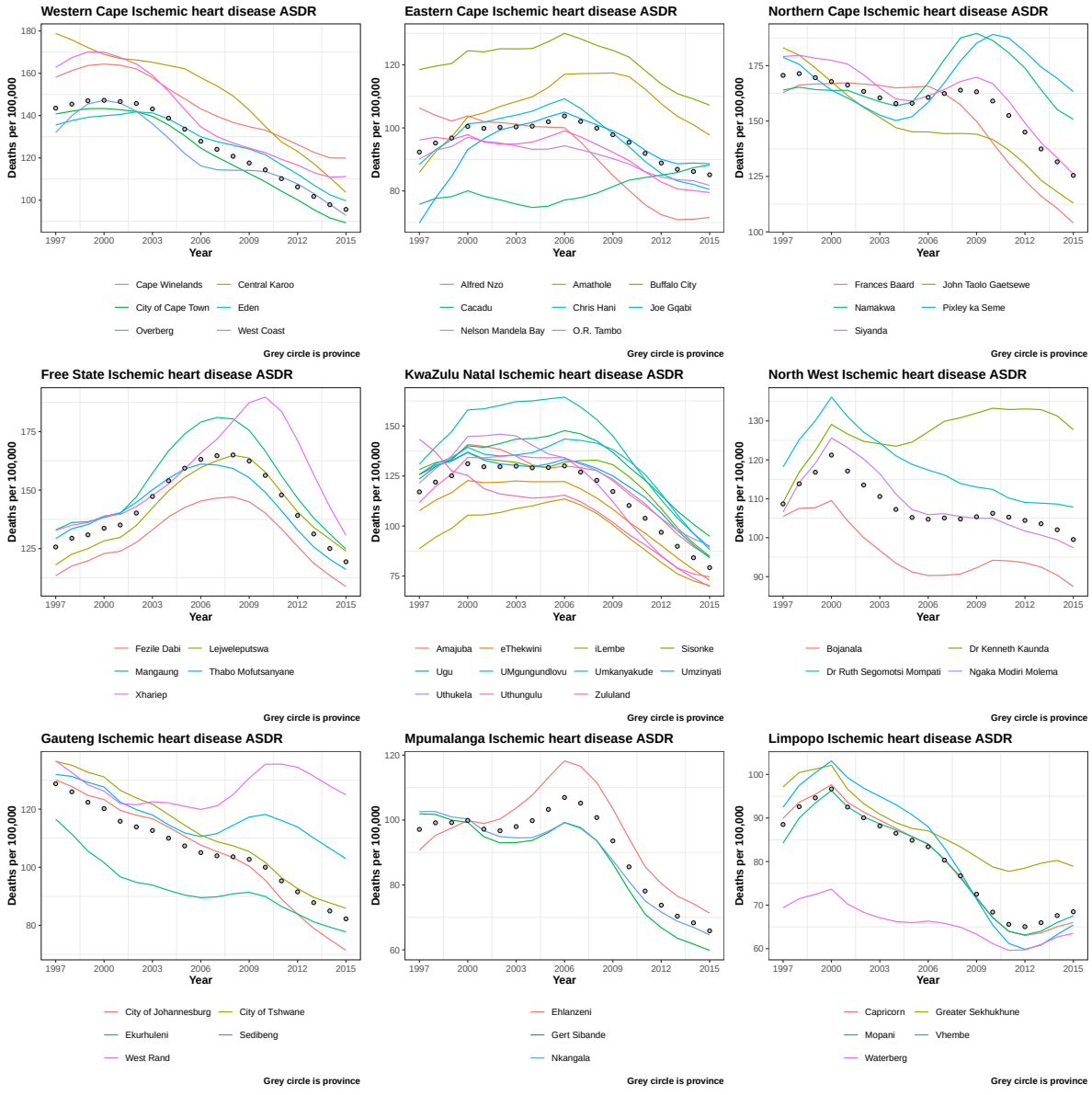

Figure 3.6: Ischemic Heart Disease ASR by district

The ASDR trends for Interpersonal violence repeat the relative patterns seen for the other two causes, i.e. an overall provincial pattern that is fed from the principal district but wide variations in actual levels. Although only 3 causes are shown here, detailed trends by district, sex, age and cause with uncertainty intervals are available in the appendix.

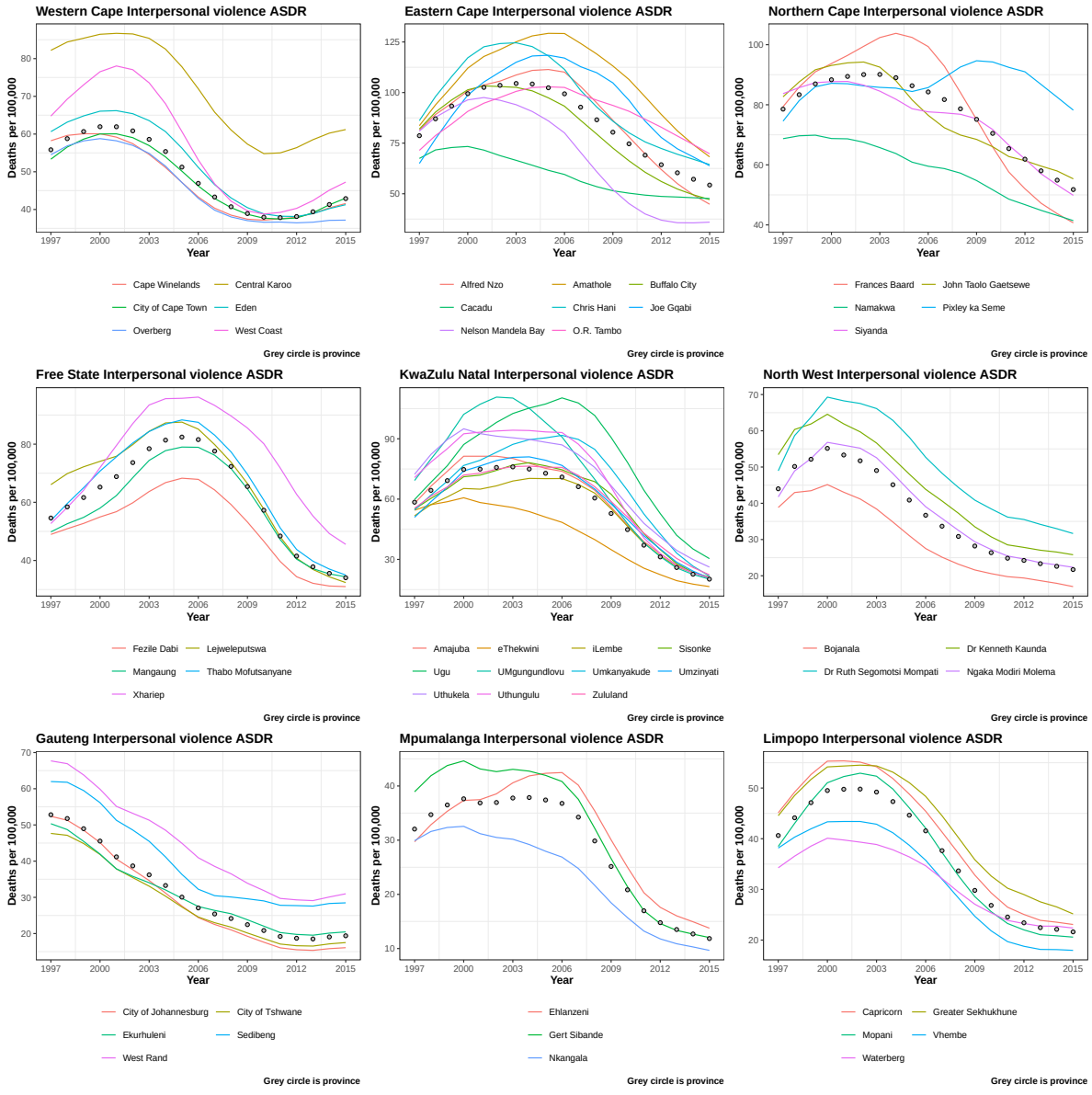

Figure 3.7: Interpersonal violence ASR by district

3.4 Discussion

This study is the first to produce district specific estimates of the major causes of death for South Africa. Building upon the reported numbers that are available from the country's vital registration system, the results produced account for both model uncertainty and uncertainty in the completeness of reporting. The model also produces estimates corrected for the misclassification of HIV/AIDS deaths and the misattribution of causes to ill-defined and garbage codes. The Dirichlet-Multinomial seed used in the 3-dimensional iterative proportional fitting insures that the marginals are strongly informed and district specific, having been estimated using the district level covariate values. In addition, iterative fitting to the province by sex, age, year and cause leads to estimates that are at the very least consistent at the aggregate, a criterion necessary for subnational estimates to be reliable.

The patterns that are observed follow directly from what is known about South African epidemiology. Mortality profiles are generally comprised of 1997 estimates being relatively low, rising to a peak in the mid-2000s due to the high rates of HIV mortality and then falling by 2015. As shown in Aim 1, this reduction has led to sustained improvements in life-expectancy as well as adult and child mortality. What this study has added are results that can be used for finer and more detailed comparisons, honing is on district differences by sex, age and cause at a granularity that was not possible before. As Figures 3.5 to 3.7 show, there are wide variations in the ASDR levels across districts and provinces and trends differ for many districts as well. The estimates produced here can be used to investigate the extent of those differences for specific age-groups, years and sexes combinations which would be informative for certain public health policy that is built to target at more specific levels. An example of this is shown in Figure 3.8, a map of South Africa's districts showing variations in self-harm mortality rates per 100,000 population for males aged 25-29 in the year 2015. According to the model these deaths are concentrated in certain metropolitan districts, the City if Cape Town and the City if Johannesburg in particular. The plot also shows that in general, rates for Eastern Cape are higher than for other provinces.

Researchers can then use such results to formulate hypotheses and investigate conditions as well as specific age-groups by sex and year, that would most likely be ignored in the absence of more detailed data.

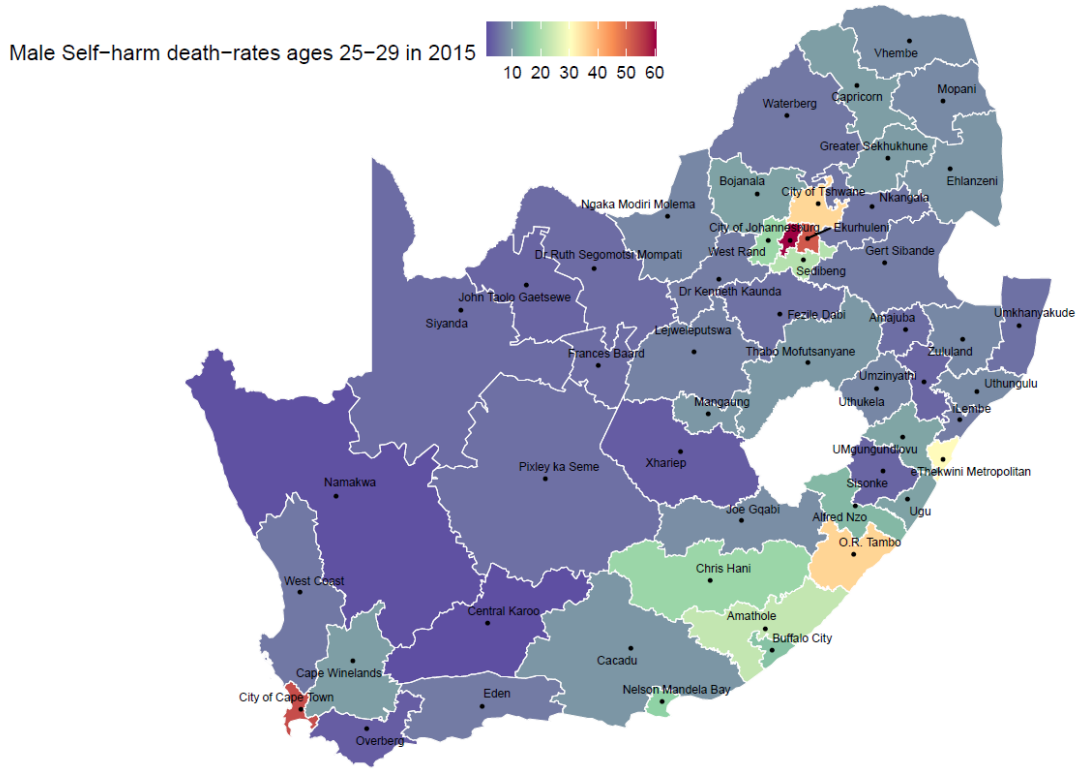

Figure 3.8: South Africa map of self-harm rates for males ages 20-24, 2015

There are limitations. The model is used to estimate the number of deaths attributable to 15 cause groupings. Although the selected list covers more than 85% of deaths for the country over the estimation period, with the remaining 15% grouped as “All Other”, the proportion covered is inversely related to age. The list of causes covers over 90% of deaths for some age-groups but accounts for 80% of all deaths aged 75-79 and this falls by age to covering 65% of deaths for the open interval age 95 and older. Noting that this proportion is at the aggregate level, we realise that this would mean for some districts and ages, the list covers more than 90% deaths whereas for others it will be less than 65%. The

limitation becomes that some single causes that are responsible for significant proportions of deaths may be hidden in the rest category, especially for the oldest ages. The challenge is not in finding or selecting these causes in the GBD results list, rather the model remaining robust in its estimation of the cause fractions if they are included. The model derives an intercept and equation for each cause and quantifies the correlation between the large numbers of variables. Increasing either the number of dependent or independent variables is not only computationally challenging but can also increase the uncertainty to levels that make the results uninformative.

As has been described, the Dirichlet regression model takes a number of variables at the province level and quantifies the relationships between those variables and the true cause-of-death fractions estimated in GBD2017. Once estimated, these "relationships" or priors within the Bayesian framework, can be used together with data specific for the district, to derive posterior distributions for the district cause-specific mortality. As with the all-cause estimation limitations described in the previous chapter, there is no gold standard data source for the district with which to either compare estimates to, assessing validity, or to adjust with to correct for known methodological bias. The assumption that the GBD2017 gives the true underlying cause at the province level is also one that has its flaws. The GBD methods are refined with each iteration and as more and in some cases even different input data are used, this may change some of the results. This has a knock on effect on the permanence of these conditional results.

Put to the case that the GBD results are 100% accurate, one still introduces potential bias when using the known information for a larger area to determine something unknown for a smaller area. This bias is broadly defined as the *ecological fallacy* [65] and closely related to it is *Simpson's paradox* [66]. The ecological fallacy refers to incorrectly inferring characteristics that are true for an aggregate area to a subdivision of that area whereas Simpson's paradox occurs when certain relationships that are identified for the aggregate are in actual fact different or even reversed for the subdivision [67]. This is of relevance

as many provinces are not uniform but have differing socio-demographic profiles. The reported data for the province is largely influenced by the reported data for the largest districts. The estimated coefficients are likewise most strongly related to these larger districts which may bias the results for the districts within the same province whose coefficients are significantly different.

REFERENCES

[1] BA Dormer et al. Tuberculosis in South Africa. *Proceedings of the Transvaal Mine Medical Officers' Association*, 27(298):63–73, 1948.

[2] Geoffrey Dean. Lung cancer among white South Africans. *British medical journal*, 2(5156):852, 1959.

[3] AM Adelstein. Some Aspects of Cardio-vascular Mortality in South Africa. *British journal of preventive & social medicine*, 17(1):29–40, 1963.

[4] Geoffrey Dean. Lung cancer in South Africans and British immigrants, 1964.

[5] Geoffrey Dean. Annual incidence, prevalence, and mortality of multiple sclerosis in white South-African-born and in white immigrants to South Africa. *British medical journal*, 2(5554): 724, 1967.

[6] JL Botha and D Bradshaw. African vital statistics-a black hole? *South African medical journal= Suid-Afrikaanse tydskrif vir geneeskunde*, 67(24):977–981, 1985.

[7] Andrew Dawes, Colin Tredoux, and Andrew Feinstein. Political violence in South Africa: Some effects on children of the violent destruction of their community. *International journal of mental health*, 18(2):16–43, 1989.

[8] Abdel R Omran. The epidemiologic transition: a theory of the epidemiology of population change. *The Milbank Quarterly*, 83(4):731–757, 2005.

[9] Stephen M Tollman, Kathleen Kahna, Michel Garenne, and John SS Gear. Reversal in mortality trends: evidence from the Agincourt field site, South Africa, 1992-1995. *Aids*, 13(9):1091–1097, 1999.

[10] Rob Dorrington, David Bourne, Debbie Bradshaw, Ria Laubscher, and Ian M Timæus. *The impact of HIV/AIDS on adult mortality in South Africa*. Medical Research Council Cape Town, 2001.

[11] Pam Groenewald, Nadine Nannan, David Bourne, Ria Laubscher, and Debbie Bradshaw. Identifying deaths from AIDS in South Africa. *Aids*, 19(2):193–201, 2005.

[12] Jeanette Kurian Birnbaum, Christopher JL Murray, and Rafael Lozano. Exposing misclassified HIV/AIDS deaths in South Africa. *Bulletin of the World Health Organization*, 89(4):278–285, 2011.

[13] Olive Shisana and Leickness Chisamu Simbayi. *Nelson Mandela/HSRC study of HIV/AIDS: South African national HIV prevalence, behavioural risks and mass media: household survey 2002*. HSRC Press, 2002.

[14] Olive Shisana. *South African national HIV prevalence, HIV incidence, behaviour and communication survey, 2005*. HSRC press, 2005.

[15] Olive Shisana, Thomas Rehle, LC Simbayi, Khangelani Zuma, Sean Jooste, Nompumelelo Zungu, Demetre Labadarios, and D Onoya. South African national HIV prevalence, incidence and behaviour survey, 2012. 2014.

[16] UNAIDS. Spectrum model. `www.unaids.org/en/dataanalysis/tools/spectrumepp2011/`, 2012.

[17] Actuarial Society of South Africa. ASSA2008 model. `aids.actuarialsociety.org.za/ASSA2008-Model-3480.htm`, 2012.

[18] Theron Moodley, Dhayendre Moodley, Motshedisi Sebitloane, Niren Maharaj, and Benn Sartorius. Improved pregnancy outcomes with increasing antiretroviral coverage in south africa. *BMC pregnancy and childbirth*, 16(1):35, 2016.

[19] Bongani M Mayosi, Alan J Flisher, Umesh G Lalloo, Freddy Sitas, Stephen M Tollman, and Debbie Bradshaw. The burden of non-communicable diseases in south africa. *The Lancet*, 374 (9693):934–947, 2009.

[20] Mohamed Seedat, Ashley Van Niekerk, Rachel Jewkes, Shahnaaz Suffla, and Kopano Ratele. Violence and injuries in South Africa: prioritising an agenda for prevention. *The Lancet*, 374 (9694):1011–1022, 2009.

[21] Andreas Plüddemann, Charles Parry, Hilton Donson, and Anesh Sukhai. Alcohol use and trauma in Cape Town, Durban and Port Elizabeth, South Africa: 1999-2001. *Injury control and safety promotion*, 11(4):265–267, 2004.

[22] Carla AbouZahr and Ties Boerma. Health information systems: the foundations of public health. *Bulletin of the World Health Organization*, 83(8):578–583, 2005.

[23] Prasanta Mahapatra, Kenji Shibuya, Alan D Lopez, Francesca Coullare, Francis C Notzon, Chalapati Rao, Simon Szreter, et al. Civil registration systems and vital statistics: successes and missed opportunities. *The Lancet*, 370(9599):1653–1663, 2007.

[24] Colin D Mathers, Doris Ma Fat, Mie Inoue, Chalapati Rao, and Alan D Lopez. Counting the dead and what they died from: an assessment of the global status of cause of death data. *Bulletin of the world health organization*, 83(3):171–177c, 2005.

[25] David E Phillips, Rafael Lozano, Mohsen Naghavi, Charles Atkinson, Diego Gonzalez-Medina, Lene Mikkelsen, Christopher JL Murray, and Alan D Lopez. A composite metric for assessing data on mortality and causes of death: the vital statistics performance index. *Population health metrics*, 12(1):14, 2014.

[26] Mohsen Naghavi, Susanna Makela, Kyle Foreman, Janaki O'Brien, Farshad Pourmalek, and Rafael Lozano. Algorithms for enhancing public health utility of national causes-of-death data. *Population health metrics*, 8(1):9, 2010.

[27] Alan D Lopez and Christopher JL Murray. *The Global Burden of Disease: A Comprehensive Assessment of Mortality and Disability from Diseases, Injuries, and Risk Factors in 1990 and Projected to 2020; Summary*. Harvard School of Public Health, 1996.

[28] World Health Organization. *International statistical classification of diseases and related health problems*, volume 1. World Health Organization, 2004.

[29] Victoria Pillay-van Wyk, William Msemburi, Ria Laubscher, Rob E Dorrington, Pam Groenewald, Tracy Glass, Beatrice Nojilana, Jané D Joubert, Richard Matzopoulos, Megan Prinsloo, et al. Mortality trends and differentials in South Africa from 1997 to 2012: second National Burden of Disease Study. *The Lancet Global Health*, 4(9):e642–e653, 2016.

[30] Haidong Wang, Mohsen Naghavi, Christine Allen, Ryan M Barber, Zulfiqar A Bhutta, Austin Carter, Daniel C Casey, Fiona J Charlson, Alan Zian Chen, Matthew M Coates, et al. Global, regional, and national life expectancy, all-cause mortality, and cause-specific mortality for 249 causes of death, 1980–2015: a systematic analysis for the global burden of disease study 2015. *The Lancet*, 388(10053):1459–1544, 2016.

[31] N Massyn, N Peer, A Padarath, P Barron, and C Day. District Health Barometer 2014/15. *Durban: Health Systems Trust*, 2015.

[32] Debbie Bradshaw, William Msemburi, Rob Dorrington, Victoria Pillay-van Wyk, Ria Laubscher, Pam Groenewald, South African National Burden of Disease Study team, et al. HIV/AIDS in South Africa: how many people died from the disease between 1997 and 2010? *AIDS*, 30(5):771–778, 2016.

[33] Richard Matzopoulos, Megan Prinsloo, Victoria Pillay-van Wyk, Nomonde Gwebushe, Shanaaz Mathews, Lorna J Martin, Ria Laubscher, Naeemah Abrahams, William Msemburi, Carl Lombard, et al. Injury-related mortality in South Africa: a retrospective descriptive study of postmortem investigations. *Bulletin of the World Health Organization*, 93(5):303–313, 2015.

[34] S Burrows, B Bowman, R Matzopoulos, and A Van Niekerk. A profile of fatal injuries in South Africa 2000: second annual report of the national injury mortality surveillance system (NIMSS) 2000. *Cape Town*, 2001.

[35] R Matzopoulos, LJ Martin, S Wadee, V Thomson, M Prinsloo, D Bourne, P Groenewald, N Naledi, and J Myers. The provincial injury mortality surveillance system (pimss): a surveillance tool for the western cape. *Injury Prevention*, 16(Suppl 1):A47–A48, 2010.

[36] Vergil N Slee. The international classification of diseases: ninth revision (icd-9). *Annals of internal medicine*, 88(3):424–426, 1978.

[37] Rafael Lozano, Mohsen Naghavi, Kyle Foreman, Stephen Lim, Kenji Shibuya, Victor Aboyans, Jerry Abraham, Timothy Adair, Rakesh Aggarwal, Stephanie Y Ahn, et al. Global and regional mortality from 235 causes of death for 20 age groups in 1990 and 2010: a systematic analysis for the global burden of disease study 2010. *The Lancet*, 380(9859):2095–2128, 2013.

[38] Victoria Pillay-van Wyk, Ria Laubscher, William Msemburi, Rob E Dorrington, Pam Groenewald, Theo Vos, Richard Matzopoulos, Megan Prinsloo, Beatrice Nojilana, Nadine Nannan, et al. Second South African National Burden of Disease Study: Data cleaning, validation and SA NBD List. *Cape Town: Burden of Disease Research Unit, South African Medical Research Council*, 2014.

[39] Samuel H Preston. *Mortality patterns in national populations: with special reference to recorded causes of death*. Elsevier, 2013.

[40] Timo Hakulinen, Harold Hansluwka, AD Lopez, and T Nakada. Global and regional mortality patterns by cause of death in 1980. *International journal of epidemiology*, 15(2):226–233, 1986.

[41] CJ Murray and Alan D Lopez. Global health statistics: a compendium of incidence prevalence and mortality estimates for over 200 conditions. 1996.

[42] Alan D Lopez, Colin D Mathers, Majid Ezzati, Dean T Jamison, and Christopher JL Murray. Global and regional burden of disease and risk factors, 2001: systematic analysis of population health data. *The Lancet*, 367(9524):1747–1757, 2006.

[43] M Naghavi, H Wang, R Lozano, A Davis, X Liang, M Zhou, et al. Gbd 2013 mortality and causes of death collaborators. global, regional, and national age-sex specific all-cause and cause-specific mortality for 240 causes of death, 1990-2013: a systematic analysis for the global burden of disease study 2013. *Lancet*, 385(9963):117–71, 2015.

[44] Ryan M Ahern, Rafael Lozano, Mohsen Naghavi, Kyle Foreman, Emmanuela Gakidou, and Christopher JL Murray. Improving the public health utility of global cardiovascular mortality data: the rise of ischemic heart disease. *Population health metrics*, 9(1):8, 2011.

[45] Haidong Wang, Tim M Wolock, Austin Carter, Grant Nguyen, Hmwe H Kyu, Emmanuela Gakidou, Simon I Hay, Edward J Mills, Adam Trickey, William Msemburi, et al. Estimates of global, regional, and national incidence, prevalence, and mortality of HIV, 1980–2015: the Global Burden of Disease Study 2015. *Lancet HIV*, 3(8):e361–e387, 2016.

[46] Kyle J Foreman, Rafael Lozano, Alan D Lopez, and Christopher JL Murray. Modeling causes of death: an integrated approach using codem. *Population Health Metrics*, 10(1):1, 2012.

[47] Judi Scheffer. Dealing with missing data. 2002.

[48] Ingrid Woolard. An overview of poverty and inequality in south africa. *Unpublished briefing paper, HSRC, Pretoria*, 2002.

[49] Matthew Evans. Structural violence, socioeconomic rights, and transformative justice. *Journal of Human Rights*, 15(1):1–20, 2016.

[50] HCJ Van Rensburg and Solomon R Benatar. The legacy of apartheid in health and health care. *South African Journal of Sociology*, 24(4):99–111, 1993.

[51] Laetitia C Rispel, Pieter de Jager, and Sharon Fonn. Exploring corruption in the south african health sector. *Health policy and planning*, 31(2):239–249, 2015.

[52] Laetitia Rispel. Analysing the progress and fault lines of health sector transformation in south africa. *South African health review*, 2016(1):17–23, 2016.

[53] Michel Garenne, Mark A Collinson, Chodziwadziwa W Kabudula, F Xavier Gómez-Olivé, Kathleen Kahn, and Stephen Tollman. Completeness of birth and death registration in a rural area of south africa: the agincourt health and demographic surveillance, 1992–2014. *Global health action*, 9(1):32795, 2016.

[54] Ahmedin Jemal, Freddie Bray, David Forman, Meg O'brien, Jacques Ferlay, Melissa Center, and D Maxwell Parkin. Cancer burden in africa and opportunities for prevention. *Cancer*, 118 (18):4372–4384, 2012.

[55] Paulo Guimaraes and Richard C Lindrooth. Controlling for overdispersion in grouped conditional logit models: A computationally simple application of dirichlet-multinomial regression. *The Econometrics Journal*, 10(2):439–452, 2007.

[56] Yiwen Zhang, Hua Zhou, Jin Zhou, and Wei Sun. Regression models for multivariate count data. *Journal of Computational and Graphical Statistics*, 26(1):1–13, 2017.

[57] Arto Klami, Abhishek Tripathi, Johannes Sirola, Lauri Väre, and Frederic Roulland. Latent feature regression for multivariate count data. In *Artificial Intelligence and Statistics*, pages 462–470, 2015.

[58] Catherine Crea, R Ayesha Ali, and Romina Rader. A new model for ecological networks using species-level traits. *Methods in Ecology and Evolution*, 7(2):232–241, 2016.

[59] Dudley L Poston Jr and Hosik Min. The multinomial regression modeling of the cause-of-death mortality of the oldest old in the us. *Journal of Modern Applied Statistical Methods*, 7(2): 24, 2008.

[60] Soheil Saadat, Mahmoud Yousefifard, Hadi Asady, Ali Moghadas Jafari, Mohammad Fayaz, and Mostafa Hosseini. The most important causes of death in iranian population; a retrospective cohort study. *Emergency*, 3(1):16, 2015.

[61] Kyle J Foreman, Mohsen Naghavi, and Majid Ezzati. Improving the usefulness of us mortality data: new methods for reclassification of underlying cause of death. *Population health metrics*, 14(1):1, 2016.

[62] James E Mosimann. On the compound multinomial distribution, the multivariate β-distribution, and correlations among proportions. *Biometrika*, 49(1/2):65–82, 1962.

[63] Andrew Gelman, Daniel Lee, and Jiqiang Guo. Stan: A probabilistic programming language for bayesian inference and optimization. *Journal of Educational and Behavioral Statistics*, 40(5): 530–543, 2015.

[64] Y Zhang and H Zhou. Mglm: Multivariate response generalized linear models. *R package version 0.0*, 7, 2016.

[65] Steven Piantadosi, David P Byar, and Sylvan B Green. The ecological fallacy. *American journal of epidemiology*, 127(5):893–904, 1988.

[66] Miguel A Hernán, David Clayton, and Niels Keiding. The simpson's paradox unraveled. *International journal of epidemiology*, 40(3):780–785, 2011.

[67] Jon Wakefield. Ecological inference for 2× 2 tables. *Journal of the Royal Statistical Society: Series A (Statistics in Society)*, 167(3):385–425, 2004.

Chapter 4

SOUTH AFRICA MORTALITY FORECASTS BY DISTRICT (2016–2030)

4.1 Introduction

The first two aims of this research describe the input data and methodology applied to estimate all-cause and cause-specific mortality for South Africa's 52 health districts for the years 1997 through to 2015, and give detailed summaries of the estimates generated. The results echo the conclusions from the NBD [1] and GBD [2] studies and show that mortality levels in South Africa have changed significantly over the final decade of the twentieth and first two decades of the twenty-first centuries. The results also show that there are wide variations across districts. As mentioned previously, following initial overall increases attributable to rising HIV/AIDS mortality in particular, the roll-out of ART in 2003 and child survival improvements paralleling global trends, the country has experienced mortality improvements [3]. These improvements are positive for the individual and for the society as a whole but do however necessitate sufficient preparedness by public and private sector health-care to meet the demands of an ageing population. To anticipate the population needs and adequately plan for them, the analysis of mortality patterns must not only be retrospective and current but prospective as well, requiring modelling and forecasting of future mortality patterns.

Until recently, observed time-series data for South Africa have been sparse and there has not been any research conducted on subnational multiple-cause mortality forecasting for the country. In addition, the complex impact of HIV/AIDS on the mortality pattern both

increased uncertainty and decreased the reliability of results even if such forecasts had been made. With the effective roll out of ART, the more estimable pattern of on-treatment HIV mortality and the accumulation of empirical data-points, more reliable forecasts for the country are now feasible and this research aims to achieve this. Specifically, this third aim seeks to answer the following two questions:

- how much improvement in overall mortality can we expect for the years 2016 to 2030, assuming the rates of change in all-cause mortality observed to 2015 persist to the end of that period?
- contingent on the projected all-cause numbers and assuming trends in cause-patterns also persist to 2030, what future levels of mortality can we expect for the causes that are estimated to be inflicting the highest mortality burden between 1997 and 2015?

To answer these questions a similar approach is taken as with previous aims. The section begins by reviewing the literature on mortality forecasting and focuses on the Lee-Carter method [4] and its underlying age-period-cohort framework. The age-period-cohort framework has been established as being one of the most robust for mortality forecasting, retaining the age-pattern of each forecast and accurately predicting mortality levels and trends in short-term as well as long-term forecasts.

In the review section, the methods used by Foreman et al. [5] to forecast out of the GBD2016 are also explored. The study by Foreman et al. [5] is the most comprehensive forecasting study to-date in terms of its inclusion of all the GBD2016 countries as well as the detailed cause-list forecasted for each.

Finally the methods used to forecast district, province and national all-cause as well as cause-specific mortality for leading causes and selected cause categories in this study are described. As with the first two aims, summary results are included herein and more detailed results can be found in an accompanying appendix.

4.2 Review of mortality forecasting methods

Booth and Tickle [6] conducted a review of mortality modelling and forecasting methods and grouped them into three broad categories. The first group comprises of the *extrapolation* methods which make use of the regularity of age patterns and trends over time. Such methods make assumptions about the connection between observed retrospective mortality trends and future trends using time-series methods. The extensive literature, established mathematical formulae for time-series analysis and the fact that the required data are relatively simple, are among the main reasons why *extrapolation* methods are the most widely utilized of the mortality forecasting methods.

A second group is made up of the *explanation* methods which utilize structural or epidemiological models of mortality from certain causes of death for which the key covariates in the causal pathway of the cause can be measured. The compartmental models such as Spectrum [7], ASSA [8] and THEMBISA [9] fall in this group. The required data as well as the computational requirements of this class of techniques are relatively more involving than for the *explanation* methods.

A third group can be defined as *expectation*, for which forecasts are based on the opinions of experts. The result is generally a fixed rate of increase or decrease for the forecasted measure based on the information available to the expert. The challenge with this approach is the subjectivity of either the direction or magnitude of the change moving forward, which may not have reproducible reasoning to support validity.

The *extrapolation* methods are the selected approach for this research. This is primarily because of the nature of the available data for South Africa; considering both the structure and the period covered by the estimated data from aims 1 and 2. We have district, province and national cause-age-sex-specific retrospective time-trends of adjusted deaths for 1997 to 2015. Based on these, we would like to forecast mortality trends to inform on the most likely health paths the different locations are travelling.

There would be a significant challenge obtaining unbiased district-level covariates with sufficient records over time that they can be forecasted and in turn used to facilitate *explanation* type forecasts for the country. There have only been three censuses in the country since 1994 to provide district-level covariates that can be used to explain district level mortality [10]. Likewise, the *expectation* type forecasts would not only be challenging, but would also potentially be uninformative, considering the number of districts-cause-age combinations to consider and the uncertainty around the estimates. The *extrapolation* methods are thus geared to be the best of the available methods based on the data at hand.

The major problem for age, cause or geography specific modelling and extrapolative forecasting of mortality is the high dimensionality of the data. Age-patterns of all-cause as well as cause-specific deaths and the population exposed for the rate estimate must be considered. In order to deal with the dimensionality problem while retaining the correct relative age relationships over time, it is necessary to use models allowing a more parsimonious representation of the data. One of the most influential of the parsimonious extrapolative mortality forecasting approaches is the Lee-Carter model [4].

4.2.1 Lee-Carter and age-period-cohort models

The basic Age-Period Lee-Carter model (AP-LC) was developed by Lee and Carter [4] and was further extended by Lee [11]. The method models $m_x(t)$, representing the central death rate for individual ages (x) and calendar years (t), using:

$$\text{AP-LC}: \quad \ln m_x(t) = \alpha_x + \beta_x \kappa_t + \varepsilon_{xt}\,, \tag{4.1}$$

where the β_x are age-specific scaling factors relating the time varying parameter κ_t to the age-specific central mortality rate, the α_x are constant age-specific mortality patterns, and time and age dependent random effects are assumed $\varepsilon_{xt} \sim N\left(0, \sigma^2\right)$.

Parameters α_x, β_x and κ_t are estimated from experienced mortality, obtaining the estimates $\hat{\alpha}_x$, $\hat{\beta}_x$ and $\hat{\kappa}_t$ [12]. Forecasts follow by modelling the values of κ_t as a time series, e.g. a random walk with drift. The bilinear multiplicative construct $(\beta_x \kappa_t)$ in equation (4.1) creates an identifiability traditionally resolved by constraining these parameters using:

$$\sum_x \hat{\beta}_x = 1\,, \quad \sum_t \hat{\kappa}_t = 0\,. \tag{4.2}$$

Starting from a given year t, forecasts of mortality rates are then computed for $s = 1, 2, \ldots$, as follows:

$$m_x(t+s) = \exp\left(\hat{\alpha}_x + \hat{\beta}_x \hat{\kappa}_{t+s}\right) = m_x(t) \exp\left[\hat{\beta}_x \left(\hat{\kappa}_{t+s} - \hat{\kappa}_t\right)\right] \tag{4.3}$$

The AP-LC approach has been used extensively in the forecasting of mortality. In the USA, for example, the model has been the standard framework for modelling and projecting mortality trends since its introduction [4, 13]. The model has also been applied in Canada [14], to Japanese mortality data [15] and to death data from the United Kingdom [16]. Subsequently, the AP-LC model has been re-evaluated by a number of researchers to try and improve the model fit and to optimize the model's properties for forecasting [17, 18, 19, 20, 21].

The proliferation of re-evaluations has led to research being conducted to determine what aspects are common to the models. Hunt and Blake [22] reviewed their structure and identified an age-period-cohort (APC) model structure. This APC framework encompasses most of the stochastic forecasting models for mortality. Currie [23] extended this to show that the majority of these types of models can be expressed as generalized non-linear models or generalized linear models. More recently, Millossovich et al. [24] have extended this work. The similarities across the plethora of LC extensions allows for an APC framework that simplifies comparing the various forecasting models.

4.2.1.1 *Generalized APC stochastic mortality models*

Most extrapolation type mortality models follow a framework similar to that of generalized linear models [22, 23]. We can D_{xt} as the number of deaths aged x in year t, d_{xt} as the observed number of deaths and N_{xt} the population at risk. Furthermore, with μ_{xt} and m_{xt} representing the force of mortality and death rates, respectively, we:

$$\hat{m}_{xt} = d_{xt}/N_{xt}$$

were the $\hat{m}_{xt}$ is an empirical estimate. Assuming constant μ_{xt} over each year of x and t, the force of mortality and death rate m_{xt} coincide. Similar to generalized linear models [25], a Generalized APC model can be expressed in terms of four parts:

1. The *random component*: assuming $\mathbb{E}(D_{xt}/N_{xt}) = \mu_{xt}$, the numbers of deaths D_{xt} follow a Poisson distribution so that $D_{xt} \sim \text{Poisson}(N_{xt}\mu_{xt})$
2. The *systematic component*: a *predictor* η_{xt} captures the effects year t, age x and cohort birth year $c = t - x$ [22] and is given by:

$$\eta_{xt} = \alpha_x + \sum_{i=1}^{T} \beta_{i,x}\kappa_{i,t} + \beta_{0,x}\gamma_{t-x}.$$

   where α_x is an age-specific constant that captures the general age-pattern of mortality, $T \geq 1$ is integer valued and indicates how many age-period terms there are to describe the mortality trends. The $\beta_{i,x}$ are used to control the age-specific mortality effect and the $\kappa_{i,t}$, $i = 1, \ldots, T$ are time-specific indices. The cohort effects are accounted for by the γ_{t-x} and the $\beta_{0,x}$ control for how that is experienced across the different ages.
3. The function g is known as the *link* and connects the systematic and random components so that using the canonical log-link,

$$g\left(\mathbb{E}\left(\frac{D_{xt}}{E_{xt}}\right)\right) = \eta_{xt}.$$

4. The *constraints for each parameter*: parameter constraints are required to be able to identify unique parameters. These is accomplished using a *constraint function* v mapping an arbitrary parameter vector

$$\theta := \left(\underbrace{\alpha_x}_{\text{General shape}} ; \underbrace{\beta_{1,x},\ldots,\beta_{T,x}}_{\text{Time index control}} ; \underbrace{\kappa_{1,t},\ldots,\kappa_{T,t}}_{\text{Time index effect}} ; \underbrace{\beta_{0,x}}_{\text{Cohort control}} ; \underbrace{\gamma_{t-x}}_{\text{Cohort effect}} \right)$$

into a transformed parameter vector

$$v(\theta) = \tilde{\theta} = \left(\tilde{\alpha}_x; \tilde{\beta}_{1,x},\ldots,\tilde{\beta}_{T,x}; \tilde{\kappa}_{1,t},\ldots,\tilde{\kappa}_{T,t}; \tilde{\beta}_{0,x}; \tilde{\gamma}_{t-x}\right)$$

which does not affect the predictor but satisfies the model constraints.

A number of the mortality forecasting models proposed in the literature can be described using the GAPC framework e.g. the original AP-LC model and all of the subsequent extensions proposed by Renshaw and Haberman [20, 26] and the Cairns, Blake, and Dowd (CBD) model and it's extensions [27]. Many other model structures dominating the literature fall within the GAPC class of models [28, 29, 30, 31, 32, 33, 34, 35]. The Generalized APC structure of six of these, which are considered in literature to be the most reliable, is summarized in Table 4.1.

Model	**Predictor**
LC	$\eta_{xt} = \alpha_x + \beta_{1,x}\kappa_{1,t}$
CBD	$\eta_{xt} = \kappa_{1,t} + (x-\bar{x})\kappa_{2,t}$
APC	$\eta_{xt} = \alpha_x + \kappa_{1,t} + \gamma_{t-x}$
RH	$\eta_{xt} = \alpha_x + \beta_{1,x}\kappa_{1,t} + \gamma_{t-x}$
M7	$\eta_{xt} = \kappa_{1,t} + (x-\bar{x})\kappa_{2,t} + \left((x-\bar{x})^2 - \hat{\sigma}_x^2\right)\kappa_{3,t} + \gamma_{t-x}$
PLAT	$\eta_{xt} = \alpha_x + \kappa_{1,t} + (\bar{x}-x)\kappa_{2,t} + \gamma_{t-x}$

Table 4.1: Model structures of main forecasting models

The *extrapolation* mortality models dominate the literature due to their not requiring extensive data for forecasting. The dependence of the mortality outcome on time and previous values alone has allowed for a number of key mortality forecasts to be made [36, 37, 38]. They have generally been used to forecast all-cause age-specific mortality and life-expectancy [39], or else single-cause mortality under the assumption that the cause-specific mortality trend has been stationary over time and is expected to persist into the forecast period [40].

The performance of these models hinges on a sufficient number of retrospective data points being available [41]. Consequently, the extrapolation type models have a number of limitations. As Hyndman et al. [41] mentions, they begin to function poorly when there are an insufficient number of observed data points relative to the number of points or parameters to be estimated. Likewise, when there are mortality spikes or the observed data points follow extreme trends that would be unreasonable to assume for the future, the retrospective trends have reduced usefulness. Another challenge is that although they make use of the association with time, the extrapolation models have no causal information. As such, one does not have any insight as to the variables influencing the trend and correspondingly, one cannot assess and compare varying mortality scenarios related to varying covariates, beyond interpreting the statistical uncertainty assumed in the stochastic structure of the model.

An example of extreme trends in mortality are the deaths due to HIV/AIDS in sub-Saharan Africa at the turn of the 21st century. After carrying a heavy mortality burden, there have been significant reductions in high prevalence countries like South Africa [42], gains which can directly be attributed to interventions and treatment. Due to the extreme changes in mortality in a short period, using the time-trend alone to predict beyond this period can lead to unrealistic estimates due to only a few data points being observed. The *explanation* type models like Spectrum [43], ASSA [44] and THEMBISA [9] utilize the links between the extent of treatment, the breadth of interventions, the level of prevalence and

population demography to estimate the mortality impact of HIV/AIDS. With these models, having forecasts of the drivers of HIV/AIDS mortality together with forecasts of HIV free mortality enables one to forecast more realistic total mortality.

4.2.2 The Singular Value Decomposition extension to Lee-Carter

In the original paper, Lee and Carter [39] point out that the $\beta_x\kappa_t$ can actually be estimated using a singular value decomposition (SVD) approach rather than maximum-likelihood because multiple maxima make optimization to identify the non-unique κ_t challenging for standard optimization algorithms. An SVD is a factorization of a $G\times N$ matrix $\mathbf{Q}$ to:

$$\mathbf{Q} = \mathbf{USV}^T \tag{4.4}$$

where

- $\mathbf{U}$ is a $G \times G$ orthogonal matrix with columns called left-singular-vectors of $\mathbf{Q}$,
- $\mathbf{V}$ is an $N \times N$ orthogonal matrix with columns called right-singular-vectors of $\mathbf{Q}$,
- and $\mathbf{S}$ is a diagonal matrix comprised of the $s_1, \ldots, s_N$ singular values of $\mathbf{Q}$. Due to how this diagonalization is constructed, the higher singular values are more important to the fidelity of $\mathbf{Q}$ and the entries of $\mathbf{S}$ are ranked in decreasing order $s_1 \geq s_2 \geq \ldots \geq s_N$.

A reduction of the number of vectors required to create $\mathbf{Q}$ can be achieved by a low-rank approximation of $\mathbf{Q}$ represented by $\tilde{\mathbf{Q}}$ which follows:

$$\mathbf{Q}_{G\times N} \approx \tilde{\mathbf{Q}}_{G\times N} = \tilde{\mathbf{U}}_{G\times c}\tilde{\mathbf{S}}_{c\times c}\tilde{\mathbf{V}}^T_{c\times N}. \tag{4.5}$$

where diagonal $\tilde{\mathbf{S}}$ is reduced $\mathbf{S}$ from the original SVD, comprised of the c largest singular values. This follows the Eckhart-Young theorem [45] which describes how one can save the factorization of the approximated matrix more effectively by exploiting that $\tilde{\mathbf{S}}$ has only c

entries. The SVD can thus be used to facilitate a reduction of the number of independent vectors required to reconstruct a matrix by estimating the c singular values - providing a method for dimensionality reduction. To apply the SVD to the LC model, we can first rearrange the LC model terms to derive a residual matrix:

$$\ln\Big(m_x(t)\Big) - \alpha_x = Q_x(t)$$

with α_x estimated as the age-specific average log-mortality across all t and $Q_x(t)$ representing the age $x \in 1,\ldots,N$ and time $t \in 1,\ldots,G$ element of the residual matrix $\mathbf{Q}$

$$\mathbf{Q}_{G\times N} = \begin{array}{c} \\ 1 \\ \vdots \\ t \\ \vdots \\ G \end{array} \begin{array}{c} \begin{array}{ccccc} 1 & \ldots & x & \ldots & N \end{array} \\ \begin{bmatrix} Q_1(1) & \ldots & Q_x(1) & \ldots & Q_N(1) \\ \ldots & \ldots & \ldots & \ldots & \ldots \\ Q_1(t) & \ldots & Q_x(t) & \ldots & Q_N(t) \\ \ldots & \ldots & \ldots & \ldots & \ldots \\ Q_1(G) & \ldots & Q_x(G) & \ldots & Q_N(G) \end{bmatrix} \end{array}$$

The SVD Lee-Carter approximation of $\mathbf{Q}$ takes the rank 1 singular value, $c = 1$:

$$\mathbf{Q}_{G\times N} \approx \tilde{\mathbf{U}}_{G\times 1}\tilde{\mathbf{S}}_{1\times 1}\tilde{\mathbf{V}}^T_{1\times N}.$$

Linking these SVD matrix and vector terms to the Lee-Carter notation, we have:

$$\tilde{\mathbf{V}}_{1\times N} = \{\beta_1, \beta_2, \ldots, \beta_x, \ldots, \beta_G\}$$
$$\tilde{\mathbf{U}}_{G\times 1}\tilde{\mathbf{S}}_{1\times 1} = \{\kappa_1, \kappa_2, \ldots, \kappa_t, \ldots, \kappa_N\}$$

For the Lee-Carter model to give an accurate fit, the rank 1 singular vector must account for more than 90% of the variation in the N columns [46]. Forecasting for the Lee-Carter model is accomplished by univariate forecasting of the κ_t using time-series methods such

as a random walk with drift (RWD);

$$\kappa_t = \kappa_{t-1} + \theta + \varepsilon_t$$

where the scalar ε_t is an independent normal random error term and θ is a constant drift term. For precise unbiased forecasts which requires low variance for ε_t and an accurate estimation of the drift θ, the approach requires a large number of years of data for which the trend in the κ_t has been fairly constant and the proportional change by age has been the same [36]. These underlying assumptions make the Lee-Carter approach problematic for a country like South Africa that only has 19 years of empirical data with HIV/AIDS mortality significantly impacting mortality differentially by age and time for a large part of the period observed. This reduces the proportion of variation explained by the first singular value and also means that θ is not constant by age and time. Consequently, one derives biased estimates if modelling κ_t as a RWD process. Despite the challenges for this context, the LC use of the SVD is informative and paves the way for other mortality models that utilize the SVD in ways that this current research builds upon.

Clark [47] gives an extensive description of how the SVD can be used to exploit the correlation by age inherent in demographic quantities like fertility and mortality and uses the SVD to develop a parameterised component model of mortality [48]. The mortality model developed by Clark, referred to as SVD-Comp, is calibrated to the relationship between child and adult mortality and mortality at other ages in the mortality schedules of the Human Mortality Database (HMD) [49]. Defining $\mathbf{Q}$ as a sex specific $A \times L$ matrix of the mortality schedules, where A are the rows representing age and L are the columns representing the set of country-year life tables constituting the database, the SVD-Comp approximates each mortality schedule $\mathbf{q}_\ell$ using the c-term sum

$$\mathbf{q}_\ell \approx \sum_{i=1}^{c} v_{\ell i} \cdot s_i \mathbf{u}_i$$

where $c \leq \rho$, the rank of $\mathbf{Q}$, $\ell \in \{1 \dots L\}$ indexes the HMD mortality schedules and $v_{\ell i}$ are the elements of $\mathbf{v}_i$. In the calibration, $c = 4$ is found to give an almost exact approximation of the observed HMD mortality schedules. Utilizing that $\mathbf{U}$ and $\mathbf{S}$ are constant across all mortality schedules and the varying elements are the $\mathbf{v}_i$, the SVD-Comp model then replaces the $v_{\ell i}$ with values related to covariates ${}_5q_0$ and ${}_1q_0$.

Using a similar formulation, Alexander et al. [50] propose a Bayesian model for estimating subnational mortality. Transposing the matrix structure proposed by Clark, they define $\mathbf{Q}$ as a an $L \times A$ matrix comprised of $L = 1550$ U.S state mortality schedules for the 50 states over a 30 year period, 1980 to 2010, and $A = 19$ age-groups. Alexander et al. [50] uses this formulation to estimate the first three right-singular values of $\mathbf{Q}$ such that specific schedules can be modelled using

$$\mathbf{q}_\ell = \sum_{i=1}^{3} \beta_{\ell,i} v_i + \epsilon$$

where $\beta_{L\times 3} = \tilde{\mathbf{U}}_{L\times 3}\tilde{\mathbf{S}}_{3\times 3}$, v_i is the ith right-singular values of $\mathbf{Q}$ and ϵ is an age, year and state specific error.

Oeppen et al. [51] use the SVD on the age-at-death distribution to model mortality for Japan. Adapting the Lee–Carter model to the Compositional Data Analysis (CoDa) framework that was pioneered by Aitchison [52], this approach enforces a unit sum constraint on the life-table deaths (d_x) and changes the coordinate system of the mortality data from a Euclidean space to an Aitchison simplex ([53]). The CoDa mortality model is of the form:

$$clr(d_{x,t}) = \alpha_x + \beta_x k_t + \varepsilon_{x,t} \tag{4.6}$$

where $\varepsilon_{x,t}$ are independent and identically distributed random variables normally distributed with mean zero. This model is clearly a variant of the Lee–Carter model but the variable of interest to be modelled is a Centered Log-Ratio (clr) transformation of the

life-table age-at-death distribution d_x. Components β_x and k_t are estimated using an SVD with α_x being the age x geometric mean in the d_x across t. Bergeron-Boucher et al. [54] builds on this model to forecast all-cause mortality for 15 Western countries.

In a presentation, Kjærgaard et al. [55] outline how the SVD can be applied to the CoDa framework in a multiple decrement life-table to estimate Cancer deaths in French and Dutch populations and to forecast these to 2050. While this forecast uses the life-table deaths, Piveteau and Tomas [56] present a similar model that creates a composition from the cause-i-specific probabilities of death $q_{x,t,i}$ as a proportion of the all-cause age-specific probabilities of death.

4.2.3 Forecasting out of the GBD2016 study

A unique strength of the GBD studies is that to measure the health of each country in the world and to estimate the levels of mortality and disability that each is having to contend with, the study quantifies covariates and risks-factors that best explain the burden of disease [57]. The iterative refinement of the GBD enterprise has been based on new data-sources available each year as well as innovations and improvements to how overall as well as cause-specific mortality and morbidity are estimated based on available data. Foreman et al. [5] leverage the GBD2016 time-series of cause-specific mortality [58, 59], the corresponding comparative risk assessment time-series [60], and data on a set of vaccines and other health related interventions, to set up a forecasting framework for cause-specific mortality and life-expectancy. The framework also incorporates some established correlates of health i.e. income, education and fertility, which are mapped onto a composite measure introduced in GBD2013 [61], referred to as the Socio-demographic Index (SDI). The forecast framework predicts the logarithm of the cause-specific mortality by adding up three components; the underlying mortality, a scalar that captures the combined effects of risk factors on the specific cause and an unexplained residual.

4.2.3.1 The underlying cause-specific mortality

The location l, aged a, at time t and cause c underlying mortality (m^u_{clat}) is modelled in log-space as a function of the Socio-demographic index (SDI) and calendar time. The SDI is a composite indicator of development status strongly correlated with health outcomes [58]. It is the geometric mean of three covariates i.e. the total fertility rate under the age of 25, mean years of education for those aged 15 and older, and lag distributed income per capita. The covariates are scaled to indices with a lower bound of 0 corresponding to covariate levels where selected health outcomes are at their worst, and a maximum of 1, representing covariate levels where selected health outcomes are at their best. These covariates were forecasted separately using different approaches:

- *Income per Capita*

For location l and time t, income was forecasted using an ensemble of models to predict $y_{l,t}$ representing the first difference in log GDP per capita i.e.

$$y_{l,t} = log(GDPpc_{l,t}) - log(GDPpc_{l,t-1})$$

The models was created by taking various combinations of demographic indicators from the UN WPP 2017 for 1970 to 2017, time series methods and weighting functions. The models were created using 1970 to 2007 observations and those giving the best 10% of the predictions according to the RMSE for the 2008 to 2017 out-of-sample prediction, were retained to forecast $y_{l,t}$ beyond 2017.

- *Education*

Education is forecasted using the annualized rate of change (AROC) which we briefly define in a general way here. For some variable x measured over time indexed by t, the

AROC approach first calculates first differences d_t as

$$d_t = f(x_t) - f(x_{t-1})$$

where $f(.)$ is a function e.g. logit. The AROC is calculated using the weighted mean of the first difference over time, with weights w_t, determined by a recency-weighting parameter ω, scaled to sum to 1

$$\delta = mean(d_T, w_t) \text{ where } w_t = (t - t_{initial} + 1)^{\omega}$$

Education was forecasted using the logit function with x_t being the complete time-series maintained for all GBD locations and years.

- *Fertility*

Total fertility for women under the age of 25 was estimated using the age-specific estimates

$$TFR = \sum^{a} n_a \dot{A}SFR_a$$

with

$$logit(ASFR_{alt}) \sim \alpha_0 + \beta_a MEDU_{alt} + \gamma_a met\_need_{alt}$$

where maternal education ($MEDU$) and met need for contraception (met_need) are independent variables and met_need was forecasted using the AROC approach with a logit function on data from 1990 to 2016. Once these covariate forecasts have been derived, they are scaled to lie between 0 to 1 and used to calculate the SDI. The SDI is in turn used to predict the underlying mortality rate according to the equation

$$log(m^u_{lat}) = \alpha_{la} + \beta_0 SDI_{<0.8} + \beta_1 SDI_{\geq 0.8} + \theta_a t$$

with location-age-specific intercepts α, a global effect on SDI β, and age-specific effects on the secular trend θ_a.

4.2.3.2 A mortality scalar attributable to risks

The scalar $\mathbb{S}$ is a function of all the GBD risk factors relevant to each cause. To derive the scalar, Foreman et al. [5] utilize a number of measures related to risk:

- *Summary Exposure Values (SEVs)*

The Summary Exposure Value (SEV) is a summary measure of exposure for each risk that was introduced in the GBD2015 comparative risk assessment [62]. It is the relative risk-weighted prevalence of exposure and can be defined as:

$$SEV = \frac{\sum_i Pr_i RR_i - 1}{RR_{max} - 1}$$

where Pr_i is prevalence of category i exposure, RR_i is relative risk of the category i, and RR_{max} is the relative risk at the highest level of exposure in theory or observed globally. For each risk factor, a single SEV is estimated by averaging of the outcome of specific SEV values for each age, sex, location, and year across causes of death c.

$$SEV_r = \frac{1}{N(c)} \sum_c SEV_{rc}$$

where $N(c)$ are all causes born of r. These univariate variables are forecasted using adjusted annualized rates of change predicting $\hat{SEV}_{rlat}$ for risk r, location l, age a and year t.

- *Population attributable fractions (PAFs)*

The population attributable fraction (PAF) is defined as the fraction of all cases (exposed and unexposed) that would not have occurred if exposure had not occurred [63]. PAFs can

be estimated using the SEV according to the following equation:

$$\hat{PAF}_{rclat} = 1 - \frac{1}{\hat{SEV}_{rlat} \times (RR_{rc}^{max}) + 1}$$

The estimated PAF are biased as a result of the SEV not being cause-specific. This is corrected by comparing the estimates to the cause-specific PAF estimated for GBD2016 for the year 2016 to estimate correction factors CF

$$CF_{rcla} = logit(PAF_{rcla2016}) - logit(\hat{PAF}_{rcla2016})$$

which are used to rescale the estimated $\hat{PAF}$

$$PAF^{*}_{rclat} = logit^{-1}\left(logit(\hat{PAF}_{rclat}) + CF_{rcla}\right)$$

- *Mediation factors (MFs)*

Mediation factors are represented by MF_{rsc} and quantify the fraction of one risk that is mediated through another. They are used to estimate the joint PAF_{clat} for all risks:

$$PAF_{clat} = 1 = \prod_{r}^{R}\left(1 - PAF^{*}_{rclat} \times \prod_{s}^{S}(1 - MF_{rsc})\right)$$

The scalar is estimated: $\mathbb{S}_{clat} = \frac{1}{1-PAF_{clat}}$

4.2.3.3 An unexplained residual

The true mortality m^{T}_{clat} is the product of the underlying mortality m^{U}_{clat} and the risk related scalar $\mathbb{S}_{clat}$. In log-space we estimate

$$log(\hat{m}_{clat}) = log(m^{U}_{clat}) + log(\mathbb{S}_{clat}) \text{ where } log(m^{T}_{clat}) \sim N(log(\hat{m}_{clat}), \sigma^2)$$

The residuals ϵ represent latent trends in total cause-specific mortality not captured by risk factors, SDI, and global secular trends.

$$\epsilon = log(m^T_{clat}) - log(\hat{m}_{clat})$$

Residuals are forecasted using a pooled $ARIMA_{1,0,0}$ model that minimizes the chance of extreme forecasts by sharing parameters within geographic super-regions (s).

$$\epsilon_{lat} \sim N(\hat{\epsilon}_{lat}, \sigma) \text{ where } \hat{\epsilon}_{lat} = \psi_{sa}\hat{\epsilon}_{lat-1} + \delta_{sat} \text{ and } \delta_{sat} \sim N(0, \tau_{sa})$$

4.2.3.4 Other components of forecasting model

There's a number of other components to the forecasting framework, key ones are:

- *Vaccine forecasts*

Coverage for DTP3 and MCV1 were predicted using the SDI

$$logit(coverage) = \alpha + \beta SDI$$

For rotavirus, PCV3 and HIB3, coverage was forecasted using methods dependent on whether the vaccine has been introduced. If yes, spatio-temporal Gaussian process regression (ST-GPR) models of coverage ratios relative to DTP3 were extrapolated to 2040 with income as a covariate. If not, survival analysis using a Weibull distribution parameterised with SDI, GAVI eligibility status, DTP3 coverage and Hib introduction date was used.

- *HIV/AIDS forecasts*

HIV/AIDS forecasting made use of Spectrum software developed by UNAIDS and modified in GBD [59]. Inputs related to prevalence, incidence, treatment, survival and CD4 progression were forecasted and used to estimate a HIV/AIDS deaths in Spectrum.

- *Population forecasts*

Four inputs are used to derive population forecasts: Starting population estimate (2016) from GBD2016 and based on UN-WPP; Future migration estimates also from UN-WPP; Forecasted mortality rates as described above; Forecasted age-specific fertility rates. The cohort-component method of projection (CCMP) is used [64], calculating future populations, N_{t+1}, from current populations, N_t, using a linear model,

$$N_{t+1} = L_t N_t + M_t$$

where L_t is the Leslie matrix and M_t is migration. The Leslie matrix contains age-specific fertilities along the first row, age-specific survival probabilities along the sub-diagonal and zeros everywhere else [65].

- *Better and worse scenarios for the risk factors*

To generate better and worse scenarios for risk factors and cause-specific mortality, the 85th and 15th percentiles of the retrospective weighted annualized rates of change across the 195 countries were estimated and substituted for the reference weighted AROC values.

4.3 District mortality forecasts

4.3.1 Methods

In this section, the methods used to forecast district, province and national all-cause and cause-specific mortality by sex and age are described.

4.3.1.1 Generalized Additive Models (GAMS)

For non-linear time series forecasting, a useful set of tools is given by Generalized Additive Models (GAMS) [66, 67]. As GAMS are used extensively in this research, they are introduced and briefly described here. GAMs are an extension of generalized linear models

(GLMs) [68]. A GLM has the structure

$$g\left(\mu_i\right) = \boldsymbol{x}_i\boldsymbol{\beta}, \tag{4.7}$$

where μ_i is the expectation of response variable Y_i such that $\mu_i \equiv \mathbb{E}\left(Y_i\right)$, g is a link function, $\boldsymbol{x}_i$ is the ith row of the covariate matrix $\boldsymbol{X}$, and $\boldsymbol{\beta}$ is a vector of unknown coefficients [68]. Akin to linear models, GLMs center around a linear predictor, $\boldsymbol{X}\boldsymbol{\beta}$, and allow for link functions other than the identity function. GLMs also allow for any distribution from the exponential family to model the dependent variable instead of just assuming it Gaussian. The exponential family consists of distributions whose probability density function can be written as

$$f_\theta\left(y\right) = \exp\left(\frac{y\theta - b(\theta)}{a(\Phi)} + c(y,\Phi)\right), \tag{4.8}$$

where a, b, and c are arbitrary functions, Φ is a scale parameter, and θ is the canonical parameter of the distribution [67]. Building upon GLMs, a GAM has the structure:

$$g\left(\mu_i\right) = \boldsymbol{x}_i^*\boldsymbol{\theta} + f_1\left(x_{1,i}\right) + f_2\left(x_{2,i}\right) + f_3\left(x_{3,i}, x_{4,i}\right) + \ldots, \tag{4.9}$$

where μ_i again is the expectation of response variable Y_i, i.e., $\mu_i \equiv \mathbb{E}\left(Y_i\right)$, the response variable Y_i follows any distribution from the exponential family, parametric model components have model matrices with rows $\boldsymbol{x}_i^*$, the vector $\boldsymbol{\theta}$ is of the corresponding parameters, and covariates x_k are smoothed with the functions f_j [67].

The smooth functions are non-parametric estimates of the actual functional relationship between the response variable and the predictor variable to which the smooth function is applied [66]. Unlike LMs or GLMs, a smooth function is non-parametric, i.e., it does not assume the response variable to follow any specific distribution. As an explanatory example, consider a model containing one smooth function of one predictor variable with

the identity function as the link function,

$$y_i = f\left(x_i\right) + \varepsilon_i, \tag{4.10}$$

where y_i is a response variable, x_i is a predictor variable, f is a smooth function, and the ε_i follow the normal distribution with a mean of zero and a variance of σ^2 [67].

For this research, the GAMS used for time-series modelling are of the form

$$y_t = f(log(t)) + \varepsilon_t$$

where y_t is the time-series variable to be forecasted and time t is counted as being 0 for 1996, 1 for 1997 etc and the smoothing function is on the $log(t)$ to determine moderate forecasts. The models used are assumed to have autoregressive lag-1 (AR-1) errors:

$$\varepsilon_t = \psi_1 \varepsilon_{t-1} + w_t$$

where $w_t \sim$ iid $N(0, \sigma^2)$. The ψ_1 correlation is estimated and accounted for in the parameter estimation for the smoother $f(\cdot)$.

4.3.1.2 Forecasting all-cause mortality for South Africa

This research builds on Oeppen et al. [51] and Bergeron-Boucher et al. [54] to model and forecast South Africa district all-cause and cause-specific mortality. In Aim 1, age-specific death rates for each district, each province and the country as a whole are estimated for each year from 1997 through to 2015. The derived output are in single-year ages and are aggregated into age-bands $x \in \{0, 1-4, 5-9, \ldots, 95+\}$. The location- and time-t-specific death-rate in age interval $[x, x+n)$, represented by ${}_nm_{x,t}$, is converted into the probability of dying in age interval $[x, x+n)$, represented by ${}_nq_{x,t}$, according to the assumption of

constant force of mortality over n as assumed for the single decrement life table i.e.

$$ {}_nq_{x,t} = 1 - exp(-n *_n m_{x,t}) $$

We are interested in ${}_nd_{x,t}$ which represents the deaths by life-table population in the age interval $[x, x+n)$ at time t. For a life-table radix of 1, this is calculated:

$$ {}_nd_{x,t} = (1 -_x q_{0,t}) *_n q_{x,t} $$

Following CoDa convention that each row represents a composition [69], the sex-specific density of death matrix for district d is transposed to give $\mathbf{d}_d$ with elements $d_{t,x}$ (shown in Equation 4.11), where each row adds up to the life table radix and where ω is the open interval age:

$$ \mathbf{d}_d = \begin{array}{c} \\ 1 \\ \vdots \\ t \\ \vdots \\ T \end{array} \begin{array}{c} \begin{array}{ccccc} 0 & \ldots & x & \ldots & \omega \end{array} \\ \begin{bmatrix} d_{1,0} & \ldots & d_{1,x} & \ldots & d_{1,\omega} \\ \ldots & \ddots & \ldots & \ddots & \ldots \\ d_{t,0} & \ldots & d_{t,x} & \ldots & d_{t,\omega} \\ \ldots & \ddots & \ldots & \ddots & \ldots \\ d_{T,0} & \ldots & d_{T,x} & \ldots & d_{T,\omega} \end{bmatrix} \end{array} \tag{4.11} $$

The $\mathbf{d}_d$ for $d \in 1 \ldots 62$ representing the 52 districts, 9 provinces and national are stacked to create $62T \times \omega$ matrix. An initial centering of the matrix to better visualize the sources of variation is performed by estimating the global geometric mean of each column,

$$ a_x = \left(\prod_{t=1}^{62T} d_{t,x} \right)^{1/(62T)} $$

The α_x vector is normalized to a unit sum and then each row of $\mathbf{d}_d$ is divided by the corresponding term in the α_x age-specific geometric mean (Equation 4.12).

$$f_{t,x} = d_{t,x} \ominus \alpha_x \tag{4.12}$$

The symbol $\ominus$ is known as a CoDa perturbation operator. The $f_{t,x}$ are also normalized. To unrestrict the data beyond the compositional plane, a centered log-ratio (clr) transformation [53] is applied to the normalized $f_{t,x}$ values to give:

$$h_{t,x} = clr(f_{t,x}) = ln\left(\frac{f_{t,x}}{g_t}\right)$$

where g_t are the time t geometric means of $f_{t,x}$ across all ages. An SVD is then applied to the matrix $\mathbf{H}$ which has elements $h_{t,x}$. A low-rank approximation of the matrix $\mathbf{H}$ is constructed by choosing the first c right-singular values of $\mathbf{H}$ and using them to construct

$$\boldsymbol{h}_t = \sum_{i=1}^{c} \beta_{t,i} v_i + \boldsymbol{\epsilon} = \boldsymbol{\beta}_t \boldsymbol{v} + \boldsymbol{\epsilon}$$

where v_i is the ith right-singular value of $\mathbf{H}$, the β are scaling factors derived using the left-singular vectors and singular values of $\mathbf{H}$ and ϵ is a random error. To determine a measure of the uncertainty around the time-varying scaling factors we use the transpose

$$\boldsymbol{h}_t^T = \boldsymbol{v}^T \boldsymbol{\beta}_t^T + \boldsymbol{\epsilon}^T$$

and assume the $\boldsymbol{v}^T$ to be data. The $\boldsymbol{\beta}_t^T$ are then estimated as linear unbiased estimators

$$\hat{\boldsymbol{\beta}}_t^T = (\boldsymbol{v}\boldsymbol{v}^T)^{-1} \boldsymbol{v} \boldsymbol{h}_t^T$$

such that their uncertainty can be drawn from a t-distribution with a covariance matrix determined by the right singular values $(\boldsymbol{v}\boldsymbol{v}^T)^{-1}$ scaled by the residuals, assuming that for some unknown σ^2, these parameters are Gaussian i.e.

$$\hat{\boldsymbol{\beta}}_t^T \sim \mathcal{N}(\boldsymbol{\beta}_t^T, \sigma^2 \left(\boldsymbol{v}\boldsymbol{v}^T\right)^{-1})$$

For each sex and district, the lower-95%, mean and upper-95% time-series of the $\beta_{t,i}$ are forecasted using the GAM specification introduced previously to generate a thousand draws for each of the three predicted time-series. A sample of a thousand forecasted time-series draws is then randomly selected from the results. This allows for draw-level low rank reconstructions of **H** as well as its forecast to 2030 using the fitted time-series:

$$\hat{\mathbf{h}}_t = \sum_{i=1}^{c} \hat{\beta}_{t,i} v_i$$

The fitted and forecasted $\hat{\mathbf{h}}_t$ are then transformed back into compositional data using the inverse centered log-ratio (softmax) according to

$$\hat{f}_{t,x} = clr^{-1}(\hat{h}_{t,x}) = C[e^{\hat{h}_{t,x}}]$$

where $C[]$ is the normalising procedure. Returning to the life-table death space requires compositionally adding back the geometric means, to obtain the predicted $\hat{d}_{t,x}$ which can in turn be used to calculate the transposed predicted mortality rates $m_{x,t}$.

Figure 4.1 shows the variance explained by each singular value arranged by rank and the cumulative variance explained. This is depicted for both sexes combined and indicates that a low rank approximation would require at least five principal components to explain 97% of the variation in **H**. The figure also shows the four right singular values explaining most of the variation in **H** for each sex. The components are orthogonal with each explaining a unique characteristic of the mortality profile; a profile varying across districts and time. The first component seems to capture the HIV/AIDS mortality pattern with high child mortality and a hump for young to middle-aged adults whereas the other components are age-specific mixtures focusing on either old age, child or young age mortality.

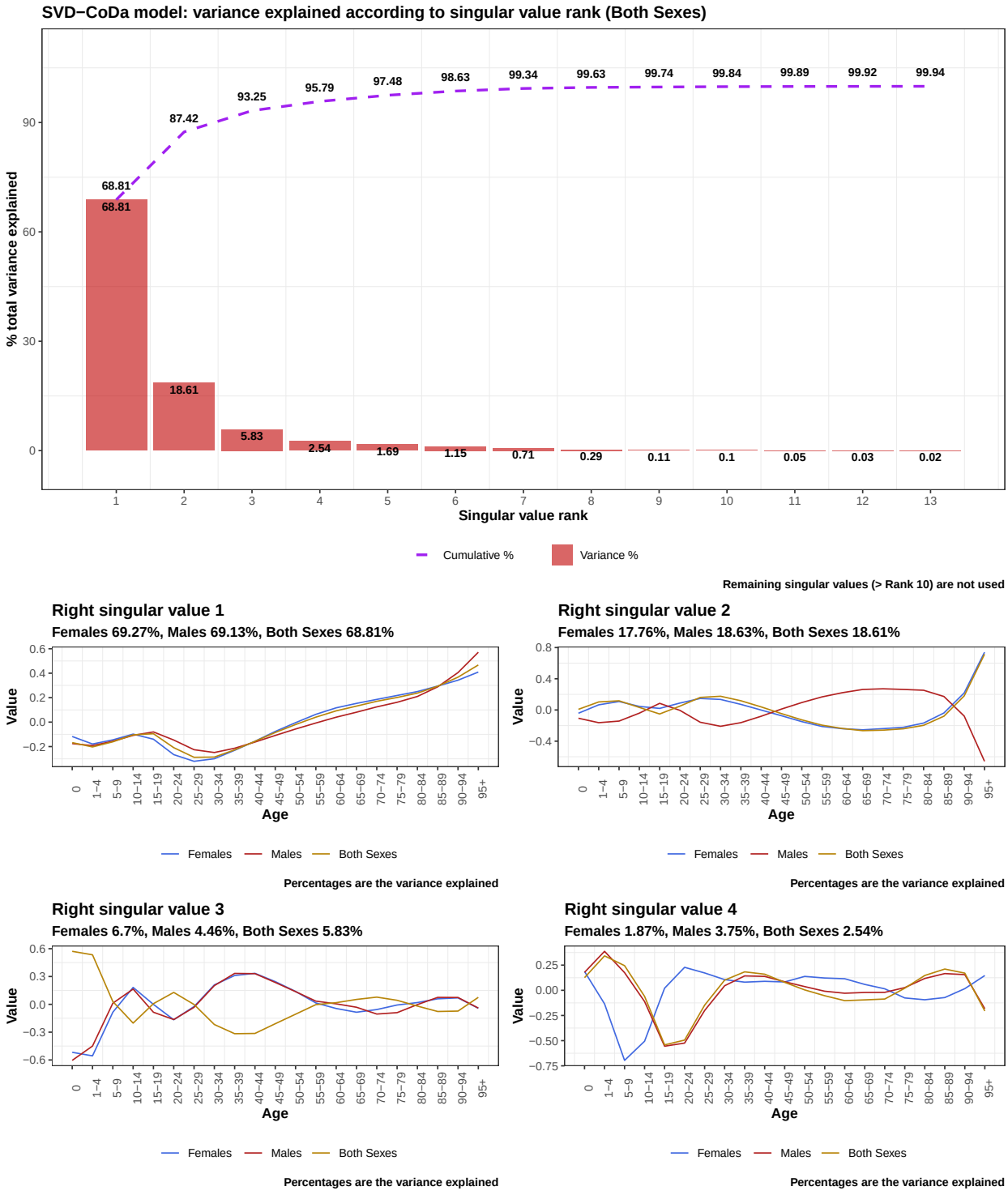

Figure 4.1: SVD-CoDa variance explained by right-singular values

4.3.1.3 *Forecasting cause-specific mortality*

The all-cause mortality forecast using this SVD-CoDa single decrement approach generates a mortality envelope which can be disaggregated according to the 16 cause-of-death groupings defined in Aim 2. Forecasts of the cause-fractions are accomplished by using a multiple-decrement extension of the all-cause approach described above [51]. The main steps of this approach are depicted in Figure 4.2.

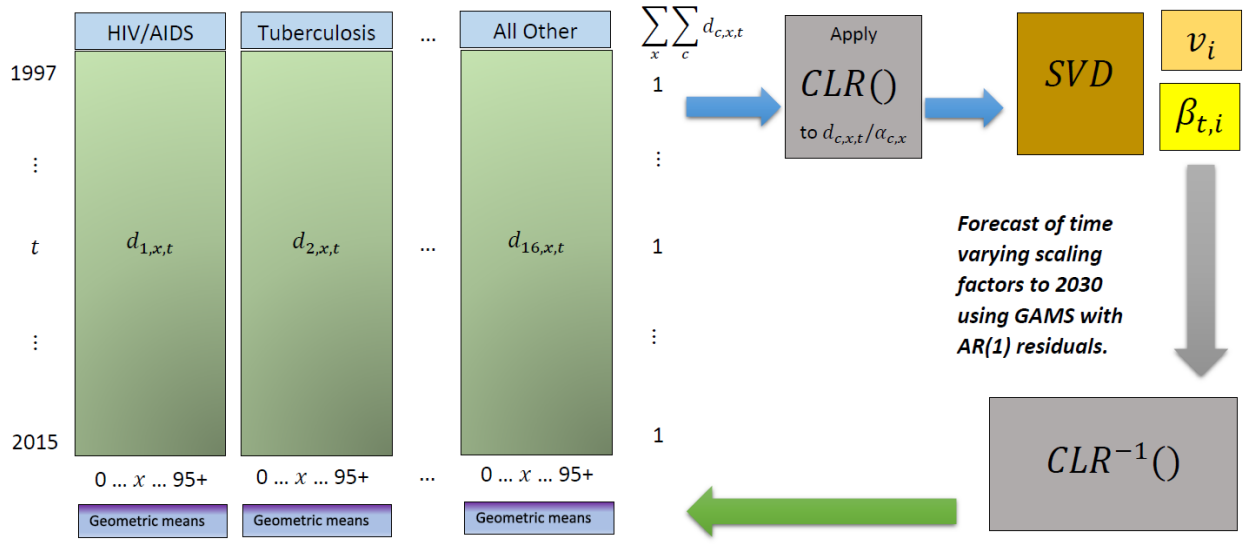

Figure 4.2: Schematic of CoDa approach for cause-specific forecast

As with the all-cause case, based on the age-specific deaths estimated for Aim 1, we have mortality rates which can be used to derive life-table deaths $d_{x,t}$. From Aim 2, the Dirichlet-Multinomial model derives estimates of cause-fractions $\theta_{c,x,t}$ which represents the time t age x proportion of deaths attributed to cause c. Elandt-Johnson et al. [70] shows that this proportion applies to the all-cause death numbers $D_{x,t}$ as well as the calculated mortality rates $m_{x,t}$, probabilities $q_{x,t}$ and crucial for our purpose, the life table deaths $d_{x,t}$. And so to obtain the cause-specific lifetimes, we use:

$$d_{c,x,t} = \theta_{c,x,t} \times d_{x,t}$$

where $d_{c,x,t}$ quantifies the life table deaths attributed to cause c. For a life table radix of 1, we have $\sum_x \sum_c d_{c,x,t} = 1$. As represented in Figure 4.2, the matrix of $d_{c,x,t}$ estimates is transposed to have time by row and age by column, with each cause stacked to the matrix horizontally. With 14 cause groupings over 19 years and 19 age-groups some of the $d_{c,x,t}$ are invariably equal to 0. To allow for a compositional centering using the geometric mean for the multi-cause zero-inflated mortality matrix made up of these $d_{c,x,t}$ elements, we add a small $\delta = 1 \times 10^{-10}$ to each $d_{c,x,t}$ value. The rows of the matrix are normalised to sum to 1 and the geometric means $\alpha_{x,c}$ for each age-cause-specific column are calculated and also normalised to sum to 1.

Figure 4.3 shows the calculated normalised $\alpha_{x,c}$ that are used to center the multi-cause matrix. The mean $\alpha_{x,c}$ captures the average age-pattern for each cause across the district, province and national data, with uncertainty given by assessing this distribution across all draws and both sexes. The negative perturbation removes what is common so that what remains is an undiluted quantification of the amount of variation in the data that is attributable to the time varying parameters. The relative levels of the $\alpha_{x,c}$ values also give some indication of the relative magnitude of the causes as each of the principal component vector is scaled by constant time-varying parameter. However, the final level of the age-specific value combines the information given by the $\alpha_{x,c}$, the time varying parameters as well as the right singular values.

An important characteristic of this approach is that unlike its all-cause counterpart which derives principle components and geometric means that are common to all districts, with only the time varying parameters being unique, the multiple-decrement forecast calculates $\alpha_{x,c}$ and principal components for each district. Over 30 parameters are required to estimate at least 95% of the variation if one stacks the life table matrices of all districts. The multiple-decrement forecast requires about 10 parameters for each district. This is more computationally involving than the all-cause case albeit still efficient as it generates 336 cause and age combinations for each district.

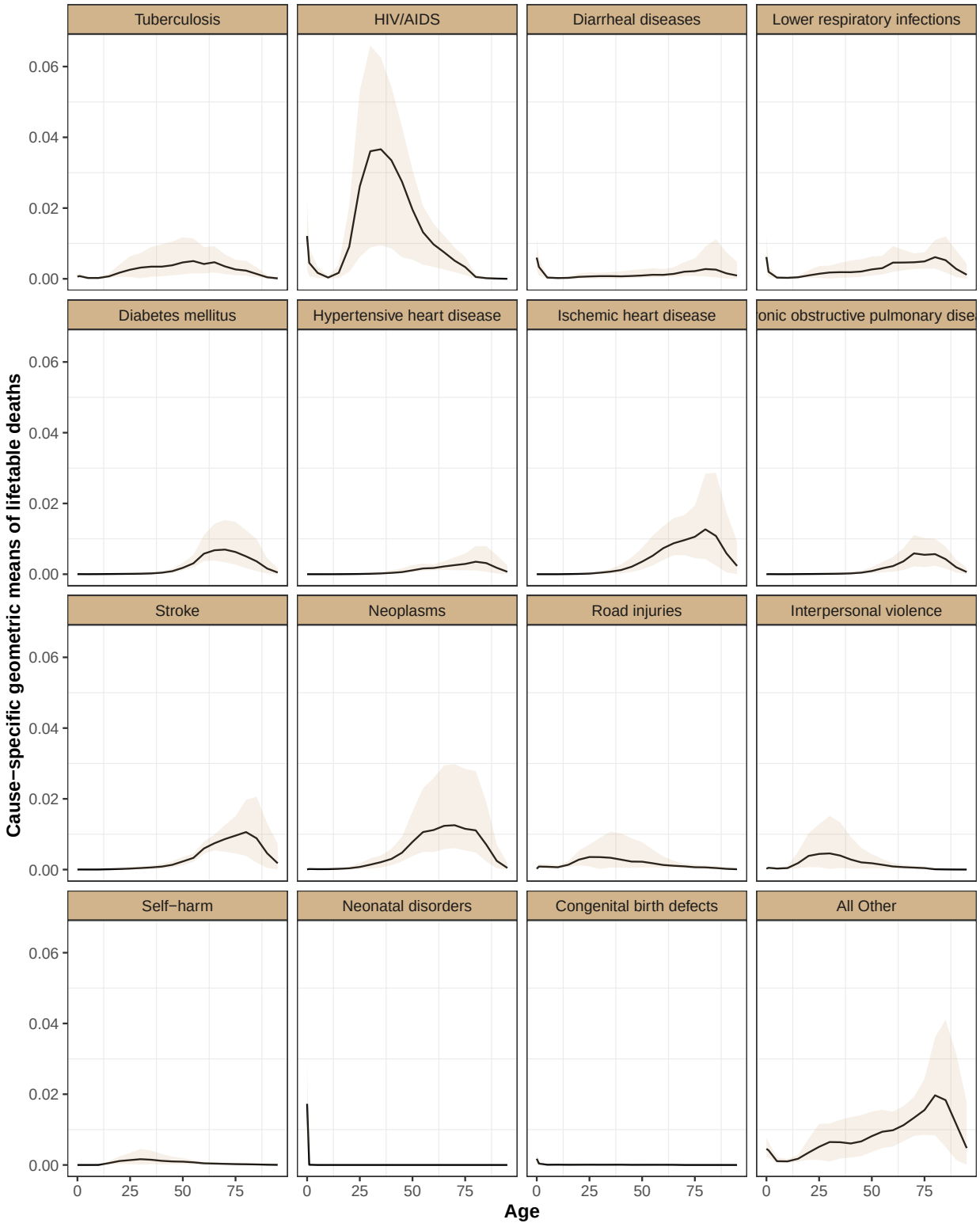

Figure 4.3: Geometric means of d_x by age and cause ($\alpha_{x,c}$)

After the geometric mean vector is derived, its inverse is compositionally perturbed from the $d_{t,x,c}$ to give matrix elements

$$f_{t,x,c} = d_{t,x,c} \ominus \alpha_{x,c}$$

The centered log-ratio (clr) transformation is applied to each row in the matrix mapping the values from the restricted simplex subspace to an unrestricted euclidean subspace, resulting in:

$$h_{t,x,c} = clr(f_{t,x,c}) = ln\left(\frac{f_{t,x,c}}{g_t}\right)$$

where g_t are the time t geometric means of the $f_{t,x,c}$ across all ages and causes. As with the all-cause forecast, an SVD is then applied to the matrix $\mathbf{H}$ to determine the principal components that can be used to perform a low-rank reconstruction. The 10 time varying scaling factors for each sex and district are forecasted to 2030 using the GAM approach with AR(1) residuals introduced earlier. These forecasted factors are matrix multiplied with the principal components which reconstructs the matrix $\hat{\mathbf{H}}$ for the 1997 to 2015 period as well as the forecasted 2016 to 2030 period. The softmax function is used to derive forecasted $\hat{f}_{t,x,c}$ estimates. These are normalized and perturbed using the age-cause-specific geometric means to give the forecasted age-cause-specific life table deaths:

$$\hat{d}_{t,x,c} = \hat{f}_{t,x,c} \oplus \alpha_{x,c}$$

Finally, coherence between cause-specific and all-cause mortality is established according to Elandt-Johnson et al. [70, Eq. 9]:

$$\hat{m}_{c,x,t} = \hat{m}_{x,t} \frac{\hat{d}_{c,x,t}}{\hat{d}_{x,t}}$$

where the $\hat{m}_{c,x,t}$ represent cause c mortality rates for age x in year t and both $\hat{m}_{x,t}$ and $\hat{d}_{x,t}$ are derived in the all-cause forecasts.

4.3.2 *Results*

In this section we summarise the results of both the all-cause and cause-specific forecasts. Detailed district level estimates for the former and latter disaggregated by age, sex and year can be found in the attached appendix. To begin with, Figure 4.4 demonstrates the performance of this model at reconstructing the mortality matrix by comparing the 2005 and 2010 mean log-mortality schedules from Aim 1 to the fitted values derived using this SVD-CoDa approach. For the two years displayed as well as all other district-province-sex-years analysed, the predicted schedules match the Aim 1 inputs very closely, with age-specific differences indiscernible from visual inspection of plots but evident from slight differences in the calculated values of ${}_5q_0$, ${}_{45}q_{15}$ and e_0.

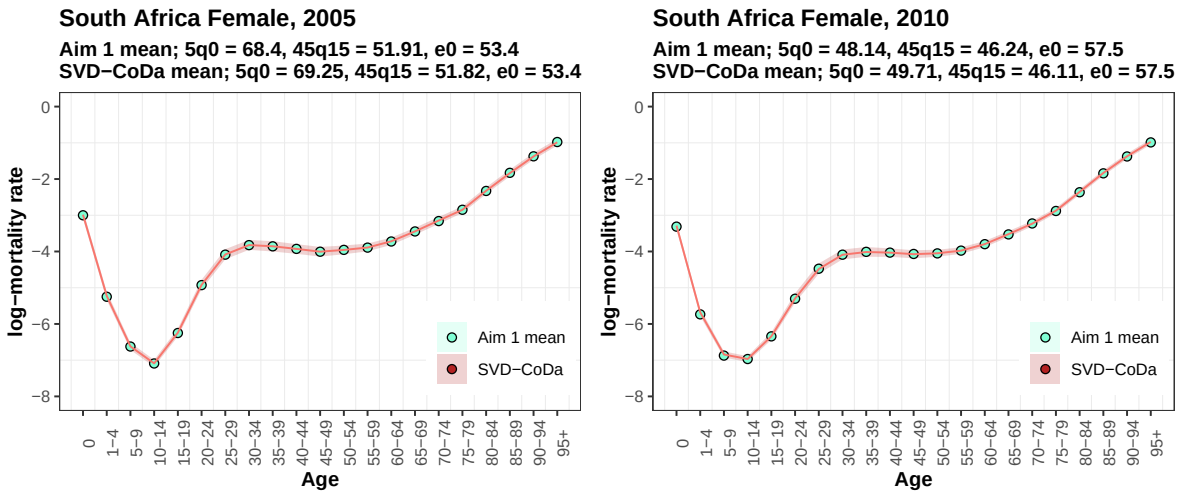

Figure 4.4: Demonstrating SVD model performance for South Africa

4.3.2.1 *All-cause mortality forecasts*

Figure 4.5 shows forecasts of the natural logarithms of the mortality rates for every three years starting in 1997 comparing the Aim 1 mean estimates to the means from the SVD-CoDa. The plot reiterates the accuracy of the SVD-CoDa at reconstructing the mortality for years 1997 to 2015.

In general, the model forecasts falling mortality for all age groups with the smallest reductions in mortality being for the oldest age-groups and the 15–19 age-group. For the provinces most affected by HIV/AIDS historically, the forecasts also predict a gradual diminishing of the characteristic AIDS hump leading to comparable mortality levels across all 9 provinces by 2030. For KwaZulu-Natal, the forecasted age-pattern for the oldest ages is less regular than for the other provinces.

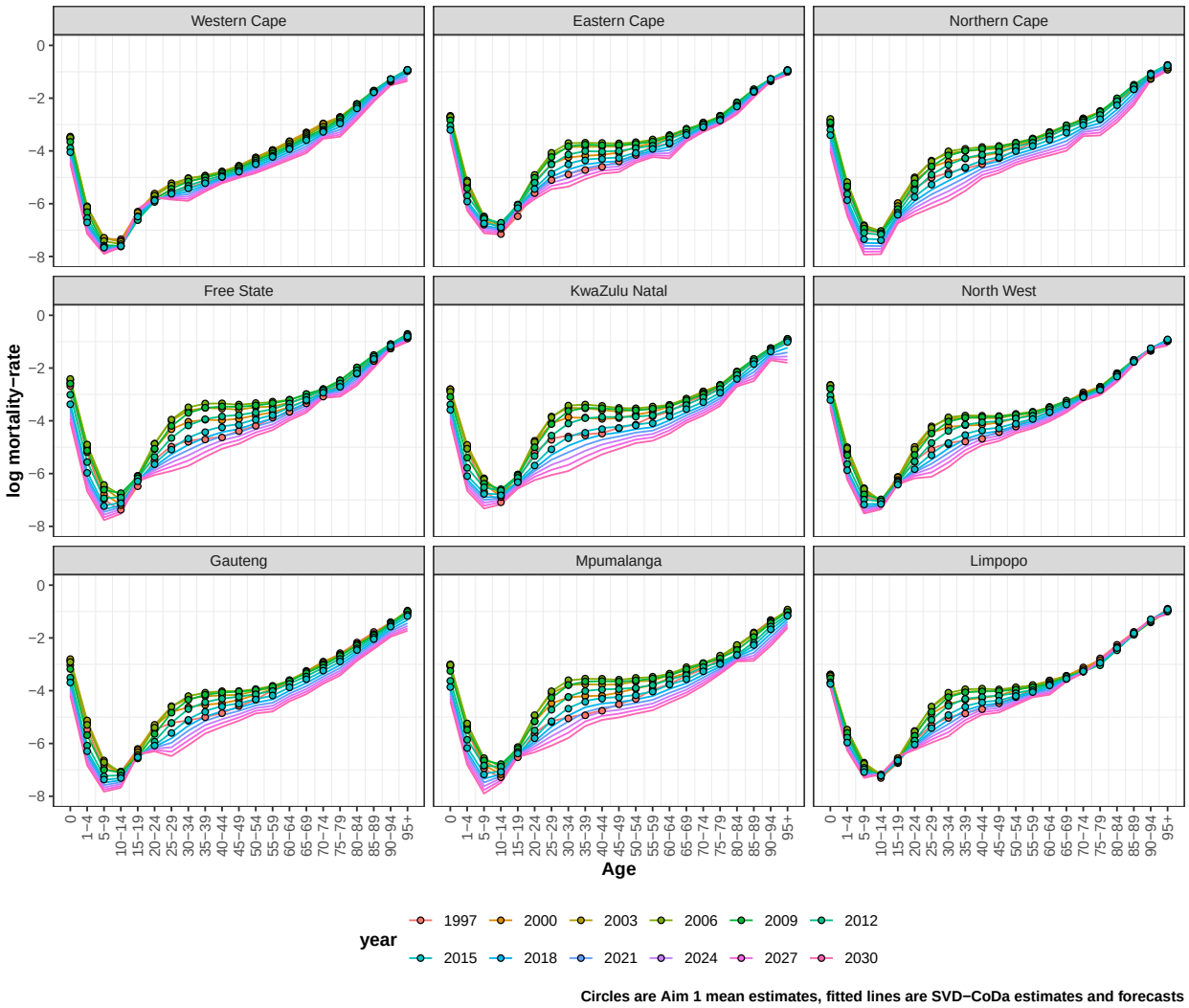

Figure 4.5: Forecasts of log-mortality by province and select year

Figure 4.6 shows the forecasts of life-expectancy at birth and adult mortality as quantified using ${}_{45}q_{15}$ per 100. The plot compares estimates derived using results from the SVD-CoDa model, GBD2017 as well as the estimates from WPP2019 [71]. For the SVD model, mean estimates for all years 1997-2030 with corresponding uncertainty intervals are shown.

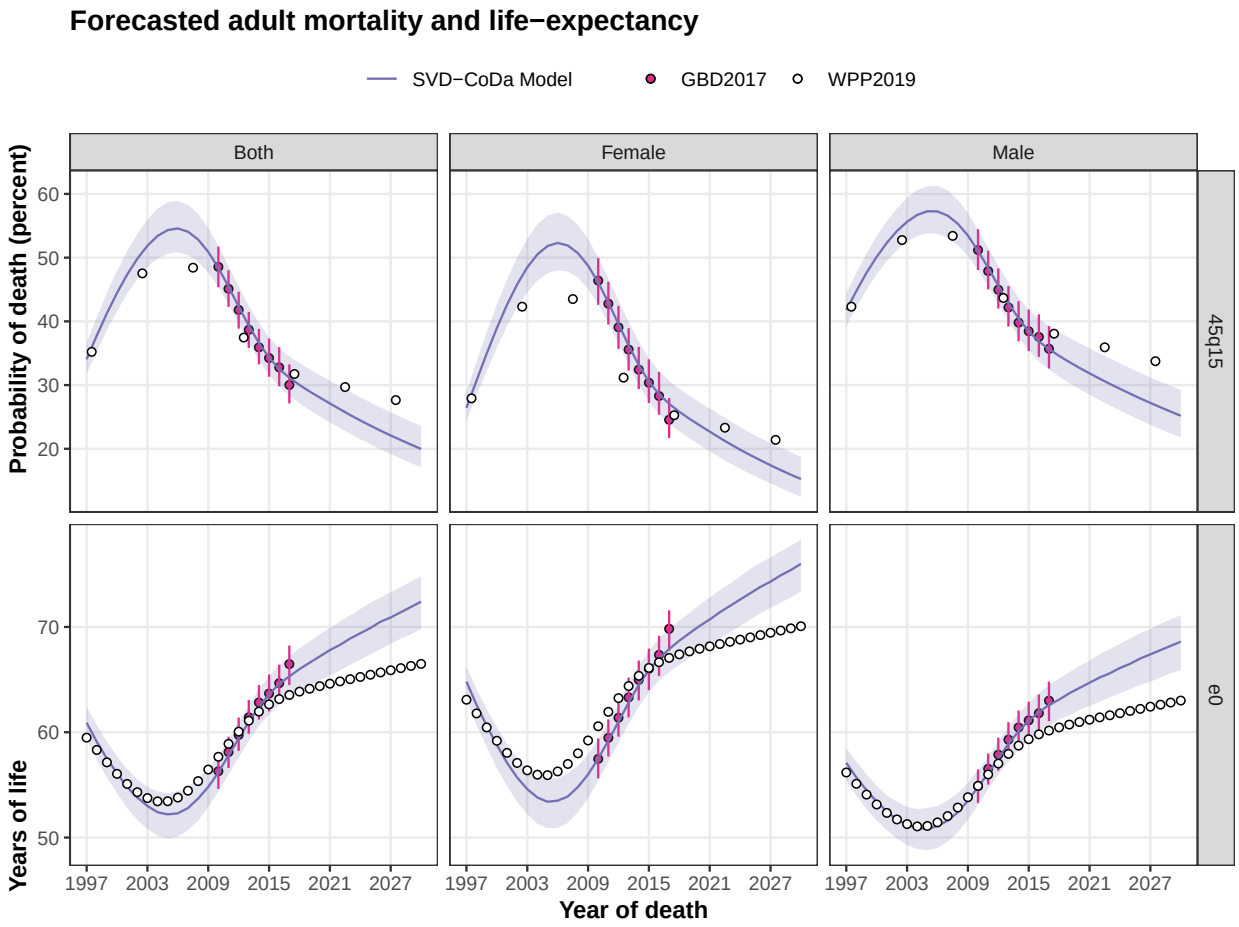

Figure 4.6: Forecasted national adult mortality and life-expectancy by sex

For the GBD2017, the most recent eight years are shown (2010 to 2017) where 2016 and 2017 are out-of-sample for the SVD model. Seeing as the model tracks the GBD very closely for the in-sample years, the difference between the GBD2017 and SVD-CoDa estimates for years 2016 and 2017 gives an indication of the out-of-sample validity of the model.

WPP2019 also has forecasts for the country based on the cohort component projection model framework which applies pre-specified fertility, mortality and migration patterns to a population to forecast its change assuming its components adhere to the demographic balancing equation. The estimates of adult mortality are generated in a 5×5 age and time framework and for the plots, are assumed to relate to the middle of the quinquennial period. The estimates for life-expectancy have been interpolated to single years in the results that are available to the public and which are shown in the plot.

Comparing the SVD-CoDa to the GBD2017, there is strong agreement in the estimates of life-expectancy and adult mortality throughout the period including 2016 and 2017. There are some slight differences for females in 2017 which suggests that either the SVD-CoDa forecast assumptions are too conservative and mortality improvements between 2016 and 2017 were larger than in previous years, or that the GBD2017 could be exaggerating mortality improvements for those two years. Relative to the SVD-CoDa, the historical time-series and forecast from WPP2019 exhibit a lower peak and slower rate of mortality improvement, respectively, . Differences between the SVD-CoDa and WPP2019 are smaller for males compared to females in the historical estimates but this is reversed for the WPP2019 female forecast which is closer to the SVD-CoDa.

Figure 4.7 shows the forecasts of child mortality (${}_5q_0$) for which the publicly available WPP2019 estimates are for both sexes combined. As with ${}_{45}q_{15}$ and e_0, there is strong agreement between the SVD-CoDa and GBD2017 for years 2010 to 2015 but less so afterwards with the improvement from 2016 to 2017 being largest in GBD2017. In contrast to the adult mortality and life-expectancy differences, there is a better agreement between the SVD-CoDa and WPP for the child mortality forecasts throughout the prediction period with the mean line for the SVD-CoDa improving at only a marginally faster rate than WPP. The uncertainty intervals for GBD2017 and SVD-CoDa overlap but the trajectory of the points point to a gradual divergence between the two that could increase with time.

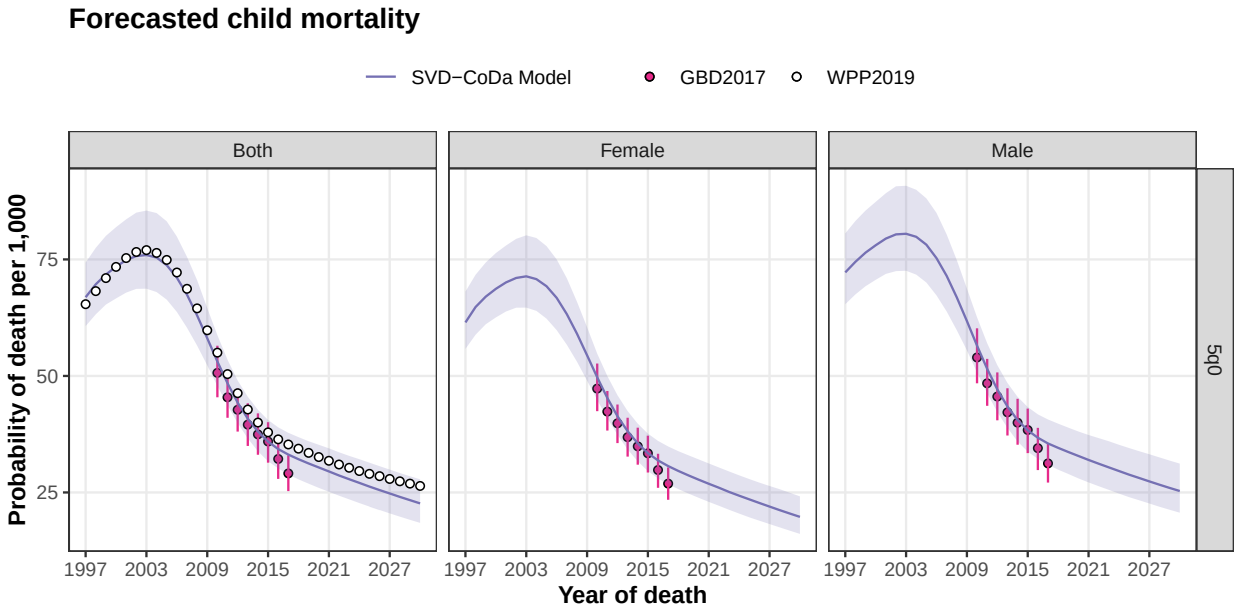

Figure 4.7: Forecasted national child mortality by sex

The SVD-CoDa model generates 1,000 draws of mortality rates for each age, sex, year and location. The model produces estimates for each district, each province as well as the national aggregate. From national results we are able to glean the following:

- Life-expectancy at birth for both sexes combined is expected to increase by about 8 years between the years 2015 and 2030, starting from 63.6 in 2015 (61.7–65.3) and increasing to 72.4 by 2030 (69.8–74.8).

- There are sex differences in the baseline estimates and forecasts with males projected to increase from 61.1 in 2015 (59.3–62.8) to 68.6 in 2030 (65.9–71.1) and females to increase from 65.9 in 2015 (63.8–67.7) to 76 in 2030 (73.4–78.3).

- The forecasted reductions in ${}_{45}q_{15}$ and ${}_{5}q_{0}$ parallel the increases in e_0. Child mortality for both sexes combined is forecasted to fall from 35.9 in 2015 (31.7–40.55) to 22.65 in 2030 (18.47–27.82).

- As expected, the differences between male and female ${}_5q_0$ are projected to be small (uncertainty intervals overlap) with males expected to fall from 38.33 in 2015 (33.76–43.33) to 25.31 in 2030 (20.66–31.19) and females to also decrease from 33.43 in 2015 (29.59–37.62) to 19.76 in 2030 (16.11–24.16).
- For both sexes combined, ${}_{45}q_{15}$ is also predicted to fall, decreasing from 34.31 in 2015 (31.57–37.5) to 19.98 in 2030 (17.09–23.57).
- Significant differences between males and females for ${}_{45}q_{15}$ are expected with males falling from 38.44 in 2015 (35.43–41.77) to 25.19 in 2030 (21.79–29.23) and females from 30.53 in 2015 (27.45–34.19) to 15.26 in 2030 (12.5–18.7).

Figures 4.8 to 4.10 show the means of the summary demographic measures, e_0, ${}_5q_0$ and ${}_{45}q_{15}$, that are derived from the district level mortality forecasts. Estimates are shown for both sexes combined and are grouped by province. The lines are colour coded by district and the estimated national means are included in each plot (dashed black line) as well as the estimated mean for the province the districts lie within (grey circles). The GBD2017 province means for 2010 to 2017 are also included in the plots (gold diamonds).

As with the national summary measures, the provincial SVD-CoDa predicts the GBD2017 well between 2010 and 2016 for e_0 and ${}_{45}q_{15}$. There are some differences for Northern Cape ${}_5q_0$ related to completeness being capped at 100% for Aim 1. Differences for 2017 are present for some provinces and in almost every case, the difference suggests a larger mortality improvement estimated for GBD2017. The result for Western Cape is unique as the GBD2017 estimates slightly worsening outcomes for 2017 relative to 2016 for adult mortality and life-expectancy. When one considers the overlap of uncertainty intervals, the differences between GBD and the SVD model up to 2017 are small. However, if the 2016 to 2017 rates-of-change persist then the GBD2017 and SVD-CoDa potentially deviate much more significantly with time. However, the mortality trend is also expected to plateau and this could reduce future differences.

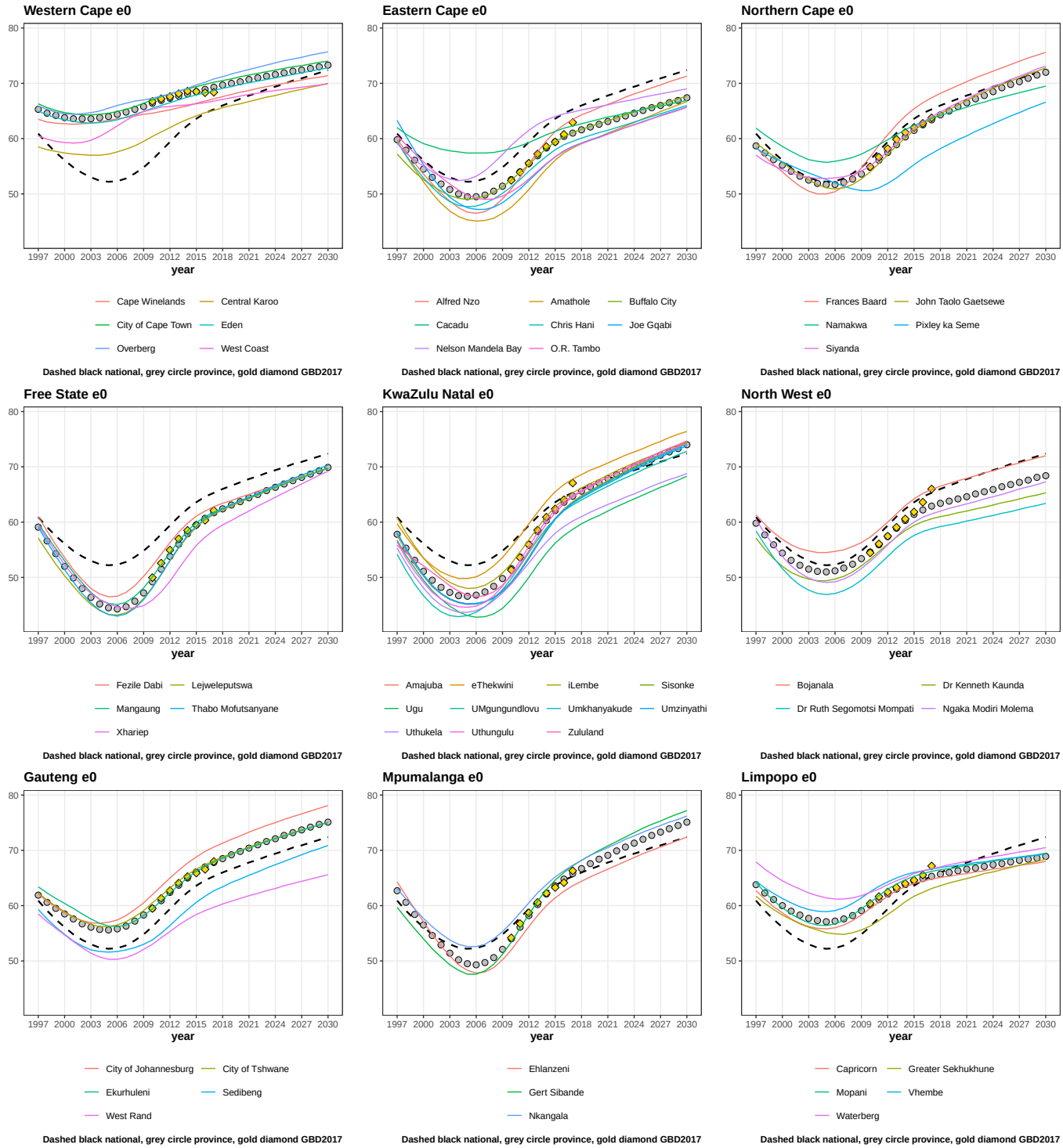

Figure 4.8: Forecasted provincial life-expectancy comparisons

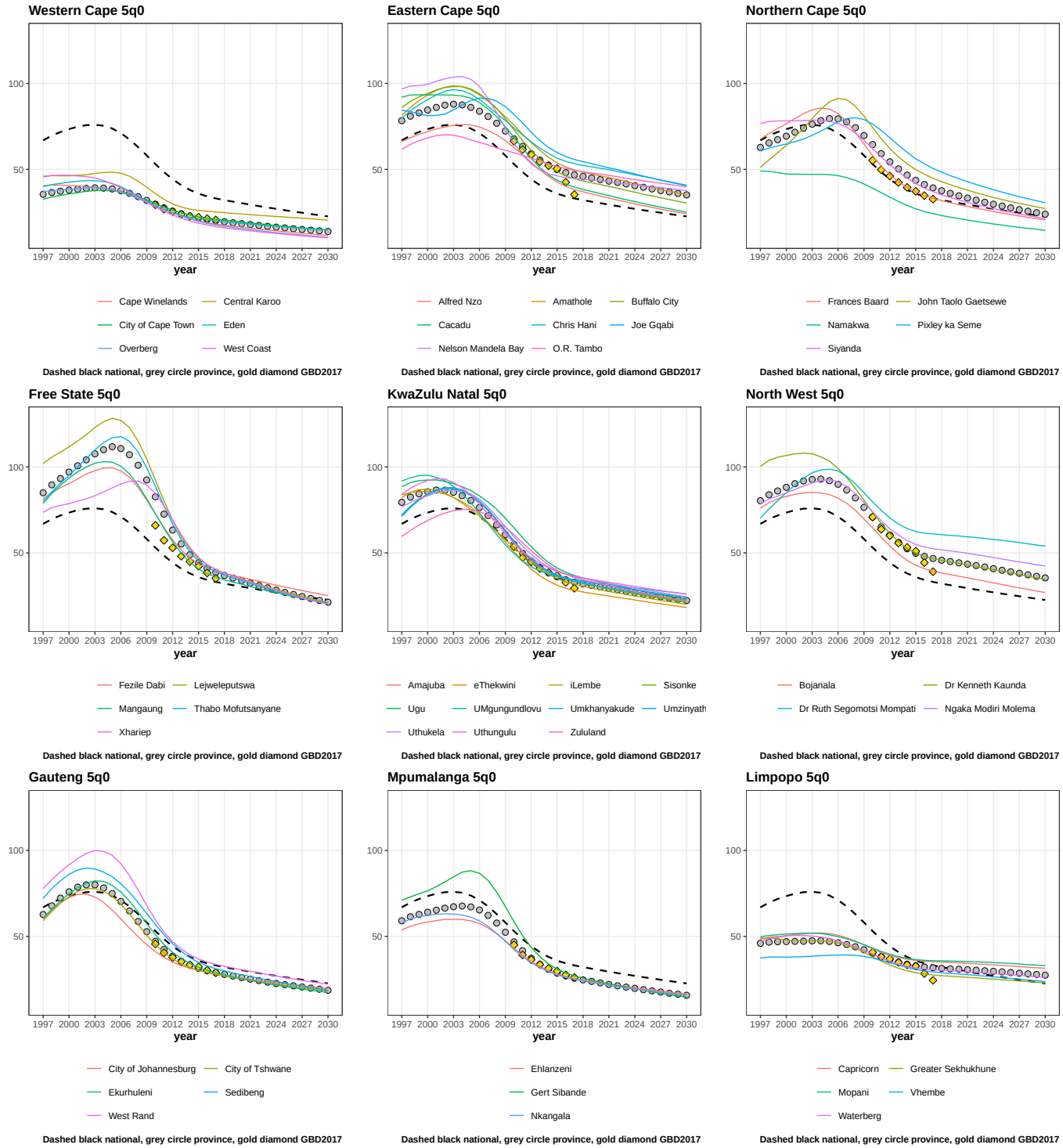

Figure 4.9: Forecasted provincial child mortality comparisons

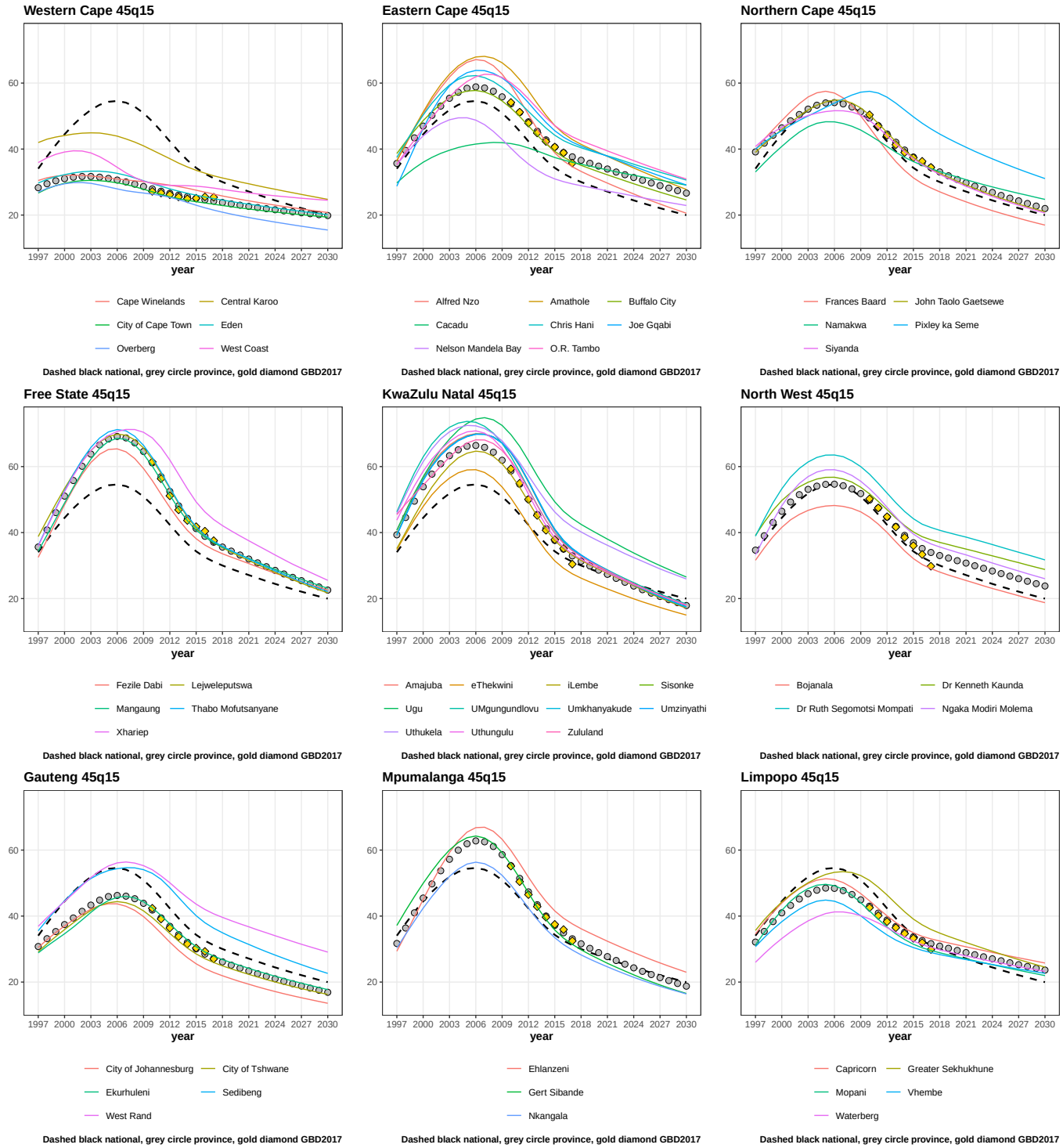

Figure 4.10: Forecasted provincial adult mortality comparisons

As with the national and provincial forecasts, gains in e_0 and decreases in ${}_{45}q_{15}$ and ${}_5q_0$ are forecasted for the districts. Figures 4.8 to 4.10 show these changes and Figures 4.11 and 4.12 illustrate them on the South Africa map.

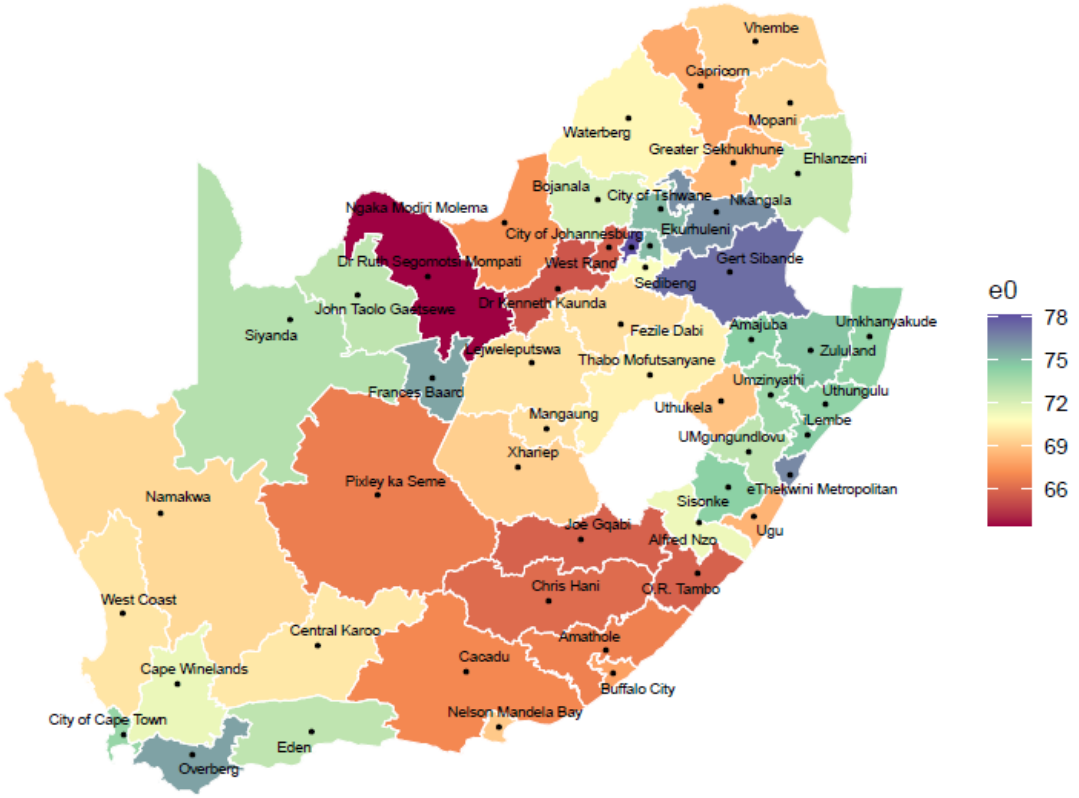

Figure 4.11: Forecasted district e_0 map, 2030

The average e_0 increase between 2015 and 2030 across the districts is 8.9 years. The districts mean increases range from 3.3 years to 13 years. The five largest average increases are forecasted for Amajuba, Sisonke, Umzinyathi and Umkhanyakude districts in KwaZulu-Natal province as well as Xhariep district in Free State, all forecasted to increase by approximately 13 years between 2015 and 2030. In contrast, the lowest improvements are forecasted for Mopani, Capricorn and Vhembe districts in Limpopo as well the City of Cape Town and the West Coast that are in the Western Cape, which are forecasted to

increase between 3 and 5 years over the period. The City of Johannesburg is projected to have the highest average e_0 in 2030 having increased from 68 years in 2015 to 78 years. In contrast, Dr Ruth Segomotsi Mompati in North West province is projected to have the lowest e_0 after rising from 57.6 in 2015 to 63.4 years in 2030.

Looking at ${}_{45}q_{15}$, the average forecasted decrease between 2015 and 2030 across the districts is 15 per 100 and the average ranges from 4.27 to 23.7. The districts with the biggest changes in e_0 also have the largest reductions in forecasted adult mortality i.e. Xhariep, Sisonke, Amajuba, Umzinyathi and Umkhanyakude, all forecasted to fall by approximately 23 per 100. Similarly, some of the districts with the lowest increases in e_0 are also among those with the lowest reductions in ${}_{45}q_{15}$ i.e. West Coast and the City of Cape Town. In addition to these two are Eden, Cape Winelands and Overberg all in the Western Cape having low reductions between 4 and 8 per 100. Once again Dr Ruth Segomotsi Mompati and the City of Johannesburg are at the extremes of the ranking with the former having the highest ${}_{45}q_{15}$ of 31 in 2015 down from from 44, and the latter the lowest ${}_{45}q_{15}$ value of 14 in 2030 down from a value of 25 per 100 in 2015.

In terms of ${}_5q_0$, Dr Ruth Segomotsi Mompati is forecasted to have the highest value of 53.9 per 1,000 in 2030 having fallen from 62.4 in 2015. The West Coast has the lowest forecasted child mortality estimate for 2030 at 10.2 per 1,000, down from 18.7 per 1,000 in 2015. On average, child mortality is forecasted to fall by 14.1 per 1,000 over the period ranging from 3.5 to 27 per 1,000. The list of districts with the biggest reductions in ${}_5q_0$ differs from the adult mortality and life-expectancy list. It comprises of Xhariep, Lejweleputswa and Thabo Mofutsanyane in the Free State as well as Pixley ka Seme and John Taolo Gaetsewe in the Northern Cape, with the largest reductions above 22 per 1,000. The districts with the smallest reductions are Central Karoo in the Western Cape and Greater Sekhukhune, Waterberg, Capricorn and Mopani in Limpopo province all falling by between 3.5 and 6 per 1,000 over the period.

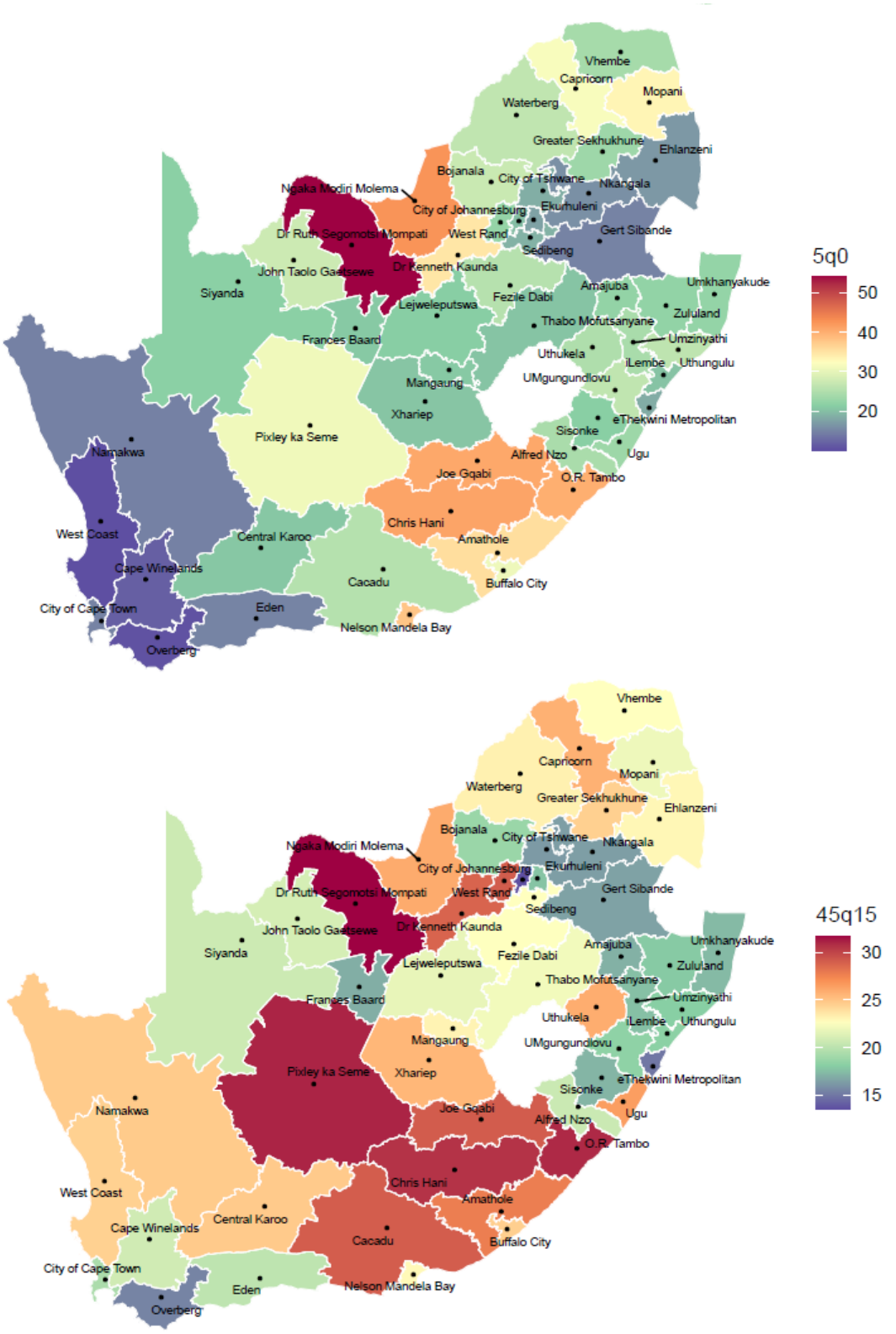

Figure 4.12: Forecasted ${}_{45}q_{15}$ and ${}_{5}q_{0}$ map, 2030

4.3.2.2 *Cause-specific mortality forecasts*

Figure 4.13 illustrates the cause-specific proportions for all deaths aggregated by province, cause and year. The slightly dulled output is from the mean Aim 2 estimates (shown previously in Figure 3.4) followed by the mean values of the forecasts by cause.

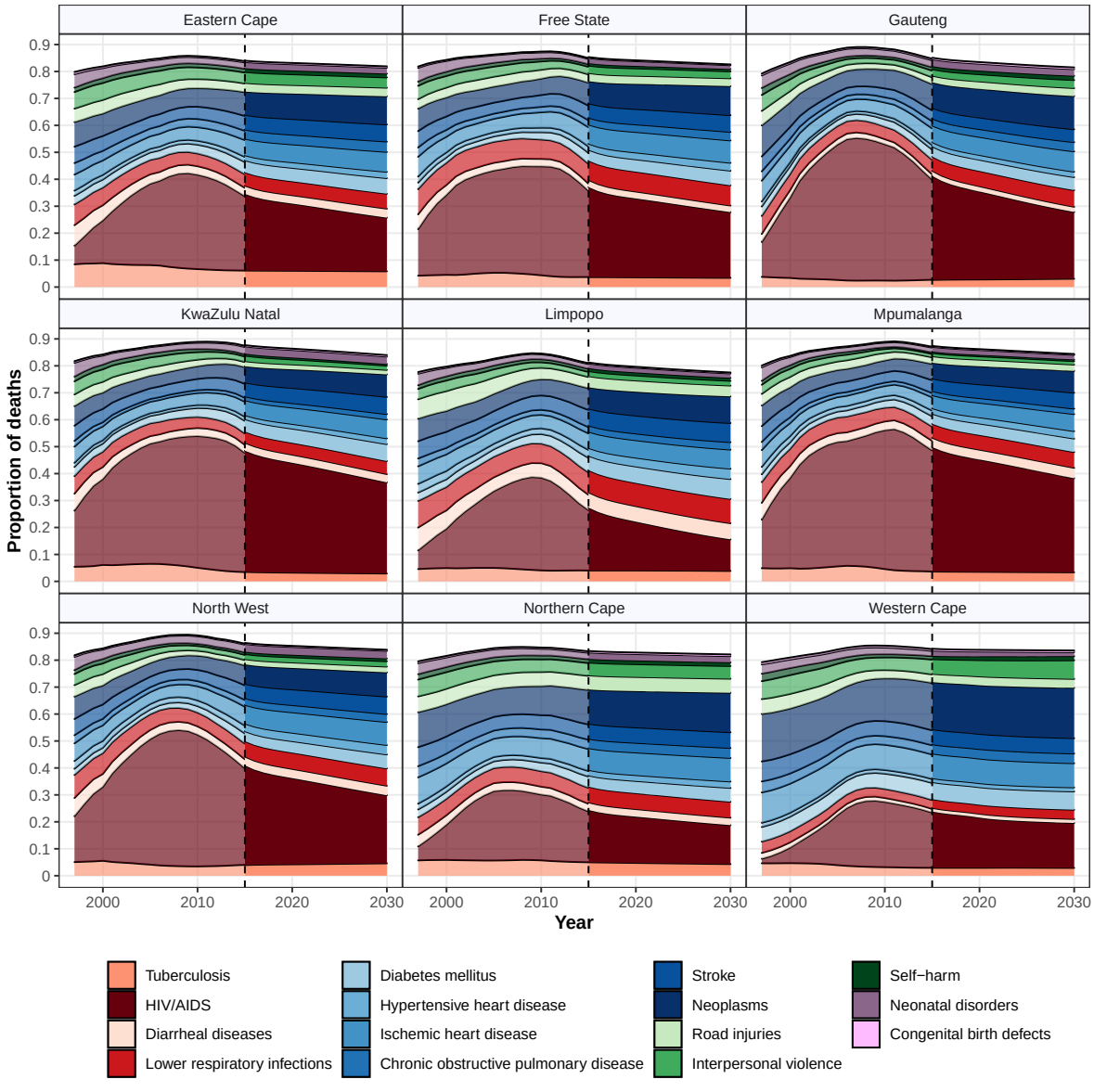

Figure 4.13: Historical and forecasted cause proportions

Figure 4.14 illustrates the overall cause-specific age-standardised death-rates per 100,000 for years 2015 and 2030, showing that the largest reductions are forecasted for HIV/AIDS and the group "All Other". Table 4.2 is of the historical and forecasted ASR as well as the percent of all deaths by cause and for years 1997, 2006, 2015 and 2030. On average the ASR for HIV/AIDS is expected to fall by more than a half between 2015 and 2030. Correspondingly, the overall HIV/AIDS cause-fraction is expected to fall by almost a third. As expected this is followed by corresponding increases in the cause-fractions of other causes albeit their ASRs are expected to fall as well.

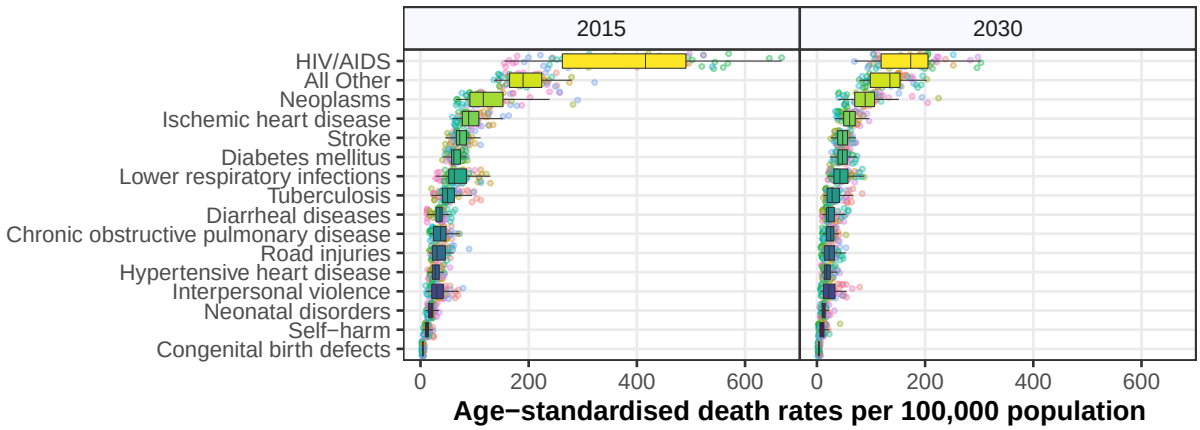

Figure 4.14: Cause-specific ASR for years 2015 and 2030

Table 4.2: Historical and forecasted ASR and percent of deaths by cause and year

Cause	1997		2006		2015		2030	
	ASR	(%)	ASR	(%)	ASR	(%)	ASR	(%)
Tuberculosis	75.79	5.2	111.35	5.07	53.12	3.96	32.45	3.81
HIV/AIDS	140.72	12.42	709.64	38.1	380.61	32.46	172.38	22.87
Diarrheal diseases	59.25	5.52	51.48	2.97	34.27	3.01	25.97	3.17
Lower respiratory infections	90	7.34	108.12	5.53	69.81	5.54	45.63	6.07
Diabetes mellitus	54.69	3.21	65.97	2.75	64.28	4.45	47.28	5.76
Hypertensive heart disease	34.28	2.23	34.11	1.5	28.46	2.06	19.91	2.61
Ischemic heart disease	119.43	7.48	122.34	5.33	93.77	6.65	59.85	7.76
Chronic obstructive pulmonary disease	55.26	3.39	48.36	2.1	37.26	2.58	25.15	3.06
Stroke	100.38	6.23	101.48	4.32	75	5.26	47.89	6.08
Neoplasms	161.23	10.08	156.55	7.24	129.1	9.29	93.2	11.35
Road injuries	56.31	5.08	65.15	3.68	34.77	3.05	24.06	3.09
Interpersonal violence	58.65	5.17	64.37	3.53	33.17	2.93	25.17	3.06
Self-harm	22.59	1.86	25	1.3	12.49	1.05	10.06	1.14
Neonatal disorders	34.14	4.5	32.18	2.5	19.93	2.24	12.87	2.07
Congenital birth defects	5.38	0.66	5.29	0.4	4.17	0.46	3.57	0.48
All Other	265.45	19.65	279.76	13.69	195.34	15.02	131	17.61

Specific for year 2030, Table 4.3 is of the age-standardised death-rates per 100,000 displayed by district and cause. The pattern shows that HIV/AIDS mortality is forecasted to still be a leading cause in 2030 the highest rates still being in KwaZulu-Natal. However, it is important to note the emergence of the non-communicable diseases and to realise that the differences across causes and districts is much lower than in the historical data e.g. Diabetes mortality in Limpopo is approximately half that of HIV/AIDS.

Table 4.3: Heatmap of ASDR by district, 2030

	Location	Tuberculosis	HIV/AIDS	Diarrheal diseases	Lower respiratory infections	Diabetes mellitus	Hypertensive heart disease	Ischemic heart disease	Chronic obstructive pulmonary disease	Stroke	Neoplasms	Road injuries	Interpersonal violence	Self-harm	Neonatal disorders	Congenital birth defects	All Other
Western Cape	City of Cape Town	17.8	104.7	9.8	21.0	40.2	9.0	57.3	22.0	36.0	104.8	22.7	49.5	10.6	9.6	5.6	105.0
	West Coast	26.5	118.6	12.0	32.2	58.5	14.5	73.3	34.4	46.1	204.7	26.9	54.9	12.7	6.1	3.6	143.2
	Cape Winelands	22.9	114.3	11.4	36.4	55.8	15.1	74.8	32.9	45.7	176.2	22.9	41.7	9.8	7.2	3.4	143.0
	Overberg	16.0	97.7	10.2	20.3	40.4	9.3	54.8	24.5	33.9	106.4	16.6	33.4	8.5	7.6	3.1	96.4
	Eden	18.0	112.7	20.2	41.0	46.5	11.2	62.0	26.9	39.8	132.9	18.2	33.3	9.0	10.5	3.8	110.2
	Central Karoo	21.8	222.0	15.3	22.3	44.8	8.6	50.8	22.2	33.2	117.1	28.3	65.4	14.1	11.4	6.8	98.6
Eastern Cape	Buffalo City	55.0	156.3	39.3	54.8	56.0	23.1	72.5	34.6	56.6	108.2	34.2	79.0	21.1	20.0	5.0	153.5
	Cacadu	64.1	189.0	28.1	50.2	58.8	23.5	69.4	33.5	61.3	109.5	33.8	42.5	15.7	14.6	5.6	164.4
	Amathole	59.7	199.6	29.8	48.1	55.5	21.1	67.4	35.3	57.2	104.2	34.5	47.0	17.8	18.2	4.4	164.1
	Chris Hani	62.2	208.9	40.0	45.6	51.9	17.8	60.0	31.9	53.4	97.1	37.8	50.3	18.1	18.1	4.2	156.2
	Joe Gqabi	66.5	221.4	42.8	51.0	56.3	20.8	67.8	39.4	60.0	104.4	32.3	41.8	15.0	9.5	4.8	174.8
	O.R. Tambo	56.5	237.6	35.7	42.5	48.0	17.4	57.9	30.2	51.2	88.4	38.7	54.4	17.7	20.3	7.1	152.7
	Alfred Nzo	83.6	142.5	46.4	39.8	44.1	17.9	57.8	41.1	53.6	88.0	21.3	29.1	10.7	5.3	4.2	137.4
	Nelson Mandela Bay	54.8	147.6	32.1	47.8	48.4	19.7	60.4	30.2	54.3	96.1	27.0	47.1	12.7	24.5	5.2	138.8
Northern Cape	John Taolo Gaetsewe	28.2	156.0	19.8	34.1	33.2	13.5	50.7	23.6	37.0	80.7	42.4	27.9	9.8	15.1	2.8	100.3
	Namakwa	37.6	163.1	16.6	59.5	56.3	22.2	80.8	36.1	50.0	194.2	36.5	34.3	12.0	7.2	3.3	134.9
	Pixley ka Seme	54.8	126.0	29.2	56.6	48.9	24.7	86.0	41.2	57.0	151.6	53.9	46.7	16.6	12.9	6.2	178.5
	Siyanda	30.0	110.8	18.1	36.0	36.9	17.1	61.5	28.7	40.4	95.3	30.2	25.2	8.2	10.8	2.8	119.8
	Frances Baard	30.1	69.4	17.3	31.5	27.3	14.0	56.3	22.0	38.8	82.4	24.6	21.9	7.2	10.0	3.4	105.6
Free State	Xhariep	26.5	252.3	21.1	56.5	47.7	21.8	62.3	25.4	47.5	85.8	26.4	22.6	10.7	10.7	2.9	134.8
	Lejweleputswa	29.1	173.0	22.6	69.7	52.7	28.5	79.1	32.2	58.6	114.7	20.9	17.7	6.7	10.2	4.6	149.8
	Thabo Mofutsanyane	26.9	172.0	25.6	63.5	47.6	26.9	77.1	31.2	55.9	90.0	21.9	20.5	6.4	10.2	2.2	151.0
	Fezile Dabi	28.1	193.1	22.2	63.2	44.8	24.3	72.8	27.8	54.4	89.2	25.8	22.9	7.5	11.1	2.3	148.5
	Mangaung	30.5	189.5	21.0	64.1	45.0	24.6	77.3	29.6	55.3	86.2	28.8	22.6	7.4	11.5	4.2	150.7
KwaZulu Natal	Ugu	29.8	303.3	23.3	46.6	58.5	19.1	53.4	19.4	48.6	118.1	13.2	12.2	5.5	13.8	3.9	123.4
	UMgungundlovu	24.8	213.4	17.2	35.6	47.6	14.4	44.8	14.2	41.7	74.9	9.7	9.0	3.7	16.6	3.6	95.5
	Uthukela	27.1	295.9	20.8	37.4	56.4	18.0	53.9	17.3	50.4	86.0	13.3	12.1	4.7	13.8	3.0	120.3
	Umzinyathi	16.0	213.0	17.6	25.4	46.1	13.6	41.9	11.0	40.6	53.6	8.8	7.8	3.3	15.7	2.7	88.6
	Amajuba	18.1	190.4	18.7	26.5	43.3	12.4	41.3	11.8	38.8	55.2	9.1	8.6	3.7	13.1	3.4	91.3
	Zululand	18.7	199.5	18.3	26.9	36.1	11.3	37.9	10.9	35.8	51.8	9.7	9.4	3.8	11.3	2.6	86.2
	Umkhanyakude	16.2	205.3	18.9	25.4	44.5	12.9	42.6	12.0	40.2	52.7	8.3	7.1	3.0	14.0	2.8	92.3
	Uthungulu	17.3	205.4	18.9	26.0	36.7	11.4	45.0	10.2	38.4	40.7	9.9	9.6	4.1	16.7	3.2	91.9
	iLembe	19.2	198.9	17.2	26.0	37.8	12.5	38.8	10.9	36.8	53.0	10.7	9.9	4.3	12.4	2.8	90.6
	Sisonke	17.3	203.2	27.4	26.3	48.2	11.9	39.7	9.7	37.6	51.7	7.2	6.4	2.7	11.7	3.0	84.9
	eThekwini	16.3	187.0	16.4	21.9	37.5	9.9	37.9	10.5	33.8	39.5	8.6	8.2	3.6	10.9	3.8	78.0
North West	Bojanala	31.8	175.2	26.6	44.2	40.6	28.4	69.0	24.2	55.5	68.7	14.0	12.7	6.7	17.6	4.4	117.1
	Ngaka Modiri Molema	47.1	224.9	53.6	56.5	48.9	30.3	79.9	30.3	65.8	84.6	20.1	20.1	10.7	18.7	4.2	142.7
	Dr Ruth Segomotsi	54.0	297.5	42.2	69.8	61.5	38.0	92.3	31.1	72.0	96.3	31.1	27.5	13.5	32.2	4.6	177.7
	Dr Kenneth Kaunda	54.1	283.6	49.8	75.9	60.8	41.8	96.3	38.8	71.7	114.8	25.9	24.4	11.4	22.4	3.6	172.9
Gauteng	Sedibeng	22.8	173.4	14.2	49.3	43.7	18.9	62.9	32.1	39.5	106.5	22.0	22.4	13.0	10.7	3.0	148.4
	West Rand	34.9	154.7	34.8	87.4	67.5	32.9	85.8	53.9	56.8	224.9	28.4	25.4	42.8	12.8	5.3	203.4
	Ekurhuleni	16.5	133.6	11.2	35.0	30.9	12.9	49.7	22.2	32.0	72.2	15.6	15.5	8.3	9.5	2.7	112.5
	City of Johannesburg	12.3	104.1	10.1	27.4	23.6	9.9	38.9	17.3	25.6	53.4	12.3	12.6	6.9	12.1	3.3	89.3
	City of Tshwane	16.1	112.7	11.2	37.5	32.9	14.5	53.1	25.7	34.0	79.6	14.2	13.8	7.7	9.6	2.7	118.1
Mpumalanga	Gert Sibande	18.2	160.2	20.3	29.5	27.7	13.8	34.0	10.7	31.5	40.6	13.5	8.6	3.8	6.9	1.5	77.6
	Nkangala	19.5	159.3	24.6	32.2	31.7	17.0	36.1	12.5	38.4	49.2	10.9	10.1	3.4	7.0	1.6	83.4
	Ehlanzeni	22.7	252.0	22.8	38.0	34.7	18.6	42.1	13.9	39.0	54.7	15.1	8.7	5.3	8.3	4.2	100.1
Limpopo	Mopani	35.2	109.2	45.2	70.7	66.1	29.7	59.3	21.4	63.7	81.7	39.8	16.9	11.4	17.7	3.2	167.2
	Vhembe	38.6	107.1	57.4	83.0	70.5	33.0	61.9	29.2	67.5	105.6	48.7	22.7	23.0	7.3	2.5	183.4
	Capricorn	43.2	113.9	50.4	76.3	65.4	30.1	61.0	24.8	63.1	93.4	47.2	20.5	15.1	11.3	3.0	186.3
	Waterberg	33.7	128.5	38.3	60.6	56.3	25.8	51.6	18.0	49.7	69.9	43.6	18.2	13.3	14.5	2.5	153.1
	Greater Sekhukhune	43.7	95.6	58.4	84.0	74.3	37.6	62.9	30.1	65.8	118.6	42.9	22.1	13.1	8.8	2.3	195.6

4.4 Discussion

This study uses a computationally efficient approach to forecast all-cause and cause-specific mortality at various levels of geographic specification. An advantage of this approach is that it utilizes the empirical measurements of deaths and population and does not require an extensive historical time-series unlike other extrapolation type approaches. Relative changes in the short term forecasts agree well with the estimates coming from the GBD2017 results for all ages and with the WPP2019 forecasts for child mortality and even suggest that the most recent GBD2017 estimate might be slightly biased.

Another strength of this approach is that within the CoDa framework applied and by determining the principal components, the age-patterns are retained as would be with a Lee-Carter type approach. Interestingly, taking the compositional framework described by Mills [72] which entails transforming the cause-fractions from the simplex space to the real number space using a transformation such as the additive log-ratio transform, forecasting the univariate age-specific and cause-specific transformed variables via a VAR or other multivariate time-series method and then transforming the forecasts back to the simplex space using the inverse transform of the ALR gives very similar proportions to those estimated using this multiple decrement approach. The problem with the univariate approach is that it is computationally more expensive even if it enforces covariance indirectly by virtue of the transformed forecasts being transformed back to proportions. By and large, the multiple decrement approach is a computationally superior approach.

One challenge with forecasting is that one has to make an assumption about the pattern of serial correlation. If one has a long time-series of historical data then it is a straightforward time-series analysis to determine the structure of the data and the nature of the correlation in the residuals. However, with a short time-series such as the one in this study for which most of it is dominated by HIV/AIDS related changes, determining the pattern of the residuals and hypothesising about how those residuals are likely to be related in a future where the effect of HIV is reduced, is not trivial. Such decisions are

made simpler by deriving the principal components and time varying parameters which capture a significant amount of information. However, decisions still need to be made about how the time varying parameters are likely to change in the future. In this research logistic growth is assumed which gives conservative estimates but for some districts the change may in fact be accelerated or linear or it may be slower than the logistic curve suggests. The logistic growth curve works well in the short term, as can be seen from the comparisons on the national forecast. There are some differences at the province and cause-specific level that seem to suggest that the projection of the time varying parameters can be improved upon to give more accurate predictions.

There is scope for improving the forecast particularly by determining covariates that have strong correlations with the time varying parameters and have established relationships with mortality e.g. income, education or HIV prevalence. The covariate framework utilised by Foreman et al. [5] using SDI and other covariates is a good example of this. The limitation in this regard, and why this study uses time as the main predictor for these principal components, is that the covariates themselves would have to be modelled to derive a comprehensive time-series for them. Unlike the current model which solely relies on the data to tell the story into the future, a covariate extrapolation approach would require assumptions to be made about how the covariates have changed over time. Currently, the best source for district level information is the census where past censuses are only for 1996, 2001 and 2011. Creating a robust time-series of covariates would require making assumptions about how the covariates behave in the intercensal period which may require modelling them against data that are annual. Consequently, a covariate based forecast by district would require assumptions to fill any gaps in the retrospective data as well as for forecasting the covariates, and depending on those assumptions, that will impact the final result. However, such a structure will also potentially be robust decreasing the number of extreme trends predicted and imposing turning or plateau points for the future directly based on future dated data.

The limitations extend to both the all-cause and the cause-specific forecasts. As with Aim 2, a major limitation is having a short-list of 15 causes which although most relevant for most, could still be deficient for some. Fortunately on the aggregate, this list still accounts for more than 80% of the deaths forecasted nationally. As a proportion, the "All Other" category accounts for slightly more deaths over time and it would be an exercise to disaggregate this group into its constituent causes to explore if there are any key causes being hidden. In addition, the cause-specific forecasts are conditional on the all-cause ones and are correlated to each other by virtue of being modelled in a composition, and so to the degree that the all-cause rates are biased, this has a compounded effect on the cause-specific estimates.

Ultimately, forecasting is not an exact science nor is it a foretelling of a certain future but it gives a reasonable prediction of what is expected to occur under regular circumstances and especially if historic rates of change persist into the future. The COVID-19 pandemic of the year 2020 is an example of an irregular circumstance such a framework is not designed to predict. With South Africa still battling many levels of inequality and the healthcare system still looking at ways to reduce the inequities that plague the nation, the journey towards a fully functioning system, covering all and giving all the highest levels of care and the highest chances at attaining the best health, is ongoing. This research provides good news in that if the work of the past few years continues, there are many real gains that will be achieved over the next 10 years. However, the results also provide a caution, as the infectious diseases fall, there are many conditions such as Diabetes, Hypertension and Cancers that have not had the same levels of intervention and for which the masses do not have the same levels of education related to lifestyle risks as well as prevention. Insufficient response towards these will lead to health burdens in the future that could be avoided if considered earlier and will make withdrawals on the country's capacity to do the best for her people.

REFERENCES

[1] Victoria Pillay-van Wyk, William Msemburi, Ria Laubscher, Rob E Dorrington, Pam Groenewald, Tracy Glass, Beatrice Nojilana, Jané D Joubert, Richard Matzopoulos, Megan Prinsloo, et al. Mortality trends and differentials in South Africa from 1997 to 2012: second National Burden of Disease Study. *The Lancet Global Health*, 4(9):e642–e653, 2016.

[2] Haidong Wang, Mohsen Naghavi, Christine Allen, Ryan M Barber, Zulfiqar A Bhutta, Austin Carter, Daniel C Casey, Fiona J Charlson, Alan Zian Chen, Matthew M Coates, et al. Global, regional, and national life expectancy, all-cause mortality, and cause-specific mortality for 249 causes of death, 1980–2015: a systematic analysis for the global burden of disease study 2015. *The Lancet*, 388(10053):1459–1544, 2016.

[3] Rob Dorrington, D Bradshaw, R Laubscher, and N Nannan. Rapid mortality surveillance report 2012. *Cape Town, South Africa: South African Medical Research Council*, 2014.

[4] R. Lee and L. Carter. Modelling and forecasting U.S. mortality. 87:659–671, 1992.

[5] Kyle J Foreman, Neal Marquez, Andrew Dolgert, Kai Fukutaki, Nancy Fullman, Madeline McGaughey, Martin A Pletcher, Amanda E Smith, Kendrick Tang, Chun-Wei Yuan, et al. Forecasting life expectancy, years of life lost, and all-cause and cause-specific mortality for 250 causes of death: reference and alternative scenarios for 2016–40 for 195 countries and territories. *The Lancet*, 392(10159):2052–2090, 2018.

[6] Heather Booth and Leonie Tickle. Mortality modelling and forecasting: A review of methods. *Annals of actuarial science*, 3(1-2):3–43, 2008.

[7] UNAIDS. Spectrum model. `www.unaids.org/en/dataanalysis/tools/spectrumepp2011/`, 2012.

[8] Actuarial Society of South Africa. ASSA2008 model. aids.actuarialsociety.org.za/ASSA2008-Model-3480.htm, 2012.

[9] Leigh Johnson, Rob Dorrington, Thomas Rehle, Sean Jooste, Linda-Gail Bekker, Melissa Wallace, Landon Myer, and Andrew Boulle. THEMBISA version 1.0: A model for evaluating the impact of HIV/AIDS in South Africa. *Centre for Infectious Disease Epidemiology and Research Working Paper February*, 2014.

[10] Tukufu Zuberi, Amson Sibanda, and Eric O Udjo. *The Demography of South Africa*. Routledge, 2016.

[11] Ronald Lee. The lee-carter method for forecasting mortality, with various extensions and applications. *North American actuarial journal*, 4(1):80–91, 2000.

[12] Arthur E. Renshaw and Steve Haberman. Lee–Carter mortality forecasting with age specific enhancement. 33:255–272, 2003.

[13] L. Lee. The Lee–Carter method for forecasting mortality, with various extensions and applications. 4:80–93, 2000.

[14] R. Lee and F. Nault. *Modeling and forecasting provincial mortality in Canada*. Paper presented at the World Congress of International Union for the Scientific Study of Population, Montreal. Unpublished, 1993.

[15] J.R. Wilmoth. Computational methods for fitting and extrapolating the Lee–Carter model of mortality change. Technical report, Berkeley: Department of Demography, University of California, 1993.

[16] Arthur E. Renshaw and Steve Haberman. A cohort-based extension to the Lee–Carter model for mortality reduction factors. 38:556–570, 2006.

[17] E. Tabeau. A review of demographic forecasting models for mortality. In E. Tabeau, A. Van Den Berg Jeths, and C. Heathcote, editors, *Forecasting mortality in developed countries: insights from a statistical, demographic and epidemiological perspective*, pages 1–32. Dordrecht:, 2001.

[18] N. Brouhns, M. Denuit, and J.K. Vermunt. A Poisson log–bilinear regression approach to the construction of projected life tables. 31:373–393, 2002.

[19] Arthur E. Renshaw and Steve Haberman. Lee–Carter mortality forecasting: A parallel generalized linear modelling approach for England and Wales mortality projections. *C*, 52(1): 119–137, 2003.

[20] A.E. Renshaw and Steven Haberman. A Cohort-Based Extension to the Lee-Carter Model for Mortality Reduction Factors. *Insurance: Mathematics and Economics*, 38(3):556–570, 2006.

[21] Rob J. Hyndman and S Ullah. Robust Forecasting of Mortality and Fertility Rates: A Functional Data Approach. *Computational Statistics & Data Analysis*, 51(10):4942–4956, 2007.

[22] Andrew Hunt and David Blake. On the Structure and Classification of Mortality Models Mortality Models. *Pension Institute Working Paper*, 2015. URL `http://www.pensions-institute.org/workingpapers/wp1506.pdf`.

[23] Iain D Currie. On Fitting Generalized Linear and non-linear Models of Mortality. *Scandinavian Actuarial Journal*, (4):356–383, 2016.

[24] Pietro Millossovich, Andrés M Villegas, and Vladimir K Kaishev. Stmomo: An r package for stochastic mortality modelling. *Journal of Statistical Software*, 2017.

[25] P McCullagh and J Nelder. *Generalized Linear Models*. Chapman & Hal, London, second edition, 1989.

[26] A.E. Renshaw and Steven Haberman. Lee-Carter Mortality Forecasting with Age-specific Enhancement. *Insurance: Mathematics and Economics*, 33(2):255–272, 2003.

[27] Andrew J. G. Cairns, David Blake, Kevin Dowd, Guy D. Coughlan, D. Epstein, A. Ong, and I. Balevich. A Quantitative Comparison of Stochastic Mortality Models Using Data from England and Wales and the United States. *North American Actuarial Journal*, 13(1):1–35, 2009.

[28] Richard Plat. On Stochastic Mortality Modeling. *Insurance: Mathematics and Economics*, 45(3): 393–404, 2009.

[29] Helena Aro and Teemu Pennanen. A User-Friendly Approach to Stochastic Mortality Modelling. *European Actuarial Journal*, 1:151–167, 2011.

[30] Steven Haberman and A.E. Renshaw. A Comparative Study of Parametric Mortality Projection Models. *Insurance: Mathematics and Economics*, 48(1):35–55, 2011.

[31] Enrico Lovász. Analysis of Finnish and Swedish Mortality Data with Stochastic Mortality Models. *European Actuarial Journal*, 1(2):259–289, 2011.

[32] Colin O'Hare and Youwei Li. Explaining Young Mortality. *Insurance: Mathematics and Economics*, 50(1):12–25, 2012.

[33] Matthias Börger, Daniel Fleischer, and Nikita Kuksin. Modeling the Mortality Trend under Modern Solvency Regimes. *ASTIN Bulletin*, 44(1):1–38, 2013.

[34] Frank van Berkum, Katrien Antonio, and Michel Vellekoop. The Impact of Multiple Structural Changes on Mortality Predictions. *Scandinavian Actuarial Journal*, 2014.

[35] Daniel H. Alai and Michael Sherris. Rethinking Age-Period-Cohort Mortality Trend Models. *Scandinavian Actuarial Journal*, (3):208–227, 2014.

[36] Federico Girosi and Gary King. Understanding the lee-carter mortality forecasting method. *Gking. Harvard. Edu*, 2007.

[37] Samir Soneji and Gary King. Statistical security for social security. *Demography*, 49(3): 1037–1060, 2012.

[38] United Nations. Department of International Economic and Social Affairs. Population Division. *World Population Prospects: The 2017 Revision, Methodology of the United Nations Population Estimates and Projections, Working Paper No. ESA/P/WP.250.* UN, 2017.

[39] Ronald D Lee and Lawrence R Carter. Modeling and forecasting us mortality. *Journal of the American statistical association*, 87(419):659–671, 1992.

[40] Christopher JL Murray and Alan D Lopez. Alternative projections of mortality and disability by cause 1990–2020: Global Burden of Disease Study. *The Lancet*, 349(9064):1498–1504, 1997.

[41] Rob J Hyndman, Andrey V Kostenko, et al. Minimum sample size requirements for seasonal forecasting models. *Foresight*, 6(Spring):12–15, 2007.

[42] Debbie Bradshaw, William Msemburi, Rob Dorrington, Victoria Pillay-van Wyk, Ria Laubscher, Pam Groenewald, South African National Burden of Disease Study team, et al. HIV/AIDS in South Africa: how many people died from the disease between 1997 and 2010? *AIDS*, 30(5):771–778, 2016.

[43] John Stover, Tim Brown, and Milly Marston. Updates to the Spectrum/Estimation and Projection Package (EPP) model to estimate HIV trends for adults and children. *Sexually transmitted infections*, 88(Suppl 2):i11–i16, 2012.

[44] Actuarial Society of South Africa AIDS Committee and others. ASSA2008 AIDS and Demographic Model, 2011. URL `http://www.actuarialsociety.org.za/`.

[45] Carl Eckart and Gale Young. The approximation of one matrix by another of lower rank. *Psychometrika*, 1(3):211–218, 1936.

[46] Zoltan Butt, Steven Haberman, and Han Lin Shang. *ilc: Lee-Carter Mortality Models Using Iterative Fitting Algorithms*, 2014. URL `http://CRAN.R-project.org/package=ilc`. *R* package version 1.0.

[47] Samuel J Clark. A singular value decomposition-based factorization and parsimonious component model of demographic quantities correlated by age: Predicting complete demographic age schedules with few parameters. *arXiv preprint arXiv:1504.02057*, 2015.

[48] Samuel J Clark. An svd component model of mortality indexed by child or both child and adult mortality. 2017.

[49] John R Wilmoth, Kirill Andreev, Dmitri Jdanov, Dana A Glei, C Boe, M Bubenheim, D Philipov, V Shkolnikov, and P Vachon. Methods protocol for the human mortality database. *University of California, Berkeley, and Max Planck Institute for Demographic Research, Rostock. URL: http://mortality. org [version 31/05/2007]*, 9:10–11, 2007.

[50] Monica Alexander, Emilio Zagheni, and Magali Barbieri. A flexible bayesian model for estimating subnational mortality. *Demography*, 54(6):2025–2041, 2017.

[51] Jim Oeppen et al. Coherent forecasting of multiple-decrement life tables: a test using Japanese cause of death data. 2008.

[52] John Aitchison. The statistical analysis of compositional data. *Journal of the Royal Statistical Society: Series B (Methodological)*, 44(2):139–160, 1982.

[53] John Aitchison. *CODA: A microcomputer package for the statistical analysis of compositional data*. Chapman and Hall London, 1986.

[54] Marie-Pier Bergeron-Boucher, Vladimir Canudas-Romo, Jim Oeppen, and James W Vaupel. Coherent forecasts of mortality with compositional data analysis. *Demographic Research*, 37: 527–566, 2017.

[55] Søren Kjærgaard, Yunus Emre Ergemen, Malene Kallestrup-Lamb, James Oeppen, and Rune Lindahl-Jacobsen. Forecasting Causes of Death using Compositional Data Analysis: the Case of Cancer Deaths. In *Fourteenth International Longevity Risk and Capital Markets Solutions Conference*, 2018.

[56] Samuel Piveteau and Julien Tomas. Mortality by Cause Of Death and Forecasts by Compositional Time Series. In *22nd International Congress on Insurance: Mathematics and Economics UNSW Sydney, 15-18 July 2018*, 2018.

[57] Alan D Lopez and Christopher JL Murray. *The Global Burden of Disease: A Comprehensive Assessment of Mortality and Disability from Diseases, Injuries, and Risk Factors in 1990 and Projected to 2020; Summary*. Harvard School of Public Health, 1996.

[58] Haidong Wang, Amanuel Alemu Abajobir, Kalkidan Hassen Abate, Cristiana Abbafati, Kaja M Abbas, Foad Abd-Allah, Semaw Ferede Abera, Haftom Niguse Abraha, Laith J Abu-Raddad, Niveen ME Abu-Rmeileh, et al. Global, regional, and national under-5 mortality, adult mortality, age-specific mortality, and life expectancy, 1970–2016: a systematic analysis for the global burden of disease study 2016. *The Lancet*, 390(10100):1084–1150, 2017.

[59] Mohsen Naghavi, Amanuel Alemu Abajobir, Cristiana Abbafati, Kaja M Abbas, Foad Abd-Allah, Semaw Ferede Abera, Victor Aboyans, Olatunji Adetokunboh, Ashkan Afshin, Anurag Agrawal, et al. Global, regional, and national age-sex specific mortality for 264 causes of death, 1980–2016: a systematic analysis for the global burden of disease study 2016. *The Lancet*, 390(10100):1151–1210, 2017.

[60] Emmanuela Gakidou, Ashkan Afshin, Amanuel Alemu Abajobir, Kalkidan Hassen Abate, Cristiana Abbafati, Kaja M Abbas, Foad Abd-Allah, Abdishakur M Abdulle, Semaw Ferede Abera, Victor Aboyans, et al. Global, regional, and national comparative risk assessment of 84 behavioural, environmental and occupational, and metabolic risks or clusters of risks, 1990–2016: a systematic analysis for the global burden of disease study 2016. *The Lancet*, 390 (10100):1345–1422, 2017.

[61] M Naghavi, H Wang, R Lozano, A Davis, X Liang, M Zhou, et al. Gbd 2013 mortality and causes of death collaborators. global, regional, and national age-sex specific all-cause and cause-specific mortality for 240 causes of death, 1990-2013: a systematic analysis for the global burden of disease study 2013. *Lancet*, 385(9963):117–71, 2015.

[62] Mohammad H Forouzanfar, Ashkan Afshin, Lily T Alexander, H Ross Anderson, Zulfiqar A Bhutta, Stan Biryukov, Michael Brauer, Richard Burnett, Kelly Cercy, Fiona J Charlson, et al. Global, regional, and national comparative risk assessment of 79 behavioural, environmental and occupational, and metabolic risks or clusters of risks, 1990–2015: a systematic analysis for the global burden of disease study 2015. *The Lancet*, 388(10053):1659–1724, 2016.

[63] JA Hanley. A heuristic approach to the formulas for population attributable fraction. *Journal of Epidemiology & Community Health*, 55(7):508–514, 2001.

[64] Kenneth C Land. Methods for national population forecasts: A review. *Journal of the American Statistical Association*, 81(396):888–901, 1986.

[65] Nathan Keyfitz. Introduction to the mathematics of population: with revisions. *Addison-Wesley Series in Behavioral Science: Quantitative Methods*, 1977.

[66] Trevor J Hastie. Generalized additive models. In *Statistical models in S*, pages 249–307. Routledge, 2017.

[67] Simon N Wood. *Generalized additive models: an introduction with R*. Chapman and Hall/CRC, 2017.

[68] John Ashworth Nelder and Robert WM Wedderburn. Generalized linear models. *Journal of the Royal Statistical Society: Series A (General)*, 135(3):370–384, 1972.

[69] Vera Pawlowsky-Glahn and Juan José Egozcue. Compositional data and their analysis: an introduction. *Geological Society, London, Special Publications*, 264(1):1–10, 2006.

[70] Regina C Elandt-Johnson, Norman Lloyd Johnson, and Mathematischer Statistiker. *Survival models and data analysis*. Number 312.0151 E37. Wiley Online Library, 1980.

[71] United Nations. World population prospects 2019. 2019.

[72] Terence C Mills. Forecasting compositional time series. *Quality & Quantity*, 44(4):673–690, 2010.